FUNCTIONAL INTERACTIONS BETWEEN MECHANICAL JUNCTION PROTEINS, CONNEXIN43 AND THE VOLTAGE-GATED SODIUM CHANNEL COMPLEX IN THE HEART

By

Halina Chkourko

A dissertation submitted in partial fulfillment
of the requirements for the degree of
Doctor of Philosophy
(Molecular and Integrative Physiology)
In the University of Michigan
2012

Doctoral Committee:

Professor Mario Delmar, Co-Chair, New York University
Associate Professor Jeffrey R. Martens, Co-Chair
Professor Lori L. Isom
Associate Professor Anatoli N. Lopatin

DEDICATION

I dedicate this work to my parents who have always offered but never imposed their wisdom on me. Your unconditional love and support have always helped me to regain strength when needed. You have taught me the importance of making my own decisions, no matter how seemingly insignificant or life-changing they might be. Mom, I have yet to meet anyone as kind, caring and generous as you are – I will always look up to you for these virtues you so effortlessly exercise. Dad, your natural curiosity, unrestricted inquisitiveness and stubbornness are features through which I am daily able to appreciate you in myself. I also dedicate this work to my husband, Edward – the man who took a leap of faith to be with me. Your kindness and love are a blessing and a great motivation. Your sharp and perceptive mind does not cease to amaze me. From the very beginning you took such a big interest in my studies and it warms my heart when I see the pride in your eyes when you look at me. I could not have wished for a better life partner. I am eternally in debt to the three of you for all the love, generosity, and support.

ACKNOWLEDGMENTS

I first would like to thank my advisor Dr. Mario Delmar for his mentorship throughout these years of graduate school. It has been a long journey and I am truly grateful for the opportunities that he provided for my intellectual growth. I have never met anyone as hard working as you and can only hope that I was able to adopt your work ethic and discipline that I admire so much.

I would like to thank Dr. Lori L. Isom, Dr. Jeffrey R. Martens, Dr. Anatoli N. Lopatin, and Dr. Mario Delmar for your time and commitment to be on my thesis committee. I especially want to thank Dr. Anatoli N. Lopatin for helping me to transition from Syracuse, NY to Ann Arbor, MI. During the few months that I worked in your laboratory I received many words of kindness and encouragement from you. I am also very grateful to Dr. Jeffrey Martens from whom I was lucky to receive mentorship. I truly enjoyed the great learning environment provided in your laboratory.

I would also like to acknowledge all the people from whom I received technical support while conducting these studies: Hassan Musa, Lin Xianming, Mingliang Zhang, Sarah Schumacher, Guadalupe Guerrero-Serna, Dr. Steven Taffet, and Wanda Coombs. I am particularly grateful to Hassan Musa, who not only introduced me to the foundations of cardiac electrophysiology but who also was a great friend who I miss.

Although I consider University of Michigan my alma mater, I am grateful to SUNY Upstate Medical University for giving me a head start in my graduate studies.

I also want to thank my great friends - Ravi Vaidyanathan and Beverly Piggott. Ravi, you have truly been like a brother to me – always offering your support, care and imparting your knowledge to me whenever the opportunity arouse. You have always been by my side - through the hard and happy times. I have always enjoyed our discussions about new findings or bouncing off ideas for experimental design. Beverly, you welcomed me to Ann Arbor and truly helped me to transition. These years of our friendship allowed me to recognize your integrity, honesty and

determination. You have always been by my side when needed. I truly hope that no matter where our career choices take us we carry these friendships through life.

TABLE OF CONTENTS

LIST OF FIGURES

Chapter I:

Chapter III:

Chapter IV:

LIST OF ABBREVIATIONS

AJ	Adherens Junctions
AnkG	Ankyrin-G
ARVMs	Adult Rat Ventricular Myocytes
CNTR	Control
Cx43	Connexin43
Dsc	Desmocollin
Dsg	Desmoglein
DP	Desmoplakin
EM	Electron Microscopy
EB1	End-Binding Protein 1
GJ	Gap Junction
ID	Intercalated Disc
IF	Immunofluorescence
I_{Na}	Sodium Current
KO	Knock out
$Na_V1.5$	α-subunit of the cardiac voltage-gated sodium channel
PG	Plakoglobin
PH	Pulmonary Hypertension
PKP2	Plakophilin-2
TTX	Tetrodotoxin
VGSC	Voltage-Gated Sodium Channel
WT	Wild-type
ZO-1	Zonula Occludens-1

ABSTRACT

Desmosomes and adherens junctions provide mechanical continuity between cardiac cells, whereas gap junctions allow for cell-cell electrical/metabolic coupling. These structures reside at the cardiac intercalated disc (ID). Also at the ID is the voltage-gated sodium channel (VGSC) complex. Functional interactions between desmosomes, gap junctions, and VGSCs have been demonstrated. Separate studies show, under various conditions, decreased abundance of gap junctions at the ID, and redistribution of connexin43 (Cx43) to plaques oriented parallel to fiber direction (gap junction "lateralization"). The mechanisms of Cx43 lateralization, and the fate of desmosomal and VGSC molecules in the setting of Cx43 remodeling, remain understudied. To study remodeling we employed the sheep pulmonary hypertension model. We found that Cx43 lateralization is a part of a complex remodeling that includes mechanical and gap junctions, but may exclude components of VGSC. Cx43/desmosomal remodeling was accompanied by lateralization of two microtubule-associated proteins relevant for Cx43 trafficking: EB1 and the kinesin protein Kif5b. Thus, we speculate that lateralization results from redirectionality of microtubule-mediated forward trafficking. Remodeling of junctional complexes may preserve electrical synchrony under conditions that disrupt ID integrity. We then further focused on the importance of the expression of Cx43 and desmosomal protein, PKP2, on the function of VGSCs in the heart. Studies of PKP2 and Cx43 deficiency (PKP2+/- and Cx43-/-) mice models demonstrated that these proteins affect the distribution and function of VGSC. In an attempt to reveal the mechanism for Cx43-mediated regulation of VGSCs we analyzed the ability of Cx43 to stabilize tubulin and for the plus-end of the microtubules to reach its anchoring point at sites rich in the adherens junction protein N-cadherin. Using Cx43 null mice and the immortal cell line of cardiac origin (HL-1) we were able to show that, in the heart, connexin43 regulates the function of VGSCs via its tubulin binding domain. Overall, the data presented in this thesis further illustrate the intimate functional interactions of the proteins residing at the ID and reinforces the idea of these proteins working together as parts of macromolecular complexes.

Chapter I

Introduction

1. Interactions Between The Proteins of the Intercalated Disc

a. Intercalated Disc

The first documentation of what is now known as the intercalated disc came from the mid-1800s, when early histological studies identified dense transverse bands, irregularly interrupting muscle fibers; these structures were recognized as boundaries of oppositions of the adjacent cells (Forbes and Sperelakis 1985). Later in history, however, intercalated discs were inaccurately characterized as "intracellular contraction bands", "tendinous incursions"(Forbes and Sperelakis 1985). Fortunately, the advancements in the technology and development of transmission electron microscopy confirmed the earlier thought and identified the intercalated discs as "lines of demarcations" between the neighboring cells opposed to each other (Beams, Evans et al. 1949).

Today, the appreciation of the importance of the intercalated disc is based on the structures that reside in it. The smooth propagation of the action potential throughout the myocardium would be impossible without excitation occurring at each cardiomyocyte due to voltage-gated sodium channels (VGSCs) and maintanance of electrical coupling between the adjacent cells by gap junctions. Each contraction generates a great amount of force which gets transmitted through the cardiac tissue. The mechanical coupling, provided by the adherens junctions and desmosomes, allows the membranes of opposing cells to stay close together for the successful formation of gap junctions and preservation of electrical coupling (Figure 1.1), as well as for the transmission of force. Together, these structures allow for the coordinate contraction and relaxation of the cardiac tissue that allows the myocardium to behave as a functional syncytium.

b. Gap Junctions

Gap Junctions are the low-resistance channels that allow for cell-to-cell communication. In the heart they are in charge of cell-to-cell electrical coupling essential for the propagation of action potential. When two hemichannels (or connexons) of the adjacent cells dock together and form disulfide bonds, they assemble into a continuous channel (gap junction) connecting cytoplasms of those cells. Each connexon is assembled from six transmembrane proteins called connexins (Cx).

Gap junctions allow for permeability of molecules with the molecular weight of up to 1 kDa such as ATP, ions, glucose, secondary messengers, metabolites, and siRNA (Valiunas, Polosina et al. 2005; Harris 2007). Nonjunctional connexons have a lower open permeability comparing to that of gap junctions, and reportedly play roles in cardiac preconditioning (Schulz and Heusch 2004; Rodriguez-Sinovas, Boengler et al. 2006; Saez, Schalper et al. 2010; Kar, Batra et al. 2012). Connexins are ubiquitously expressed throughout a body and thus the role they play in the wellbeing of a cell is tissue-specific (Figure 1.2).

There are 21 different types of connexins expressed in a human body and five of them are expressed in the heart (Cx43, Cx40, Cx45, Cx30.2, Cx37) (Sohl and Willecke 2004). Ventricular cardiomyocytes express connexin43, whereas atrial cells also express connexin40 (Severs, Bruce et al. 2008). Connexins 40, 45, and 30.2 are connexins of conduction tissue (Kreuzberg, Sohl et al. 2005). Cx40, Cx43 and Cx37 are expressed in the cardiac vasculature (Pfenniger, Derouette et al. 2010). Each connexin molecule consists of four transmembrane domains, two extracellular loops, one cytoplasmic loop, and cytoplasmic amino- and carboxy-terminals. The regulation of gap junction- mediated intercellular coupling occurs via interaction of connexins43 with various binding partners or post-translational modifications at mainly, but not only, carboxy-terminus (Herve, Bourmeyster et al. 2007; Colussi, Rosati et al. 2011).

One of the key binding partners of connexin43 is a membrane-associated guanylate kinase (MAGUK) family protein zonula occludens (ZO-1). ZO-1 is a PDZ- containing protein that binds connexin43 and modifies growth of gap junction plaques (Giepmans and Moolenaar 1998; Toyofuku, Yabuki et al. 1998; Toyofuku, Akamatsu et al. 2001). Connexin43 has been shown to directly bind to the second-PDZ domain of ZO-1 and this interaction is regulated by Src-tyrosine- mediated phosphorylation of Cx43 (Toyofuku, Akamatsu et al. 2001). The inhibition of Cx43-ZO-1 interaction leads to the increase of the gap junction plaque size and redistribution of

nonjunctional connexons to the existent plaque whereas overexpression of ZO-1 results in smaller plaques (Hunter, Barker et al. 2005; Rhett, Jourdan et al. 2011). These findings led to the idea that by binding to the periphery of gap junction plaque, ZO-1 regulates the rate of plaque accretion. Duolink, is a novel technology, that allows validating the subcellular Cx43 - ZO-1 interaction through the interaction-dependent (<40nm) fluorescent signal (Rhett, Jourdan et al. 2011). Rhett et al demonstrated that gap junction plaque is surrounded by ZO-1 interacting with connexons and this region is called *perinexus*. The disruption of the interactions within the perinexus leads to the increase of the connexons docking to the gap junction plaque and increase of coupling between the adjacent cells (Rhett, Jourdan et al. 2011). In the patients with the end-stage congestive heart failure, the interaction of Cx43 and ZO-1 was shown to be altered (Bruce, Rothery et al. 2008). In these hearts, the expression of ZO-1 was significantly increased; whereas the total expression of Cx43 was decreased when compared to control. However, the fraction of Cx43 that interacts with ZO-1 was significantly higher in the diseased heart (Bruce, Rothery et al. 2008).

A recently discovered atypical role of connexin43 is of particular interest as it may provide an insight on the mechanism of cross-talk between connexin43 and other residents of the intercalated disc. In the mouse embryonic fibroblasts, connexin43 was shown to regulate microtubule dynamics (Francis, Xu et al. 2011). From the previous studies, connexin43 is known to directly bind tubulin at 234-243 residues of the carboxy terminus (Giepmans, Verlaan et al. 2001; Giepmans, Verlaan et al. 2001). It came as a surprise, however, that the loss of connexin43 leads to a significant reduction of stabilized detyrosinated tubulin (Francis, Xu et al. 2011). Detyrosinated tubulin is a result of the removal of tyrosine from the carboxy terminus of α-tubulin by an unknown carboxypeptidase (yielding glu-tubulin) (Webster, Gundersen et al. 1987; Hammond, Cai et al. 2008). Coincidently, glu-tubulin is the most abundant post-translationally modified tubulin in the healthy ventricular cardiomyocytes (Belmadani, Pous et al. 2004). Some motor proteins (i.e. Kinesin-1) actually have preferential binding to detyrosinated as opposed to tyrosinated tubulin (Liao and Gundersen 1998). It was not, however, a gap junction-mediated communication that regulated stabilization of microtubules, since the communication-deficient mutants of connexin43 were able to maintain the microtubule stability.

Francis et al suggested that connexin43 tethers microtubules to the cell membrane through its tubulin-binding domain(Francis, Xu et al. 2011).

c. Mechanical Junctions: Desmosomes

Desmosomes are disk-shaped intercellular adhesion junctions usually found in the cells undergoing mechanical stress, and in the myocardium they insure the distribution of the force among the cardiac cells. Desmosomes are composed of the proteins encoded by three family of genes: cadherins, armadillo proteins and plakins (Huber 2003; Getsios, Huen et al. 2004; Al-Amoudi and Frangakis 2008; Delmar and McKenna 2010). Desmocollin and desmoglein are the desmosomal cadherins which provide calcium-dependent hemophilic or heterophilic extracellular interactions (Al-Amoudi and Frangakis 2008). Through its intracellular domain, desmosomal cadherin interact with armadillo proteins, plakophilin and plakoglobin (also known as γ-catenin). Interestingly, plakoglobin is the protein that is present in both desmosomes and adherens junctions (Cowin, Kapprell et al. 1986). In the heart, γ-catenin binds to a desmoplakin, a plakin family protein, which in turn binds to the desmin, intermediate filaments of the heart (Figure1.3A). The electron microscopy reveals the intracellular part of desmomes as electron-dense plaque consisting of outer or inner elements based on its relation to the membrane (Figure 1.3B) (North, Bardsley et al. 1999; Al-Amoudi and Frangakis 2008). Diseases linked to the mutations of every desmosomal protein have been reported making the importance of these junctions self-evident (Figure 1.3C) (Delmar and McKenna 2010).

d. Mechanical Junctions: Adherens Junctions

Adherens junctions is another type of mechanical junctions that provides the transmission of the force from one cell to another during contraction of the heart. N-cadherin is a type of classical cadherins expressed in adherens junctions of cardiomyocytes. Unlike desmosomal cadherins, classical cadherins form only calcium-dependent homophilic interactions (Tepass, Truong et al. 2000). N-cadherin also has a single transmembrane domain and a highly conserved cytoplasmic domain which interacts with a family of cytoplasmic proteins, catenins. N-cadherin binds to β- or γ-catenin which in turn bind to α-catenin (Meng and Takeichi, 2009). α-catenin, then binds to actin filaments. By binding to the sarcomeric actin, adherens junctions directly link contractile apparatus of the neighboring cells together.

Cell-to-cell adhesion is not the only role of β-catenin. A portion of β-catenin is not assembled into adherens junctions but resides in the nucleus and participates in Wnt signaling transduction pathway as a transcriptional activator. Structurally, plakoglobin is very homologous to β-catenin and may compete for the binding site. In the normal heart, the majority of the plakoglobin is assembled into the adherens junctions or desmosomes. However, when the structure of desmosomes is compromised, plakoglobin is "cut loose" and accumulates in the nucleus resulting in the suppression of Wnt/β-catenin signaling pathway (Garcia-Gras, Lombardi et al. 2006; Lombardi, Dong et al. 2009).

e. Voltage-Gated Sodium Channel (VGSC)

Voltage-gated sodium channels (VGSC) carry sodium current (I_{Na}) and are essential for excitability in neurons, cardiac myocytes, and skeletal muscles as they regulate the rapid upstroke of the action potential (Catterall 1992; Cannon 1996; Escayg, MacDonald et al. 2000; Dhar Malhotra, Chen et al. 2001; Lossin, Wang et al. 2002; Papadatos, Wallerstein et al. 2002; Yu, Yarov-Yarovoy et al. 2005; Patino, Claes et al. 2009). VGSCs form macromolecular complexes which include at least one α-subunit and one β-subunit (Catterall 1992). $Na_V1.5$ is the predominant isoform of α-subunit expressed in the heart and is encoded by *SCN5A* gene. In the heart, $Na_V1.5$ is localized at the intercalated disc as well as T-tubules. The localization affects the function properties of the channel (Cohen 1996; Scriven, Dan et al. 2000; Kucera, Rohr et al. 2002; Lin, Liu et al. 2011). In his recent work (Lin, Liu et al. 2011) used the cell-attached macropatch technique to demonstrate that the amplitude and the gating properties of the sodium current differ between the channels localized at the intercalated disc and those of the lateral membrane. It was shown that the amplitude of I_{Na} is significantly higher at the intercalated disc and it depends on the preservation of the cell-cell contact. $Na_V1.5$ carries tetrodoxin (TTX)-resistant sodium current. Alpha subunits which carry TTX-sensitive current ($Na_V1.1$, $Na_V1.3$, and $Na_V1.6$) are also expressed in the heart and their location is restricted to T-tubules (Maier, Westenbroek et al. 2002). All five isoforms of β-subunit (β1, β1B, β2, β3, β4) are expressed in the heart and encoded by *SCN1B-SCN4B (*Brackenbury and Isom 2011*).*

Just like gap junctions, VGSC do not reside at the membrane as isolated molecules but interact with the binding partners forming macromolecular complexes. (Meadows and Isom

2005). $Na_V1.5$ interacts with syntrophin, an adaptor protein that forms a macromolecular complex with dystrophin, an actin binding protein (Peters, Adams et al. 1997; Gee, Madhavan et al. 1998; Gavillet, Rougier et al. 2006). Multiple interactions were reported between syntrophins and $Na_V1.5$ in non-cardiac cells, and the interaction between C-terminus of $Na_V1.5$ and PDZ domain of γ2- syntrophin in the intestinal smooth muscle cells is thought to be involved in mechanosensitivity (Gee, Madhavan et al. 1998; Ou, Strege et al. 2003). In cardiac cells, the PDZ-binding domain of Nav1.5 (SIV), consisting of the last three residues of the C-terminus (2014-Ser-Ile-Val-2016), interacts with the syntrophin –dystrophin complex (Gavillet, Rougier et al. 2006). Studies of the mouse model of Duchenne muscular dystrophy, dystrophin- deficient (mdx^{5cv}) animal, demonstrated the decrease in the expression of $Na_V1.5$ as well as decrease in I_{Na} (Gavillet, Rougier et al. 2006). Despite of its obvious importance in the localization and function of $Na_V1.5$ neither dystrophin nor syntrophin are present at the intercalated disc, but rather at the lateral membrane of cardiomyocytes (Kaprielian, Stevenson et al. 2000; Stevenson, Cullen et al. 2005). Mdx hearts had a reduced velocity of action potential propagation when compared to the control hearts. The cells from mdx hearts had decrease of immunoreactive $Na_V1.5$ at the lateral membrane. On the other hand, SAP97, another PDZ domain protein, is a member of membrane associated guanylate kinases (MAGUK) family that is localized at the intercalated disc. Pull-down assay had demonstrated the interaction between SAP97 and $Na_V1.5$, and that this interaction is not global for all MAGUK proteins since no interaction of $Na_V1.5$ and ZO-1 was detected. Silencing of SAP97 caused decrease of surface expression of $Na_V1.5$ in HEK293 cells and decrease of I_{Na} in HEK293 and cardiomyocytes (Petitprez, Zmoos et al. 2011). These studies revealed two pools of cardiac $Na_V1.5$.

Ankyrins belong to a family of adaptor proteins participating in the targeting of the membrane proteins. There are two types of ankyrins expressed in the heart: ankyrin-G and ankyrin-B (Mohler, Rivolta et al. 2004; Bennett and Healy 2009). Only ankyrin-G is located at the intercalated disc and T-tubules and interacts with $Na_V1.5$ (Mohler, Rivolta et al. 2004). This interaction is essential for the function of the channel. Loss of ankyrin-G leads to the decrease of $Na_V1.5$ expression in the cell and the localization of the protein on the membrane (Lowe, Palygin et al. 2008). This change in the expression is directly linked to the function of the channel resulting in the significant decrease of amplitude of I_{Na}. The disruption of ankyrin-G - $Na_V1.5$

interaction due to the mutation in the ankyrin-G binding motif of $Na_V1.5$ (E1053K) results in a human Brugada Syndrome (Mohler, Rivolta et al. 2004).

Besides syntrophin, ankyrin-G and SAP97, other proteins were shown to interact with $Na_V1.5$. Some of them are: calmodulin, protein tyrosine phosphatase H1 (PTPH1), 14-3-3η, nedd-4-like enzyme, and MOG1(Tan, Kupershmidt et al. 2002; van Bemmelen, Rougier et al. 2004; Allouis, Le Bouffant et al. 2006; Jespersen, Gavillet et al. 2006; Wu, Yong et al. 2008) (Figure 1.4). Localization and function of $Na_V1.5$ is also regulated through post-translational modifications: phosphorylation and glycosylation (Frohnwieser, Chen et al. 1997; Watson and Gold 1997; Zhou, Yi et al. 2000; Zhou, Shin et al. 2002; Hallaq, Yang et al. 2006; Montpetit, Stocker et al. 2009).

f. Cross-talk Among the Residents of the Intercalated Disc

For a long time proteins of mechanical junctions, gap junctions and ion channel complexes had been thought of to exist as separate entities. Close examination of the diseased phenotypes frequently links the disturbances and alterations in the expression and/or function of these complexes together. Today, a body of evidence demonstrating the interactions between the proteins of these complexes suggests the idea that residents of the intercalated disc in fact function as one macromolecular complex (Delmar 2012; Delmar and Liang 2012).

The first knowledge that localization of Cx43 at the intercalated disc depends on the desmosomal integrity came from the study of a patient with Naxos disease caused by the plakoglobin mutation (McKoy, Protonotarios et al. 2000; Kaplan, Gard et al. 2004). Just like other forms of arrhythmogenic right ventricular cardiomyopathy (ARVC), Naxos disease manifests itself through the high prevalence of lethal arrhythmias and sudden cardiac death. The study showed that hearts with mutated plakoglobin had severe reduction of gap junction plaques at the intercalated disc (Kaplan, Gard et al. 2004). The body of evidence confirming the importance of desmosomal proteins for the preservation of gap junction- mediated electrical coupling has grown with the number of mutations that were discovered in all the rest of the desmosomal proteins: desmoglein-2, desmocollin-2, plakophilin-2, and desmoplakin (Rampazzo, Nava et al. 2002; Gerull, Heuser et al. 2004; Pilichou, Nava et al. 2006; Syrris, Ward et al. 2006; Delmar and McKenna 2010). Moreover, the role of desmosomes in the

formation, maintenance and function of gap junctions was confirmed by the study of loss of plakophilin-2 in cells in culture. The loss of the protein led to the decrease in connexin43 expression, redistribution of the protein from the cell-cell contact to the intracellular space, and decrease of gap junction- mediated coupling between cardiac myocytes (Oxford, Musa et al. 2007). It comes as no surprise that ARVC is known as a disease of the "cardiac desmosomes" (Rizzo, Pilichou et al. 2012).

Loss of adherens junctions results in remodeling of connexin43 and thus creates an arrhythmogenic substrate. The cardiac-specific tamoxifen-induced N-cadherin knockout mouse has a high prevalence of sudden death occurrence within 50 days of tamoxifen administration (Li, Patel et al. 2005). The death was preceded with a dramatic change in the electrocardiographic recordings. The optical mapping studies revealed significant reduction of conduction velocity and loss of gap junction electrical coupling. These animals had a severe decrease in the expression of both connexin43 and connexin40. The model became a great tool demonstrating the importance of adherens junctions for the maintenance of connexin43 at the intercalated disc and the detrimental implications the loss of N-cadherin has on the function of the heart.

Originally viewed as completely segregated structures, desmosomes and adherens junctions are frequently found to be mixed together forming the *"*area composita" (Figure 1.5A). The ability of desmosomal protein, plakophilin-2, to interact with αT-catenin, a member of N-cadherin-catenin adhesion complex, in the cardiomyocytes allows for the formation of these "hybrid junctions" (Chen, Bonne et al. 2002; Goossens, Janssens et al. 2007; Bass-Zubek, Godsel et al. 2009). Recent studies show that loss of αT-catenin in the heart leads to a selective loss of plakophilin-2 from the area composita (Li, Goossens et al. 2012). The importance of plakophilin-2 for the localization of connexin43 explains why αT-catenin knockout animals have decreased expression of connexin43 at the intercalated disc, the latter facilitating ischemia-induced arrhythmogenesis.

The functional interactions between desmosomal protein plakophilin-2 and $Na_V1.5$ have been demonstrated by studying protein-protein interactions between these proteins. GST-pull down assay showed that plakophilin-2 pulls down $Na_V1.5$ (Sato, Musa et al. 2009). Furthermore, the

loss of plakophilin-2 in neonatal rat ventricular myocytes led to a significant decrease in the I_{Na} density and gating properties of the current. Changes in the sodium current and previously demonstrated decrease in electrical coupling resulted in slowing of conduction in the plakophilin-2 -deficient cells (Oxford, Musa et al. 2007; Sato, Musa et al. 2009). Furthermore, the co-immunoprecipitation studies revealed that $Na_V1.5$ - interacting partner, ankyring-G, also interacts with plakophilin-2 and connexin43 in the heart (Figure 1.5B). The immunocytochemical analysis revealed that ankyrin-G and plakophilin-2 reciprocally regulate each other's localization. Loss of either plakophilin-2 or ankyrin-G leads to redistribution of $Na_V1.5$ and reduction of amplitude of I_{Na} (Lowe, Palygin et al. 2008; Sato, Coombs et al. 2011).

Loss of connexin43 and $Na_V1.5$ are common phenotypes of various heart conditions which manifest themselves through arrhythmias. It was not until recently that connexin43 has been implicated in the regulation of $Na_V1.5$ expression at the membrane (Borlak and Thum 2003; Valdivia, Chu et al. 2005). Study of the hearts from genetically-modified animals which had induced reduction of connexin43 showed that only a number of the analyzed hearts was susceptible to the arrhythmias (Jansen, Noorman et al. 2012). The analysis of the arrhythmogenic hearts revealed significantly reduced immunoreactive signal of connexin43 together with $Na_V1.5$ comparing to the changes occurring in non-arrthmogenic animals. The same study demonstrated that in isolated rat cardiomyocytes silenced for connexin43 sodium current was significant reduced comparing to control. That finding confirmed the importance of connexin43 protein for the expression and function of $Na_V1.5$. The mechanism by which connexin43 may regulate $Na_V1.5$ function remains to be determined.

2. Trafficking of Connexin43

Connexin43 is a highly dynamic molecule with a half-life ranging from only 1 to 5 hours (Beardslee, Laing et al. 1998; Shaw, Fay et al. 2007). The localization of connexin43 at the intercalated disc at any given point comes from the balance of anterograde trafficking, lateral diffusion, and retrograde trafficking (Figure 1.6) (Smyth and Shaw 2012).

The majority of connexin43 turnover processes occur after the protein has been assembled into a connexon. The ability of connexin43 to be solubilized in 1% Triton X-100 reflects its subcellular localization. The newly synthesized intracellular connexin43 is soluble in this

detergent whereas the protein incorporated into a gap junction plaque is not (Musil and Goodenough 1991). Sucrose gradient velocity sedimentation technique allows for the separation of proteins based on molecular mass and shape. The combination of sucrose gradient sendimentation and cross-linking techniques demonstrated that assembly of connexin43 into a connexon occurs inside of the cell as opposed to assembly at the plasma membrane (Musil and Goodenough 1993).

To further pinpoint the location of connexon assembly the method of blocking endoplasmic reticulum-to-Golgi apparatus trafficking is frequently used. Such blocking in NRK cells resulted in a complete block of connexon assembly leading to a conclusion that connexin43 assembles into a connexon inside the Golgi apparatus, and most likely upon its exit from trans- Golgi network (TGN) (Musil and Goodenough 1993). It is worth mentioning that connexin43 is delivered to the plasma membrane in a non-phosphorylated form. The fact that Triton X- 100 insoluble fraction of connexin43 is phosphorylated points to the idea that assembly of connexons into an intercellular channel occurs concomitantly with phosphorylation of conneixn43 molecule (Musil and Goodenough 1991).

Microtubules are essential for the delivery of connexin43 to the plasma. The formation of gap junction plaques at cell-cell contact is highly dependent on the microtubules and was disturbed by the treatment of cells with a microtubule-depolymerizing agent, nocodazole (Shaw, Fay et al. 2007). Surprisingly, treatment with taxol, a microtubule- stabilizing agent, had also led to a decrease in a number of connexin43 plaques at the border (Shaw, Fay et al. 2007). It is important to note that taxol acts by binding to the β-tubulin subunit of microtubule and prevents normal dynamic GTP-dependent exchange of α/β-tubulin heterodimer at the growing plus end of microtubules. It makes microtubules stable, rigid and resistant to Ca^{2+} and cold temperature – induced depolymerization (Xiao, Verdier-Pinard et al. 2006). The functional differences between taxol-stabilized microtubules and physiologically stable microtubules found in a cell during a normal cycle are not clear.

Being a very dynamic structure, microtubules undergo constant polymerization and depolymerization which are also referred to as growth and catastrophe. The microtubule plus end is a growing end and thus is highly unstable whereas the minus end is attached to the

microtubule organizing center (MTOC) and is far more stable. The dynamics of the plus end are controlled by the plus-end tracking proteins (+TIPs) (Akhmanova and Hoogenraad 2005). In cardiomyocytes, the role of one +TIP, EB1, particularly strands out. Shaw et all suggested that EB1 through association with its binding partner p150 (Glued) participates in tethering of microtubules to adherens junctions (Shaw, Fay et al. 2007). The study demonstrated that by mutating EB1 or by inhibiting the expression of either EB1 itself or p150(Glued), the formation of gap junction plaque was disrupted (Shaw, Fay et al. 2007; Smyth, Hong et al. 2010). Furthermore, Smyth et al suggested that in the diseased heart the oxidative stress displaces EB1 off of the microtubule plus end, resulting in a less microtubules being tethered to the plasma membrane (Smyth, Hong et al. 2010). Smyth et al offered a model entailing that the oxidative stress-mediated decrease in microtubule dynamics leads to a decreased anterograde trafficking of connexin43. This model offers an explanation for why in an ischemic heart the decrease of Triton X-100 insoluble (junctional) connexin43 is accompanied by the loss of immunoreactive EB1 signal from the intercalated disc.

There are two possibilities for connexin43 gap junction plaque to form and grow - connexin43 can be directly targeted from inside of the cell to the plaque or the plaque can also grow by accretion of connexon molecules. The photo-bleaching study in conjunction with inhibition of ER-Golgi trafficking revealed that, until depleted, connexon molecules will laterally diffuse to the gap junction plaque from nonjunctional membrane (Lauf, Giepmans et al. 2002). The extent of this accretion is most likely regulated by ZO-1 (Hunter, Barker et al. 2005; Rhett, Jourdan et al. 2011).

Kinesins are motor proteins participating in the anterograde trafficking of the membrane proteins. Fort et al had demonstrated that kinesin delivers connexin32 to the basolateral-membrane of hepatocytes (Fort, Murray et al. 2011). Live-cell imaging of a fluorescently-tagged protein allowed the detection of the movement of connexin32 vesicles with an average speed of 0.25μm/sec. The movement was accelerated up to 0.4-0.5 μm/sec once the 50μM ATP was added. The recent study by Chkourko et al alludes to Kinesin-1 as a potential motor protein participating in delivery of connexin43 to the intercalated disc in the normal heart (Chkourko, Guerrero-Serna et al. 2012).

Microtubules are not the only trafficking pathways for the anterograde trafficking of connexin43, filamentous actin is also involved. The abundance of intracellular vesicles that are either stationary or move very slowly (0.09 μm/sec) led to the suspicion that microtubule-mediated trafficking may not be the only way for connexin43 to get to the membrane. Treatment with an actin-disrupting agent, Latrinculin A, led to the disruption of connexin43 trafficking (Smyth, Vogan et al. 2012). This inhibition of actin-mediated trafficking of connexin43 is reminiscent of the ischemia-induced disruption of connexin43-actin interaction. Smyth et al suggested that actin plays an important role in forward trafficking of connexin43 serving in a sense as a "depot" by allowing vesicles to "pause and rest" before being re-railed to the microtubules and speeding up to the membrane (Smyth, Vogan et al. 2012).

Due to its rapid turnover of connexin43, the role of internalization and retrograde trafficking are important for degradation and recycling. While new connexons are added to the plaque sidewise, the old connexons get removed/endocytosed from the center of a plaque (Gaietta, Deerinck et al. 2002; Lauf, Giepmans et al. 2002). Internalization can occur either through endocytosis of uncoupled connexons or by internalizing the whole plaque including the membranes of adjacent cells into one (Smyth and Shaw 2012). The latter internalization will result in the formation of a structure called "annular gap junctions" (AGJ) (Jordan, Chodock et al. 2001; Laird 2006). AGJ were shown to be processed through autophagic pathway of degradation (Hesketh, Shah et al. 2010).

There are several options for connexin43 to be degraded. Prior to being internalized, Connexin43 undergoes ubiqutination. Hyperphosphorylation of connexin43 has been shown to occur concurrently with ubiquitination and internalization which suggests that phosphorylation regulates endocytosis (Leithe and Rivedal 2004). The monoubiquitination and degradation of connexin43 was triggered by activating protein kinase C (PKC) (Leithe and Rivedal 2004). The PY motif of connexin43 was shown to bind E3 ubiquitin ligase Nedd4 (Leykauf, Salek et al. 2006). The ubiquitination may follow by proteosomal and/or lysosomal degradation (Laing and Beyer 1995; Laing, Tadros et al. 1997; Qin, Shao et al. 2003; Fernandes, Girao et al. 2004; Leithe and Rivedal 2004). Although recycling of connexin43 was reported in the cells undergoing mitosis, no evidence of recycling have been reported in cardiomyocytes (Boassa, Solan et al. 2010).

Despite of this extensive knowledge of the connexin43 life cycle, many questions remain regarding the molecular machinery participating in the trafficking of connexin43 in the cardiac myocytes.

3. Trafficking of $Na_V1.5$

Trafficking of $Na_V1.5$ is heavily dependent on the post-translational modifications and interactions with its binding proteins (Hallaq, Yang et al. 2006). Reportedly, β-adrenergic stimulation increases the delivery of $Na_V1.5$ at the cell membrane (Schreibmayer, Frohnwieser et al. 1994; Frohnwieser, Chen et al. 1997; Lu, Lee et al. 1999; Schreibmayer 1999). One of the mechanisms of this stimulation is through the masking of RXR-type ER retention motif of $Na_V1.5$ (Zhou, Shin et al. 2002). Generally, the ER retention motif prevents a protein exit from ER in a chaperon-dependent manner. β-adrenergic stimulation leads to the PKA phosphorylation of the retention motif resulting in release of $Na_V1.5$ from the intracellular compartment. Moreover, the binding partners that were mentioned earlier (plakophilin-2, ankyrin-G, syntrophin, SAP97) also play an important role in the delivery and/or maintenance of $Na_V1.5$ at the membrane.

Cytoskeleton plays an essential role in the delivery of $Na_V1.5$ to the membrane. Disruption of F-actin polymerization by cytochalasin D decreases the open probability state of the channel and thus reduces a cell peak current in ventricular cardiomyocytes (Undrovinas, Shander et al. 1995). It also slows the inactivation of sodium current resulting in the increase of the persistent activity (Undrovinas, Shander et al. 1995; Maltsev and Undrovinas 1997). The microtubule manipulations were done with taxol. Taxol is a drug that has been used for treatment of a broad range of cancers and it is a tubulin-stabilizing agent. Unfortunately, administration of this drug to the patients was reportedly associated with cardiac toxicity manifesting itself as arrhythmias (transient asymptomatic bradycardia, tachyarrhythmias, atrioventricular and bundle branch blocks) as well as cardiac ischemia (Rowinsky, McGuire et al. 1991; Rowinsky and Donehower 1995). Bradyarrythmia as well as atrioventricular and bundle branch block are types of cardiac disturbances that can be attributed to the alterations of $I_{Na.}$ Moreover, *in vitro* measurements of I_{Na} in HEK293 cells expressing only $Na_V1.5$ or $Na_V1.5$ together with β_1-subunit protein and treated with Taxol had shown 50% decrease in the amplitude of the current (Casini, Tan et al.

2010). Immunocytochemistry analysis also revealed taxol-mediated decrease of membrane labeling of $Na_V1.5$ and increase in intracellular staining. Unlike in the cells expressing $Na_V1.5$ only, the treatment with taxol did not completely abolish membrane $Na_V1.5$ in the cells expressing both subunits suggesting that β_1-subunit increases amplitude of the I_{Na} by increasing the membrane expression of the channel. The discrepancy however emerges when the contribution of β1 subunit in HEK293 system is compared to the data gathered from the cardiomyocytes. Lopez-Santiago et al had demonstrated that beta 1 knockout (*Scn1b* null) mice had 33% increase in the expression of $Na_V1.5$ protein and 50% increase in I_{Na} (Lopez-Santiago, Meadows et al. 2007). Although these findings implicate actin and microtubules in the forward trafficking of $Na_V1.5$, the complete molecular machinery may differ in the heart when compared to the heterologous system.

Although Casini and et al clearly demonstrated the importance of microtubules for the membrane expression of $Na_V1.5$ the interaction of the α-subunit with tubulin directly or through the binding partners has yet to be shown(Casini, Tan et al. 2007). Impairment of anchoring the protein to the membrane may also result in the aberrations of $Na_V1.5$ localization. Membrane expression of $Na_V1.5$ has been shown to be highly dependent on ankyrin-G (Mohler, Rivolta et al. 2004). The importance of ankyrin-G for the membrane expression of $Na_V1.5$ became apparent after deciphering the localization of human E1053K mutation of $Na_V1.5$. This mutation is associated with Brugada Syndrome, a cardiomyopathy that manifests itself through incomplete right bundle branch block and high risk of sudden cardiac death (Priori, Napolitano et al. 2002). E1053K is a mutation located in loop 2 of $Na_V1.5$ and is at the ankyrin-binding domain. Immunohistochemistry analysis of the adult cardiomyocytes expressing HA-tagged E1053K mutant protein showed the absence of the protein from the membrane surfaces of the intercalated disc and T-tubule regions. The surprising twist came when the expression of the same mutation in HEK293 cells did not prevent targeting of the protein to the membrane surface but did affect gating properties of I_{Na}. This finding led to the speculation that heart had evolved a more specialized targeting machinery for $Na_V1.5$ (Mohler, Rivolta et al. 2004). Ankyrin -G belongs to the family of cytoskeleton-anchoring proteins members of which are known to directly bind to tubulin (Davis and Bennett 1984). It is unclear whether ankyrin-G binds tubulin and if it does whether it participates in anterograde trafficking itself.

Various interacting partners were demonstrated to regulate the membrane expression of $Na_V1.5$, but the precise mechanism of this regulation as well as the molecular machinery of $Na_V1.5$ trafficking remain to be elucidated.

4. Remodeling

Alterations in the expression and distribution of connexin43 gap junctions are associated with the changes in the conducting properties of the heart and are linked to a number of heart diseases (Peters, Green et al. 1995; Peters, Coromilas et al. 1997; De Mello 1999; Akar, Spragg et al. 2004; Severs, Bruce et al. 2008). These alterations are known as remodeling. There are three aspects to remodeling that can occur at the different stages of the disease progression. The first aspect is the loss of total connexin43 and/or the loss of connexin43 from the intercalated disc. The second aspect is the change in the phosphorylation state of connexin43. It has been widely reported that pathological conditions lead to the loss of phosphorylated Cx43 and increase in the abundance of dephosphorylated form. The third aspect is the change in the localization of connexin43 from its normal location at the intercalated disc to the lateral membrane.

The level of the decrease of connexin43 that causes the detrimental effect on the function of the heart varies from species to species. Gutstein et al showed that in the cardiac specific connexin43 knockout mice, for the arrhythmogenesis to manifest itself, the loss of total Cx43 has to reach the level of almost 90% (Gutstein, Morley et al. 2001). Although Morley et al showed that a 50% loss of connexin43 does not alter cardiac conduction, the connexin43 heterozygous mice are nonetheless more susceptible to the ischemia-associated ventricular arrhythmogenesis that control animals (Morley, Vaidya et al. 1999; Lerner, Yamada et al. 2000). The diseased human heart exhibits arrhythmias with the reduction of only 50% (Severs, Coppen et al. 2004). The decrease in protein expression is often accompanied by the reduction of the connexin43 mRNA as well (Dupont, Matsushita et al. 2001). These alterations in the expression level are not only associated with the end-stage heart failure but other heart diseases such as myocarditis, idiopathic dilated cardiomyopathy, hypertrophic heart and congestive heart failure (Peters, Green et al. 1993; Dupont, Matsushita et al. 2001; Kostin, Rieger et al. 2003). It is predicted that the expression of the total connexin43 affects the gap junction mediated coupling. It is, however, not the only factor leading to arrhythmogenesis. The heterogeneity of connexin43 expression

throughout myocardium is assumed to be the leading arrhythmia-induced factor. The heart failure model of a dog generated by the rapid pacing led to the decreased connexin43 expression in the endocardial and epicardial levels making the expression almost the same in both layers; whereas in the normal heart connexin43 expression is significantly higher in the epicardium (Akar, Spragg et al. 2004). Heterogeneity of gap junction expression may create differences in the resting potential throughout the myocardium, affecting excitability, refractoriness and homogeneity of action potential propagation (Severs, Dupont et al. 2004). The detrimental effect of heterogeneity of gap junctions expression was demonstrated by Gutstein et al on the chimeric mice that had "patchy" expression of connexin43 (Gutstein, Morley et al. 2001). The connexin43-deficient mice that had homogeneous loss of connexin43 exhibited overall slowing of the conduction velocity. The chimeric mice, however, exhibited significant disturbances in the conduction as demonstrated by optical mapping. Moreover, echocardiography showed significant fractional shortening that results from disturbed contractile function of cardiomyocytes (Gutstein, Morley et al. 2001). Although the loss of Connexin43 is undoubtedly an important factor in the development of heart disease, the heterogeneity of the expression is far more important aspect of it.

Significant increase of connexin43 fraction that interacts with ZO-1 in the hearts with idiopathic dilated or ischemic cardiomyopathy implicates ZO-1 to the mechanism of remodeling (Bruce, Rothery et al. 2008). The ubiquitous expression of ZO-1 in the cell of different type led to the erroneous belief that ZO-1 is expressed in the lateral membrane of cardiomyocytes (Gutstein, Liu et al. 2003; Li, Patel et al. 2005). However, co-labeling of ZO-1 with CD31, an endothelial marker, enabled Bruce et al to decipher the specific localization of ZO-1 (Bruce, Rothery et al. 2008). Bruce et al concluded that that ZO-1 localizes only at the intercalated disc in the control and diseased heart. Due to its role as a regulator of the size of connexin43 plaque, increase in ZO-1 and connexin43 interaction may lead to the decrease in the size of connexin43 plaque and gap junction mediated coupling.

Phosphorylation is known to affect the function of connexin43 and therefore the disease-associated changes in the phosphorylation state of connexin43 contribute to the generation of arrhythmogenic substrate (Moreno, Saez et al. 1994; Beardslee, Laing et al. 1998; Sasano, Honjo et al. 2007; Procida, Jorgensen et al. 2009). The normal heart maintains the majority of the

connexin43 in the phosphorylated state. The progressive accumulation of dephosphorylated connexin43 accompanied by the loss of phosphorylated protein was observed over the course of the induced acute ischemia in a rat heart (Beardslee, Lerner et al. 2000). The canine heart failure (non-ischemic) model of a dog had also demonstrated abnormal abundance of hypophosphorylated Cx43 (Akar, Spragg et al. 2004). Western blot demonstrated a shift in the migration of connexin43 bands from 46 (P2) and 44kDa (P1) to the 41kDa (P0). Besides the accumulation at the intercalated disc, the dephosphorylated Cx43 was also shown to be accumulating to the lateral membrane in the injured heart (Matsushita, Kurihara et al. 2006). The suggested mechanism for ischemia-induced dephosphorylation is decrease of intracellular ATP and thus "the inhibition of thermodynamic driving force for ATP-dependent phosphorylation" (Beardslee, Lerner et al. 2000).

A direct link between susceptibility to remodeling and phosphorylation of connexin43 came from a recent study on connexin43 phosphomutant mice. Serines 325/328/330 are known to be targeting sites for connexin43 phosphorylation by casein kinase (CK1δ) (Cooper and Lampe 2002; Lampe, Cooper et al. 2006). The knockin mice (S3E) carrying phosphatase-resistant phosphomimetic glutamic acids at these three residues were resistant to the ischemia-mediated remodeling and developing an arrhythmogenic substrate (Remo, Qu et al. 2011). In the opposite, mice that had serines substituted for nonphosphorylatable alanines had a higher susceptibility to arrhythmogenesis.

The change in the subcellular localization of connexin43 gap junctions is the last and the most puzzling aspect of remodeling. The localization of Cx43 at the intercalated disk is essential for the preservation of the anisotropic flow of the current. With the lesser resistance along the long longitudinal direction of the cells the conduction is faster than in the transverse direction. Thus, neoformations of gap junctions at the lateral membrane can be a potential substrate for arrhythmogenesis. On the other hand, with the loss of the connexin43 at intercalated disc, lateralized gap junctions-mediated pathway for wave propagation may be the only option to the conduction block. The heart failure model of a dog demonstrated a two-fold increase in connexin43 that was lateralized and was not co-localized with N-cadherin (Akar, Spragg et al. 2004). The detailed information on the ultrastructure of remodeled Cx43 gap junctions comes from a later study of the same model (Hesketh, Shah et al. 2010). The study reported that in this

diseased model lateralized Cx43 did not colocalize with the adopter protein ZO-1. Transmission electron microscopy identified noticeable membrane bending at the areas where lateralized gap junctions were located. Furthermore, internalized gap junctions were identified in the form of multilamellar concentric rings which were reminiscent of the previously described annular gap junction (AGJs) formations, which resulted from the internalization of the entire gap junction plaque and included membranes from both cells (Jordan, Chodock et al. 2001; Piehl, Lehmann et al. 2007). The method of Triton X-100 extraction and sucrose density centrifugation allowed Hesketh et al to separate membrane into the dense fraction and a buoyant (detergent resistant) fraction which is also known to be a fraction rich in cholesterol and sphingolipid-rich membrane, named lipid rafts (Hesketh, Shah et al. 2010). Surprisingly, the lipid raft-rich fraction had predominantly slowly migrating form of Cx43 (P2) which under the treatment with alkaline phosphatase was mobilized faster (P1 and P0). The same fraction also had an autophagosomal marker, LC3, and was devoid of ZO-1 or mechanical junctions. The study indicated increased autophagosomal formation in the canine model of heart failure. Because the lipid raft-rich fraction from the heart failure samples had a 3.5 fold higher amount of Cx43 comparing to the same fraction from the normal heart whereas the total amount of Cx43 was two folds less in the heart failure. The authors offered an interesting conclusion suggesting that upon reaching the final hyperphosphorylation state, lateralized Cx43 enters lipid rafts and undergoes internalization by authophagy (Hesketh, Shah et al. 2010).

In the diseased heart different aspects of Cx43 remodeling occur sequentially and are associated with changes in the electrophysiological properties. The canine heart failure model had shown that expression of total Cx43 is the first occurring change (Akar, Nass et al. 2007). Change in the phosphorylation occurs gradually with almost two fold increase in dephosphorylated Cx43 at the late stage. The redistribution of Cx43 to the lateral membrane is the last occurring change and is the most highly correlate with the changes in the conduction velocity and even mechanical function measured by left ventricular end-dyastolic pressure parameter (Akar, Nass et al. 2007).

Despite the numerous studies of gap junction remodeling, the mechanism or remodeling remains unclear. It is not self-evident how connexin43 ends up to be localized at the lateral membrane. First, connexin43 trafficking can be redirected leading to the targeted delivery of

connexin43. Second, connexin43 is redistributed by lateral diffusion from intercalated disc to the lateral membrane.

5. Statement of Objectives

The intercalated disc serves as a harbor for the successful interactions and function of gap junctions, mechanical junctions and ion complexes. In the healthy heart, due to the physical proximity and/or high affinity direct or indirect binding between the proteins, very elaborate interactions of these proteins are formed. Thus, the proteins residing at the intercalated disc become a part of one macromolecular complex that acts as a precise mechanism to support the function of the heart. Although there are two different mechanical junctions at the intercalated disc, there is really no redundancy in function and a failure of one protein to perform can lead to the domino effect of the detrimental events as seen in the diseased heart.

Remodeling of gap junctions is a common phenotype of a vast spectrum of heart conditions. Subcellular redistribution of the gap junctions during remodeling is of a particular interest and has been well documented. It is not clear, however, whether redistribution of connexin43 occurs through the redirection of the forward trafficking or through the lateral diffusion of the nonjunctional connexons to the lateral membrane. My first objective is further characterization of the molecular machinery participating in the trafficking of connexin43, with particular attention to the mechanisms of connexin43 remodeling.

Unlike gap junctions, the fate of the other members of the macromolecular complex during remodeling is yet unknown. My second objective is to describe the morphological and functional changes that occur with the proteins of mechanical junctions and VGSC complex when gap junctions undergo remodeling. Hopefully, this will shed light on the question of whether other residents of intercalated disc share the similar mechanism of delivery. The question of whether redistribution of gap junctions to the lateral membrane is beneficiary or detrimental to the heart remains controversial. Perhaps revealing the fate of the other proteins may help to answer this question.

The localization and function of $Na_V1.5$ at the cell membrane was clearly shown to be regulated by each member of "the intercalated disc community." The cytoskeleton plays a crucial

role in that process, but there is little information on the molecular machinery participating in either anterograde or retrograde trafficking of $Na_V1.5$. Besides its typical role in the channel-dependent maintaining of electrical coupling, connexin43 just recently emerged as a regulator of microtubule stability. Importantly, some motor proteins have a preferential motility along stable microtubules versus dynamic ones (Cai, McEwen et al. 2009). Moreover, connexin43 was also shown to regulate the function and localization of $Na_V1.5$ at the membrane (Jansen, Noorman et al. 2012). My third objective is to elucidate whether maintaining of microtubule stability is the mechanism by which connexin43 mediates the function and membrane expression of $Na_V1.5$.

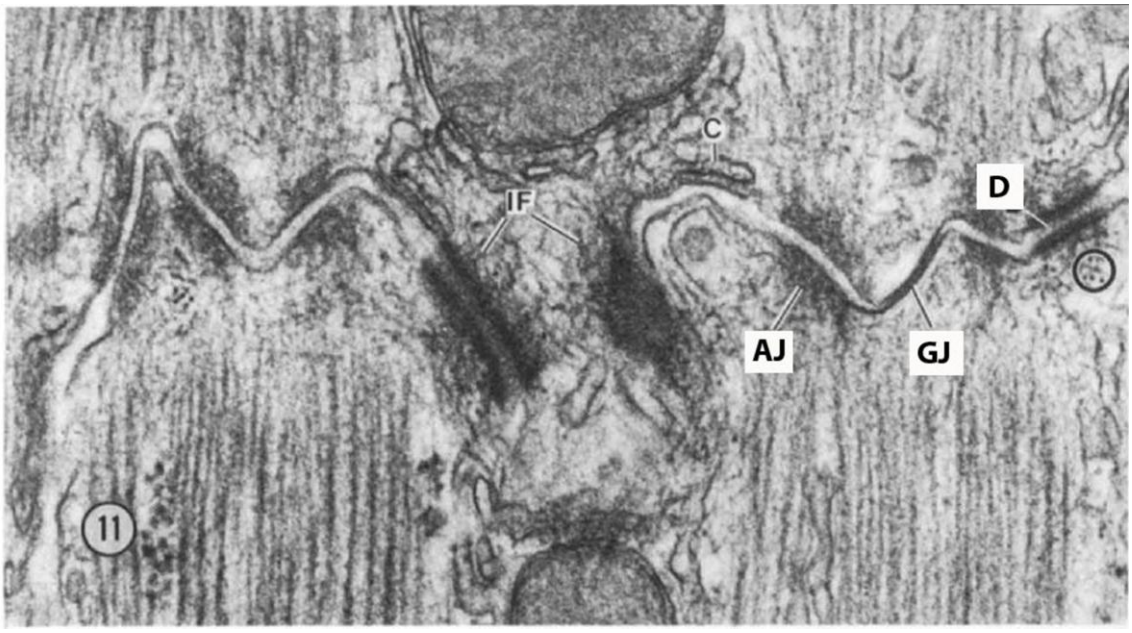

Figure 1.1 Electron micrograph of intercalated disc from a mouse right atrium. AJ – adherens junctions, GJ- gap junctions, D- desmosomes, IF- intermediate filaments. X75,000 Reprinted from Publication (Forbes and Sperelakis 1985) with permission from Elsevier, license # 2982030291756.

Connexin

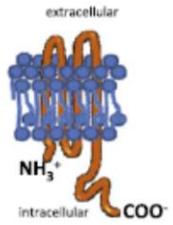

Role	Organ
Cell death	Brain, Inner ear, Kidney, Liver
Differentiation	Bone, Brain, Inner ear, Heart, Ovary, Lung, Liver
Proliferation/ survival	Brain, Bone, Heart, Lens, Ovary, Testis, Liver

Gap junction Channels

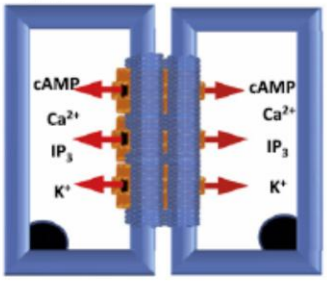

Role	Organ
Ionic conduction	Brain, Inner ear, Heart, Kidney, Lens, Lung, Liver
Metabolic coupling	Brain, Lens, Liver
2nd Messenger diffusion	Inner ear, Ovary, Lung, Liver

Hemichannels

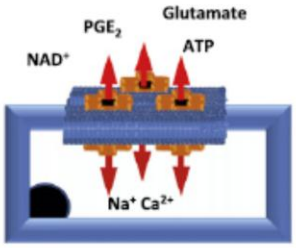

Role	Organ
Injury protection	Heart
preconditioning	Brain, Heart
Extracellular cell signaling	Bone, Brain, Kidney, Ovary, Lung, Liver
Mechanical stimulation response	Bone, Ovary

Figure 1.2 Illustration of the function of connexins as individual proteins, when assembled into a hemichannel (connexon) or as a channel in various organs. Reprinted from Publication (Kar, Batra et al. 2012) with permission from Elsevier, license # 2982031351174.

A

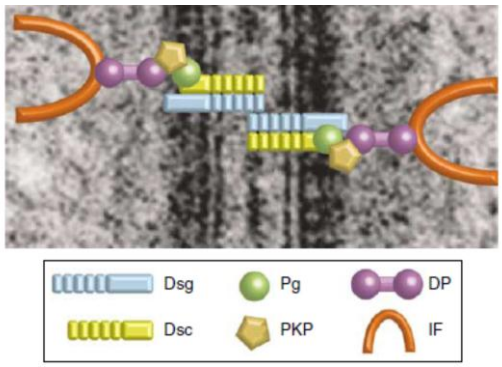

B

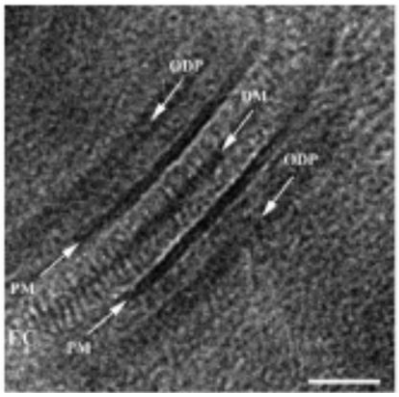

C

Table. Summary of Desmosomal Genes and Encoded Proteins Implicated in Inherited Human Disease

Gene Superfamily	Gene	Chromosomal Location	Encoded Protein	Mutation-Associated Phenotypes
Armadillo	*JUP*	17q21	Plakoglobin	Naxos disease (AR arrhythmogenic cardiomyopathy with PPK and woolly hair)
				AD arrhythmogenic cardiomyopathy
	PKP1	1q32	Plakophilin-1	Ectodermal dysplasia and skin fragility syndrome
	PKP2	12p11	Plakophilin-2	AD arrhythmogenic cardiomyopathy
				AR arrhythmogenic cardiomyopathy
Desmosomal cadherin	*DSG1*	18q12	Desmoglein-1	Striate PPK
	DSG2	18q12	Desmoglein-2	AD arrhythmogenic cardiomyopathy
				? AR arrhythmogenic cardiomyopathy
	DSG4	18q12	Desmoglein-4	Inherited hypotrichosis
Desmosomal cadherin	*DSC2*	18q12	Desmocollin	Arrhythmogenic cardiomyopathy
				Arrhythmogenic cardiomyopathy with palmoplantar keratoderma and woolly hair
Plakin	*DSP*	6p24	Desmoplakin	Striate PPK
				Keratoderma, keratin retraction, skin fragility and woolly hair/alopecia
				AD arrhythmogenic cardiomyopathy
				Carvajal syndrome
				Lethal acantholytic epidermolysis bullosa

AD indicates autosomal dominant; AR, autosomal recessive.

Figure 1.3 A, Schematic representation of a cardiac desmosome. Reprinted by permission from Macmillan Publishers Ltd: Journal of Investigative Dermatology (Green and Simpson 2007), license # 2982041043142. **B,** Electron micrograph of a desmosome reveals the outer dense plaque (ODP) and inner dense plaque (IDP). DM, dense midline; EC, extracellular core; PM, plasma membrane. Scale bar: 35 nm. Reprinted from Publication (Al-Amoudi and Frangakis 2008) with permission from Elsevier, license # 2982051038837. **C,** Table summarizing the link between a desmosomal gene and a disorder. Reprinted from Publication (Delmar and McKenna 2010) with permission from Wolters Kluwer Health, license # 2982050588388.

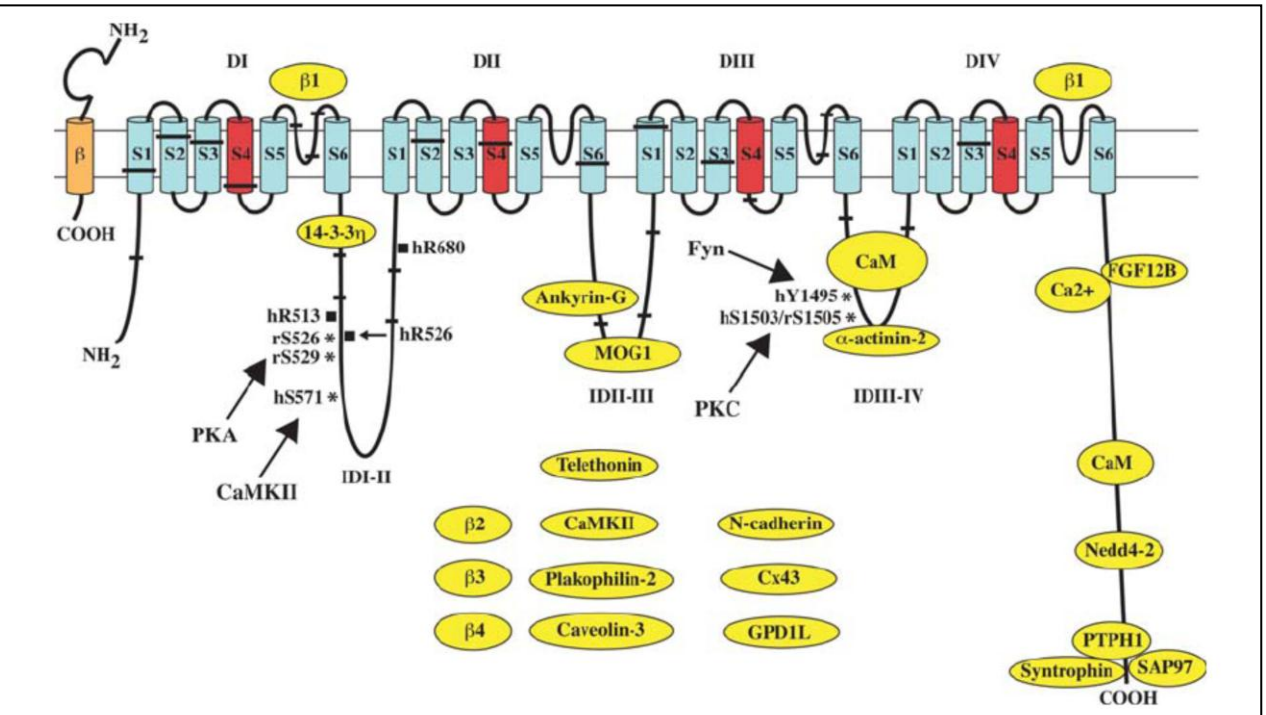

Figure 1.4 Schematic representation of a membrane topology of the α- and β-subunits of the cardiac sodium channel and the proteins they interact with. DI-DIV indicates the homologous domains; S5 and S6, pore-lining segments; green S4, voltage sensor; yellow ovals, interacting proteins of $Na_V1.5$ and their relative binding region. Reprinted from Publication (Rook, Evers et al. 2012) by permission from an Oxford University Press, license # 2982021276383

A

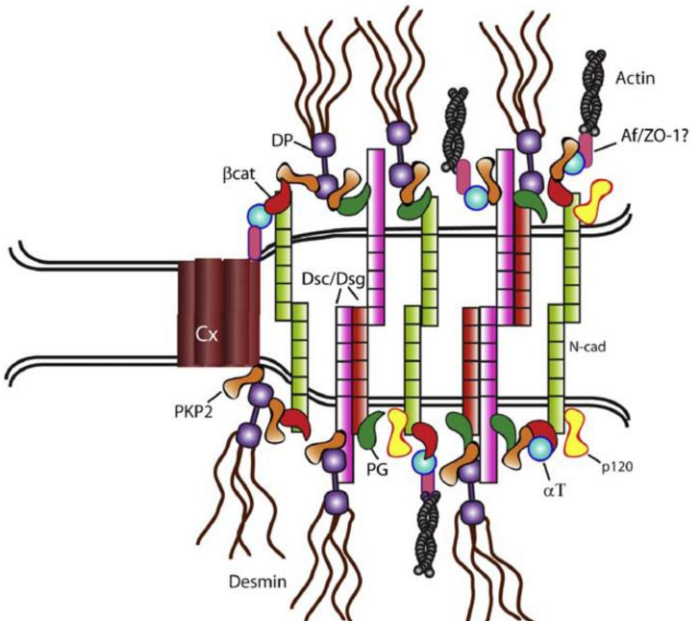

B

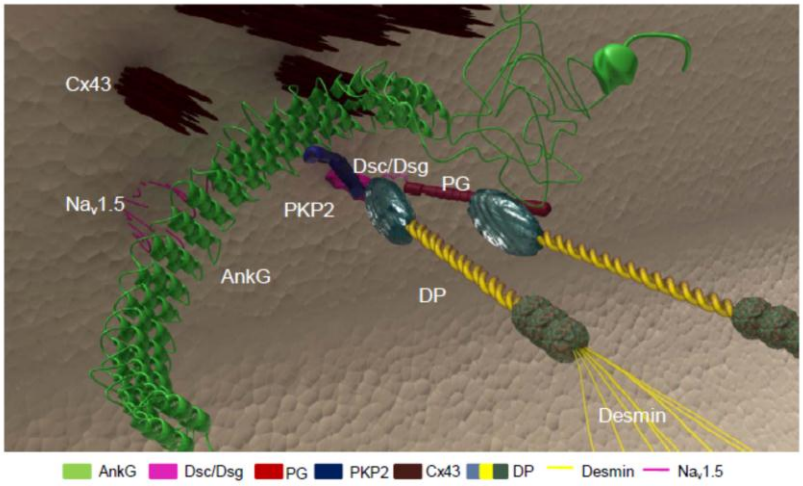

Figure 1.5A, Illustration of the area composita in cardiac myocyte. These mixed junctions containing components of desmosomes and adherens junction are reinforced by the interations of plakophilin2 and αT-catenin. The interaction of gap junctions and area composita through connexin43-plakophilin2 binding. Reprinted from Publication (Bass-Zubek, Godsel et al. 2009) with permission from Elsevier, license # 2982051321048. **B,** Schematic representation of the interactions between proteins of mechanical junctions, connexin43 and $Na_V1.5$ within a macromolecular complex. Reprinted from Publication (Sato, Coombs et al. 2011) with permission from Wolters Kluwer Health, license # 2982060420423.

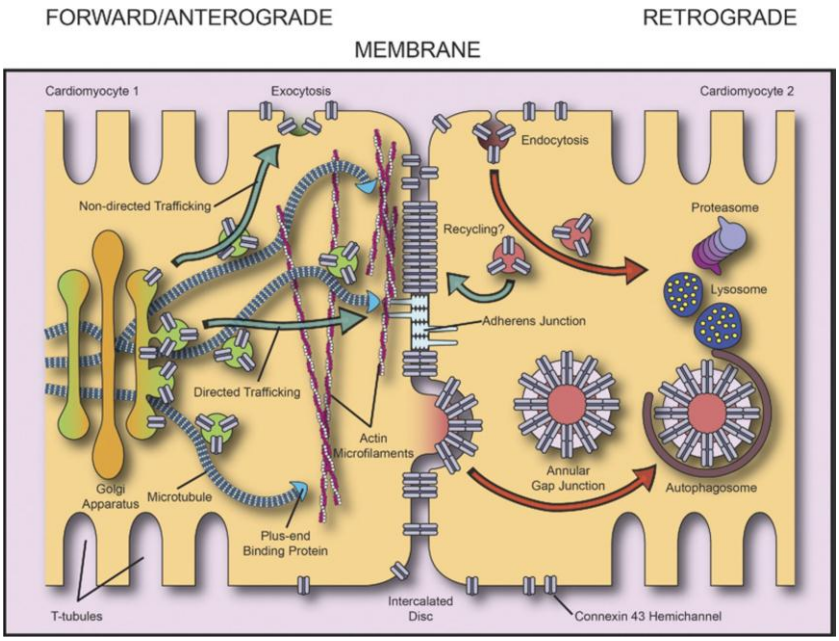

Figure 1.6 Schematic diagram of the connexin43 life cycle. Reprinted from Publication (Smyth and Shaw 2012) with permission from Elsevier, license # 2982070120297.

Chapter II

Materials and Methods

Chapter 2 describes all the experimental procedures relevant to the data described in the chapters 3 and 4.

I performed all immunochemistry studies and all the confocal imaging. TIRF imaging was done with the assistance of Dr. Eli Rosenberg. The analysis of immunochemistry data in chapter 3 was done by me and Nedal Darwish. The analysis of immunochemistry data in chapter 4 was done by me. All the statistical analysis of immunochemistry data was done by me. I performed all the western blots. Cell culture and transfections were done by me. Dr. Xianming Lin performed all enzymatic dissociations of Adult Rat Ventricular Myocytes (ARVMs). The electrophysiology was done by either Dr. Hassan Musa or Dr. Xianming Lin. Dr. Mingliang Zhang generated all the vectors. Dr. Guadalupe Guerrero-Serna performed sheep tissue preservation. Preservation of mouse tissue and cryosectioning were done by me.

Sheep Pulmonary Hypertension model

A large animal model was generated by the laboratory of Dr. Keith Cook to simulate chronic pulmonary hypertension with right ventricular hypertrophy. This model effectively reproduces pulmonary hemodynamics experienced by lung transplant candidates with pulmonary hypertension secondary to respiratory dysfunction, and is described in more detail elsewhere (Weitzenblum, Ehrhart et al. 1983; Della Rocca, Pugliese et al. 1997; Vizza, Lynch et al. 1998; Venuta, Rendina et al. 2000; Thabut, Mal et al. 2003; Thabut, Dauriat et al. 2005; Lettieri, Nathan et al. 2006; Sato, Hall et al. 2008). Sephadex beads (0.375 g) were suspended in sterile saline and injected into the pulmonary circulation of adult sheep every day for 60 days. Ketorolac (60 mg intravenous) was administered prior to the injection of beads. Anesthesia was induced with 60–90 mg/kg of propofol and maintained after endotracheal intubation with 1%–

3% inhaled isoflurane. Animals were monitored during anesthesia by continuous tracking of arterial heart rate and blood pressure and intermittent examination of jaw tone. Euthanasia was carried out by intravenous injection of Fatal-Plus (pentobarbital sodium at 86.2 mg/kg). All animal use was consistent with guidelines from the National Institutes of Health and approved by institutional committees. Prior to heart harvest, sheep were anesthetized, a left thoracotomy was performed, and hearts instrumented according to published methods to measure mean pulmonary artery pressure, mean left atrial pressure and cardiac output. Details on the model, and hemodynamic parameters of the animal population used for these studies, have been published elsewhere (Sato, Hall et al. 2008).

Genetically engineered mice

Connexin43 deficient mice were a gift from Dr. Fishman (Gutstein, Liu et al. 2003). As Gutstein et al described, to generate a cardiac restricted connexin43 null mouse (a-MHC-Cre:Cx43flox/flox) we crossed a heterozygous mouse (a-MHC-Cre:Cx43+/flox) with a cre-deficient mouse (Cx43flox/flox). These mice die within the first post-natal month, thus all the experiments on these animals were done within 2-3 weeks. Cx43flox/flox littermates or age-matched animals were used as control.

PKP2+/- mice were a gift from Dr. Toon A van Veen and Dr. Harold V van Rijen. The method by which the mouse was generated was described elsewhere (Grossmann, Grund et al. 2004; Cerrone, Noorman et al. 2012). Wild type littermates or age-matched animals were used as control.

Enzymatic dissociation of adult mouse ventricular myocytes (AMVMs)

Isolation of adult mouse ventricular myocytes was performed using enzymatic dissociation. Briefly, 0.25mL of heparin injection was followed by thoracotomy. Aorta of an excised heart was cannulated while submerged in a cold cardioplegic solution (180.16 mM glucose, 74.56 mM KCl, 84.01 mM NaHCO3, 182.2 mM Mannitol). The cannulated heart was mounted onto a Langendorff apparatus and perfused sequentially with Ca^{2+} and Mg^{2+}- free collagenase (type 2; Worthington) dissociation solution (10 mM HEPES, 0.6 mM Na_2HPO_4, 113 mM NaCL, 4.7 mM KCL, 12 mM $NaHCO_3$, 0.6 mM KH_2PO_4, 1.2 mM $MgSO_4$, 10 mM

$KHCO_3$, 30 mM Taurine). When digested, the ventricles were minced and then gently triturated with a Pasteur pipette. The cell suspension was strained using 100 μm cell strainer and pelleted by centrifugation. Cells were then resuspended and Ca^{2+} concentration was gradually increased to 1 mM. Cells were used for electrophysiological recording within 8 hours after isolation. Cells for immunofluorescence samples were plated on 18 mm glass coverslips coated with laminin in a 12-well plate and incubated for an hour at 37C. Cells were then fixed with either ice cold methanol for 3 minutes or 4% parafarmaldehyde for 10 min.

Cell culture and transfection

The HL-1, mouse atrial cardiomyocyte, cell line was used to generate stable cell lines with silenced connexin43 and PKP2 proteins (Claycomb, Lanson et al. 1998). Lenti-PKP2-shRNA clone, clone ID TRCN0000123349, was packaged with TransLenti Viral Packaging System (Open Biosystem). The hairpin sequence targeting 3'-UTR of PKP2 gene: CCGGGCATCATTATTCAGGCTTATACTCGAGTATAAGCCTGAATAATGATGCTTTTT G. Lenti-GJA1- shRNA clone, Clone ID TRCN0000068473, hairpin sequence targeting 3'-UTR of GJA1 gene: CCGGCCCACCTTTGTGTCTTCCATACTCGAGTATGGAAGACACAAAGGTGGGTTTTT G. Non-silencing Lenti vector was also packaged and used as a control to infect HL-cell. The infected HL-1 cells were selected in Claycomb medium containing puromycin.

HL-1 cells were plated on 18 mm glass coverslips coated with fibronectin gel. 24 hours after plating cells were transiently transfected with 2 μg of plasmid DNA and 2μl of Lipofectamine2000 (Life Technologies) in antibiotic- and serum- free OPTI-MEM media. After 4 hours of incubation at 37°C cells the media was aspirated and replaced with a Complete Claycomb Medium.

Immunochemistry of tissue and cells

For tissue preparations, fragments of sheep hearts were flash frozen in Tissue Tec O.C.T. (Optimal Cutting Temperature Compound, Sakura, Sakura Finetek U.S.A., Inc., Torrance, CA) and stored at –80°C until they were sectioned. Mouse hearts were cannulated and perfused with ice cold PBS Ca^{2+}- and Mg^{2+}- free PBS solution. The hearts were then submerged into 30%

sucrose in PBS solution and left overnight at 4C. The following day the tissue samples were flash frozen in Tissue Tec O.C.T. The tissue was later sectioned at 5 μm thickness.

Tissue sections were rehydrated by incubation in PBS and then fixed in 4% parafarmaldehyde in PBS. Sections were then immersed in blocking buffer (2% Normal Goat Serum (NGS) 0.1% Triton-X100 in PBS) for 30 min at room temperature, followed by a one-hour incubation in primary antibodies. Sections were washed with PBS and incubated for 30 minutes with secondary antibodies (both primary and secondary antibodies were diluted in blocking buffer). Sections were washed and during the last wash they were incubated for 10 min in TO-PRO-3 (1 uM) in PBS. Samples were mounted using ProLong Gold (Invitrogen). Cardiomyocytes used for microtubule staining were fixed with ice cold methanol for 3 minutes.

The protocol differs for the immunostaining of tissue or cells with Nav1.5 antibodies (Sigma, S0819). Samples were incubated with the blocking buffer (0.1% Triton- X100 and 2% BSA/PBS) for 1 hour followed by the overnight incubation with primary antibodies in 10% NGS/PBS at room temperature. The following day the samples were blocked again with the blocking buffer for 30 minutes followed by the incubation with secondary antibodies in 2% NGS/PBS and 0.1% Triton-X100.

Immunostained preparations were analyzed by confocal microscopy (Leica SP5) to determine protein localization in relation to cell morphology. TIRF (total internal reflection fluorescence) microscopy was used to conduct high spatial resolution imaging of Kif5b and Cx43 molecules at the cell membrane.

List of antibodies used for immunochemistry

Primary antibodies were: for Cx43, #AB1728; rabbit; epitope: carboxyl-terminal domain, Chemicon International Inc, Temecula, CA; for Cx43, #C8093; mouse; Sigma-Aldrich, St. Louis, MO; for Cx43NT1, clone P1E11, mouse; epitope: N-terminus; Fred Hutchinson Cancer Research Center, Seattle, WA; plakophilin 2, #K44262M, Biodesign International, Saco, ME; for desmoplakin1/2, #2722–5204, AbD Serotec, Oxford, UK; Plakoglobin #610254, BD Transduction Laboratories, for desmoglein 1& 2, # 10R-D105A, Fitzgerald, Acton, MA; for

Ankyrin G #33–8800, mouse, Invitrogen, Camarillo, CA; for N-cadherin, #610921, mouse, BD Transduction Laboratories; for Kinesin, # ab5629, rabbit, abcam, Cambridge, MA; for EB1, #610534, mouse, BD Transduction Laboratories; for Nav1.5, # ASC-013, rabbit, Alomone, Israel; for Nav1.5, #ab56240, rabbit, abcam, Cambridge, MA; for Nav1.5, # S0819, rabbit, Sigma-Aldrich, St.Louis, MO; for anti-detyrosinated tubulin, # AB3201, rabbit, Millipore, Temecula, CA. Secondary antibodies included goat anti-mouse and anti-rabbit IgG antibodies conjugated to Alexa Fluor 594 (Molecular Probes, Eugene, OR), goat anti-mouse and anti-rabbit IgG antibodies conjugated to Alexa Fluor 488 (Molecular Probes), goat anti-mouse IgG antibodies conjugated to Alexa Flour 647 and goat anti-rabbit IgG antibodies conjugated to Alexa Fluor 555.

Analysis of immunochemistry data

For the analysis of the heart tissue, a "plaque" was defined as a cluster of 15 or more contiguous pixels showing an identifiable immunoreactive signal (smaller clusters were not measured). Most plaques were best defined as ellipsoids, with a long axis oriented either parallel (0 to 45 degrees) or perpendicular (46 to 90 degrees) to the orientation of the fibers (defined by the long axis of the nuclei of the cells surrounding the plaque). In cases where plaques did not have a well-defined long axis (plaques that were circular or irregularly shaped), the plaque orientation was considered as "ambiguous." Numbers of plaques of a given direction were counted to establish the prevalence of lateralization of a particular protein in PH sheep versus control. The extent of co-localization of Cx43 with another protein (regardless of orientation) was defined by a Pearson's Colocalization Coefficient, estimated using MacBiophotonics ImageJ and WCIF ImageJ (NIH).

Immunoreactive fluorescent signal of compressed Z-stacks (maximal projection) were quantified for all the tissue samples, isolated cardiomyocytes and HL-1 cells. ImageJ (NIH) software was used to measure intensity fluorescence of the immunoreactive signal.

Western blot

Collected tissue was frozen and stored at −80°C. Prior to use, tissue was thawed and homogenized in a lysate buffer that contained a cocktail of protease inhibitors (Roche).

HL-1 cells were rinsed with PBS and lifted on ice in Tris-EDTA buffer with protease inhibitor. The samples were then collected and centrifuged at 14,000 rpm for 5 minutes at 4°C. The supernatant was aspirated and the pellets were resuspended with lysis buffer. The cells were incubated on ice for an hour and frequently vortexed. The samples were then spun down at 14,000 rpm for 10 min at 4°C and the supernatant was collected.

Protein assay was performed to measure the amount of protein in each sample. Samples were heated for 10 min at 55°C except for samples probed for Cx43 and $Na_V1.5$ which were incubated at room temperature. Samples were loaded in a 4–12% 10- or 15-well Tris-Glycine gel, and run at 120 V, followed by transfer to a nitrocellulose membrane at 110 V for 90 min. Blocking of the nonspecific signal was done by incubating membranes in "blocking buffer" (5% NFM in T-PBS). Incubation with primary antibodies was done overnight at 4°C in blocking buffer. Incubation with secondary antibodies was done for an hour at room temperature in PBS. Protein detection was performed using Odyssey infrared imaging system (LI-COR).

Antibodies used for western blot

Primary antibodies used for western blot: for Cx43 #C6219, rabbit, Sigma-Aldrich, St.Louis, MO; for Ankyrin G, # sc-28561, rabbit, Santa Cruz Biotechnology, N-cadherin, # 610921, mouse, BD Transduction Laboratories; Plakoglobin #610254, BD Transduction Laboratories; for PKP2, #K44262M, mouse, Meridian Life Science, Inc, Saco, ME; for Nav1.5, #ab56240, rabbit, abcam, Cambridge, MA; for anti-detyrosinated tubulin, # AB3201, rabbit, Millipore, Temecula, CA; for α-tubulin, # T5168, mouse, Sigma-Aldrich or # ab18251, rabbit, abcam; for α-tubulin, ab18251, rabbit, abcam, Cambridge, MA; for HSP90, #610419, BD Transduction Laboratories. Secondary antibodies: IRDye 800CW Donkey anti-rabbit IgG, # 926–32213, LI-COR, Lincoln, Nebraska and IRDye 680 Conjugated Goat anti-mouse IgG, # 926–32220, LI-COR.

Total internal reflection fluorescence (TIRF)

TIRF was conducted on immunolabeled isolated mouse myocytes. Immediately following dissociation, cells were plated on laminin coated glass bottom dishes (MatTek), fixed (4% paraformaldehyde) and immunolabeled as described above.

Electrophysiology

Whole-cell cardiac sodium current (I_{Na}) was recorded from freshly isolated sheep myocytes, mouse myocytes or cultured HL-1 cells using standard methods. All recordings were conducted at room temperature, in a low-sodium extracellular solution containing (in mM): NaCl, 5; $MgCl_2$, 1; $CaCl_2$, 1.8; $CdCl_2$, 0.1; HEPES, 20; CsCl, 132.5; glucose, 11. The pipette solution contained (in mM): NaCl, 5;CsF, 135; EGTA, 10; MgATP, 5; HEPES, 5. Recordings were performed using an Axopatch-200B Amplifier (Molecular Devices Sunnyvale, CA) and data acquisition and analysis were performed utilizing pClamp10.2 software (Molecular Devices Sunnyvale, CA). Pipette resistances ranged from 2–3 MΩ. Access resistance was compensated to 1–2 MΩ. Input resistance was 500 MΩ to 1 GΩ. To characterize the voltage dependence of the peak I_{Na}, single cells were held at −160 mV, and 200 msec voltage steps were applied from −100 to +10 mV in 5 mV increments. Interval between voltage steps was 3 sec. Voltage-dependence of inactivation was assessed by holding cells at various potentials from −140 to −40 mV followed by a 30 msec test pulse to −40 mV to elicit I_{Na}. Recovery from inactivation was studied by holding cells at −160 mV and applying two 20-msec test pulses (S1, S2) to −45 mV separated by variable inter-pulse intervals, to a maximum S1–S2 interval of 80 msec. The S1–S1 interval was kept constant at 3 sec.

The dual whole-cell voltage clamp technique was used to record gap junction currents. G_j was measured from cells in side-to-side apposition. Both cells in the pair (cell 1 and cell 2) were independently voltage clamped at the same holding potential (−40 mV). The prejunctional cell (cell 1) was stepped to +20 mV, creating a potential difference across the junction (V_j) of +60 mV during repetitive 10−30-s steps. Patch pipettes were filled with a solution containing cesium (in mM: 130 CsCl; 0.5 $CaCl_2$; 10 HEPES; 10 EGTA; 2.0 Na_2ATP; 3.0 MgATP; pH 7.2). Pipette resistance was 3.0–5.0 MΩ. During recording, cells were kept at room temperature in a cesium-containing solution (in mM: 160 NaCl; 10 CsCl; 2.0 $CaCl_2$; 0.6 $MgCl_2$; 10 HEPES; pH 7.4).

Statistical analysis

Statistical significance for measurements of sodium and gap junction current properties was assessed by unpaired two-tailed *t* test (Origin Version 7.0; Origin Laboratory Corporation). For immunochemical data, statistical significance was assessed by unpaired 2-tailed Student's *t* test, and, for multiple groups, Tukey's Multiple Comparison One-way ANOVA (GraphPad Prism 5 Software). All data are presented as mean value ± S.E.M. Statistical significance was set at $p < 0.05$.

Chapter III

Remodeling of Mechanical Junctions and of Microtubule-Associated Proteins Accompany Cardiac Connexin43 Lateralization

All the preservation of the tissue samples for this chapter was done by Dr. Guadalupe Guerrero-Serna. All immunohistochemistry, confocal imaging, and western blotting were performed by me. Patch clamp experiments were done by Dr. Hassan Musa and Dr. Xianming Lin. The analysis of the data was performed by Nedal Darwish and me. TIRF microscopy was performed by me with assistance of Dr. Rothenberg. The experiments were done under the guidance and supervision by Dr. Mario Delmar and recommendations by Dr. Jeffrey Martens.

This chapter is reprinted from Publication (Chkourko, Guerrero-Serna et al. 2012) with permission from Elsevier (license # 2991471133827).

Introduction

Intercellular communication is essential for cardiac function. Mechanical continuity is provided by desmosomes and adherens junctions, whereas gap junctions provide a pathway for passage of ions and small molecules between cells. These complexes preferentially reside at the site of end-end contact between myocytes, within the intercalated disc (ID). Also resident to the ID are "non-junctional" molecules, which are, not involved in providing a physical continuum between neighboring cells. Conventionally, the various ID molecules, junctional or not, have been considered separate entities. Yet, this view is rapidly changing and the emerging picture is that of the ID as a protein interacting network involved in maintaining synchrony within cell populations (Sato, Musa et al. 2009; Delmar and Liang 2011; Sato, Coombs et al. 2011).

The importance of gap junctions in normal electrical function is well established. Recent studies have shown that under various pathological conditions, there is reduced presence of gap junction plaques at the ID, often replaced by neoformation of gap junctions at sites other than the cells' edge (see, e.g.,(Uzzaman, Honjo et al. 2000; Emdad, Uzzaman et al. 2001; Barker, Price et al. 2002; Kostin, Rieger et al. 2003; Kostin, Dammer et al. 2004; Spragg, Akar et al. 2005; Cabo, Yao et al. 2006; Akar, Nass et al. 2007; Fialova, Dlugosova et al. 2008; Qu, Volpicelli et al. 2009; Tan and He 2009)). Changes in total abundance of connexin43 have also been reported (e.g., (Qu, Volpicelli et al. 2009)). This process of gap junction "remodeling" has been described as potential substrate for cardiac arrhythmias (Peters, Coromilas et al. 1997; Akar, Nass et al. 2007). Yet, it can be argued that, if the lateral membrane junctions are functional, lateralization may help to maintain action potential propagation. Either as an arrhythmogenic, or as an antiarrhythmic event, gap junction remodeling is a process intrinsic to cardiac pathology and, likely, highly relevant to the heart rhythm.

The formation of Cx43-mediated gap junctions requires pre-formation of mechanical junctions (Rohr 2007). Thus, we speculate that, to be functional, redistribution of Cx43 should be accompanied by remodeling of mechanical junctions. Moreover, the mechanisms that transport Cx43 to its new location remain unclear. We propose that Cx43 lateralization involves redirection of microtubule-mediated Cx43 trafficking to the lateral membrane (Lauf, Giepmans et al. 2002; Thomas, Jordan et al. 2005). Furthermore, while intercellular junctions associate with the voltage-gated sodium channel (VGSC) complex at the ID (Kucera, Rohr et al. 2002; Maier, Westenbroek et al. 2004; Dominguez, de la Rosa et al. 2008), the fate of that interaction, once remodeling has been triggered, remains undefined. Here, we have characterized junctional remodeling in an ovine model of right ventricular pressure overload (Pohlmann JR ; Weitzenblum, Ehrhart et al. 1983; Della Rocca, Pugliese et al. 1997; Vizza, Lynch et al. 1998; Venuta, Rendina et al. 2000; Thabut, Mal et al. 2003; Thabut, Dauriat et al. 2005; Lettieri, Nathan et al. 2006; Sato, Hall et al. 2008). The data show substantial Cx43 lateralization. Cx43 plaques oriented parallel to fiber direction co-localized with mechanical junction proteins, and with the microtubule-associated proteins EB1 (Shaw, Fay et al. 2007) and Kifb5 (Argyropoulos, Stutz et al. 2009; Zadeh, Cheng et al. 2009; Fort, Murray et al. 2011). Separate electron microscopy studies demonstrated the presence of desmosomes and gap junctions at sites of side-

side contact. In contrast, our data suggest that VGSC remodeling may follow a process different from that of junctional proteins, with consequent functional changes in the amplitude and kinetics of sodium current. Overall, this is the first characterization of the fate of the desmosome-gap junction-VGSC complex under pressure-overload induced remodeling. These observations provide a fundamental background to understand intercellular communication in cardiac disease, particularly in cases affecting mechanical continuity between cells.

Results

Cx43 remodeling in right ventricle of sheep subjected to right ventricular pressure overload

In control animals, Cx43 signal in right ventricular tissue was oriented primarily in a direction perpendicular to fiber orientation (corresponding to the ID; see Figure 3.1A). In contrast, long clusters of immunoreactive signal oriented parallel to the fibers were found in right ventricle of sheep subjected to right ventricular pressure overload (Figure 3.1B). From a total of 84 plaques analyzed in control tissue, 60 were deemed perpendicular (71% of total), only 8 were found to be parallel to the orientation of the fibers and 16 were classified as "undefined" (Figure 3.1C). In contrast, out of 403 plaques analyzed in right ventricular tissue of PH animals, only 34% were oriented in the perpendicular direction (Figure 3.1D). These results indicate that in this animal model, Cx43 undergoes extensive and consistent remodeling, with an increase in predominance of plaques oriented parallel to the axis of the fibers. For simplicity, plaques oriented in the perpendicular or parallel direction will be referred to as "ID" (for "intercalated disc") or "LM" (for lateral membrane), respectively. Regions of interest with an ambiguous orientation were not included in the colocalization analysis.

Proteins of the mechanical junctions accompany Cx43 remodeling

Immunostaining of the desmosomal/adherens junction protein plakoglobin (PG) showed a pattern similar to that observed for Cx43, with plaques localized to the intercalated disc in control (Figure 3.1E) and redistributed in a parallel direction in PH hearts (Figure 3.1F). From a total of 79 PG plaques analyzed in control tissue, 59 were identified as perpendicular (75%), 13 (16%) were undefined, and 7 (9%) were parallel (Figure 3.1G). In PH hearts, only 42% of plaques (out of 437 total) were perpendicular (i.e., at the ID; Figure 3.1H). Overlay of signals

showed co-segregation of Cx43 and PG to the same cellular region (Figure 3.1I and 1J). An enlarged image of the plaque formed at the lateral membrane displays the characteristic pattern of co-localization of desmosomal and gap junction proteins (Maass, Shibayama et al. 2007) with either overlapping or closely alternating pixels positive for one protein or another (Figure 3.1; panels a, a' and a''). A Pearson's coefficient analysis showed that, compared to control, the probability of ID co-localization was significantly decreased in PH hearts (Figure 3.1K). Pearson's coefficient for signals oriented parallel to fibers (i.e., in LM) was not carried out in control preparations, given the very low number of regions of interest oriented in that direction (see also Fig 3.1C). Yet, in PH hearts, we observed a degree of co-localization similar to that found in the ID, suggesting that displacement of Cx43 to lateral membranes is accompanied by redistribution of mechanical junction proteins. To further extend this concept, we examined the localization of the desmosomal cadherins desmocollin (Figure 3.2) and desmoglein (Figure 3.3), the desmosomal components plakophilin-2 (Figure 3.4) and desmoplakin (Figure 3.5) as well as N-cadherin (a component of the area composita;(Borrmann, Grund et al. 2006; Franke, Borrmann et al. 2006) Figure 3.6). Consistently, we observed a decrease in the fraction of plaques at the ID, and an increase of those parallel to the fibers, in PH hearts. We also observed a decrease in extent of co-localization (Pearson coefficient) of Cx43 with other junctional proteins at the ID, except for DSC and N-cadherin, in PH hearts when compared to control. Pearson coefficient values at the lateral membranes were significantly lower than at the ID (except in the case of PG); yet, for all proteins of the area composita tested, probability of co-localization with Cx43 at the lateral membrane was higher than 20% and significantly larger than zero. These data suggested that lateralization of Cx43 was not an isolated event, but part of a complex remodeling process that includes the molecules necessary to form mechanical junctions between cells. Western blot analysis was limited by the availability of antibodies imunoreactive to ovine tissue. Changes in protein abundance were not detected (Figure 3.7).

Desmosomes and gap junctions in the lateral membranes of cardiac tissue.

The data in Figure 3.1-3.6 suggest that desmosomal and gap junction molecules are able to form new complexes even if displaced from the ID. More direct demonstration was obtained by electron microscopy studies (Figure 3.8). The low resolution image in 8A reveals the preserved morphology of a thin section from the right ventricle of a PH-afflicted heart. Fiber

orientation can be clearly distinguished. An enlargement of the area demarcated by the red box, corresponding to a site where cardiac cells are in close lateral (not end-end) proximity, is presented in 3.8B. The image shows two types of electron-dense structures interrupting the continuity of the intercellular space: one with the morphological characteristics of a desmosome and the other, with the morphological features of a gap junction plaque. These results provide direct evidence that junctional structures can be formed at the lateral membranes of cardiac myocytes. Formation of these structures likely facilitates preservation of electrical coupling even when the molecular organization of the intercalated disc is disturbed.

Junctional remodeling and the fate of the VGSC complex

Previous studies show that the most abundant alpha subunit of the cardiac sodium channel complex, $Na_V1.5$, localizes primarily to the intercalated disc and associates with molecules of the mechanical (Sato, Musa et al. 2009) and electrical junctions (Kucera, Rohr et al. 2002; Maier, Westenbroek et al. 2004; Dominguez, de la Rosa et al. 2008) We therefore explored whether the sodium channel complex is also redistributed to the lateral membrane in PH-afflicted hearts. $Na_V1.5$-immunoreactive plaques at the intercalated disc were clearly visible in control tissue, co-localizing with Cx43 (Figure 3.9A; columns labeled CNTR; $Na_V1.5$ in red, Cx43 in green; overlay in bottom panels; box labeled "a" enlarged in right panels). In contrast, the $Na_V1.5$ plaques were very sporadic in PH hearts. Most of lateralized Cx43 signals were void of a co-localizing $Na_V1.5$ signal (see boxes labeled "b") though occasional overlap was seen at the ID area ("c"). As a result, the Pearson coefficient for co-localization of Cx43 and $Na_V1.5$ was significantly decreased, particularly when we analyzed Cx43 signals at the lateral membranes (Figure 3.9B). In fact, in contrast to what we observed for junctional proteins, the Pearson coefficient value for LM signals was not different from zero (two-tailed t test). Furthermore, the analysis of variance- Bonferroni test for all LM Pearson coefficient values showed that the extent of co-localization of Cx43 with Nav1.5 was significantly less than that obtained for junctional molecules (Figure 3.9C). These data suggest that while junctional molecules reorganize to form junctional complexes "in exile," $Na_V1.5$ molecules do not follow. Ankyrin G detection was hampered by high background and as such, quantitative analysis for co-localization at the lateral membranes was not possible; yet, the immunofluorescence images suggest that in the PH hearts, ankyring G localization at the ID decreased significantly (see

Figure 3.10). As a next step, we asked whether the reported changes in protein localization associated with modifications in sodium current properties.

ID remodeling and electrophysiological properties

Electrophysiological recordings were obtained from cardiac myocytes isolated from the left or right ventricle of afflicted animals, as well as from the right ventricle of control animals. As shown in Figure 3.11A, average current density recorded from left ventricular cells was slightly larger than that from cells dissociated from control right ventricle. This difference became more noticeable when cells from the right ventricle of afflicted animals were tested (Table 3.1). The decrease in peak current density was accompanied by a slight shift in the peak current voltage relation (Figure 3.11A), a significant decrease in $V_{1/2}$ activation (Figure 3.11B; Table 3.1), and a slowing in recovery from inactivation (Figure 3.11D) without a noticeable change in voltage dependence of steady-state inactivation (Figure 3.11C). Overall, these results indicate that pressure overload led to changes not only in distribution but also in function of the VGSC complex. Similarly, as shown in 3.11E, we observed an ~30% decrease in junctional conductance measured between myocytes from an afflicted right ventricle, when compared to control. Of note, ventricular arrhythmias, or unexplained sudden death, have not been observed in these animals and are not clinical features of patients with pulmonary hypertension (Vizza, Lynch et al. 1998; Lettieri, Nathan et al. 2006).

Lateralized Cx43 and redistribution of molecules involved in Cx43 forward trafficking

The mechanism by which Cx43 reaches the lateral membrane of the cell remains poorly understood. We speculate that Cx43 lateralization results, at least in part, from the re-routing of Cx43 forward trafficking to a new microdomain. A key molecule in Cx43 forward trafficking is the microtubule-associated end-plus protein EB1, which tethers to N-cadherin for delivery of Cx43 (Shaw, Fay et al. 2007). In Figure 3.12 we show that under control conditions, EB1 (green) co-localized with Cx43 (red) at the intercalated disc (box and panels labeled “a”). In PH hearts, EB1-Cx43 co-localization was maintained, but in this case, plaques oriented parallel to the cells (box and panels labeled “b”). Overlay images (bottom of Figure 3.12) showed that regardless of the position of the plaque, there was an overlap or a close alternation of immunofluorescent signals, indicating the close proximity of the two proteins. These results demonstrate that

pressure overload led to lateralization of EB1. Separately, we showed that kinesin protein Kif5b, a microtubule-associated motor protein in the heart, also co-localized with Cx43, both in control and in PH hearts (Figure 3.13A). This is the first demonstration of co-localization of Cx43 with a kinesin molecule in heart cells. To confirm this observation and minimize the influence of background fluorescence, we utilized total internal reflectance fluorescence microscopy (TIRF) in isolated adult mouse cardiac myocytes. As shown in Figure 3.13B, there was abundant co-localization of Cx43 and Kif5b at the end of the cell, consistent with the hypothesis that this kinesin participates in the microtubule-dependent trafficking of intercalated disc proteins, including Cx43.

Discussion

Mechanical junctions are an integral component of cardiac mechanical and electrical function. Yet, the fate of mechanical junction proteins in the setting of heart disease remains understudied. Here, we utilized an animal model of right ventricular pressure overload to characterize the morphology of intercellular junctions that are formed outside the area of the intercalated disc. We show that gap junction neo-formation is concurrent with remodeling of mechanical junction proteins and that together, they form junctional complexes that have the potential to preserve intercellular communication. Yet, these new complexes showed limited association with $Na_V1.5$ and functionally, a reduction in amplitude and change in kinetics of the I_{Na}. While Cx43 remodeling has been previously described, this is the first characterization of the fate of the desmosome-gap junction-VGSC complex in a model of cardiac pressure overload. While Cx43 remodeling has been previously described, this is the first characterization of the fate of the desmosome-gap junction-VGSC complex in a model of cardiac pressure overload. It is important to emphasize that we did not implement this model to study cardiac arrhythmias, rather, as a system to characterize, in a living animal, the fate of various ID proteins. In fact, we speculate that in this case, redistribution of junctional proteins allows for partial preservation of electrical communication. Electrophysiological recordings showed only a minor decrease in junctional conductance (see Figure 3.11). It is worth noting that no Cx43 lateralization (only loss of Cx43 plaques) has been reported in hearts of patients with arrhythmogenic right ventricular cardiomyopathy, an inherited disease associated with mutations in desmosomal proteins. It is

interesting to note that in our case, N-cadherin was also prominent at the lateral membrane, in contrast to what has been observed in cases of ARVC.

We have previously shown that loss of expression of the desmosomal protein PKP2 (Sato, Musa et al. 2009), as well as loss of Cx43 expression (Sato, Coombs et al. 2011), affect sodium current function. In the PH heart, gap junctions and desmosomes formed at a new site, but $Na_V1.5$ did not reorganize in a similar manner. We speculate that, as opposed to gap junctions and desmosomes, trafficking of $Na_V1.5$ requires molecules that are unable to redirect to the lateral membranes. Furthermore, our data showed slowing of recovery from inactivation for I_{Na}. Interestingly, similar effects were recently reported for $Na_V1.5$ channels exposed to membrane stretch (Beyder, Rae et al. 2010). It is tempting to speculate that kinetics can be changed by moving channels from a rigid but stretch-free ID to lateral membranes more prone to strain. Also, of note, slow recovery from inactivation was observed in our previous studies after silencing PKP2, suggesting that composition of the macromolecular complex that includes $Na_V1.5$, can influence its kinetic properties (Sato, Musa et al. 2009).

Cx43-containing connexons are delivered to the plasma membrane in vesicles, moving along microtubules (Lauf, Giepmans et al. 2002; Thomas, Jordan et al. 2005). EB1 serves as a guide for the microtubule growth and vesicle delivery (Shaw, Fay et al. 2007). N-cadherin plays an essential role by tethering EB1 and as a result, Cx43-containing vesicles to the membrane (Shaw, Fay et al. 2007). Immunohistochemical studies revealed that EB1 signal is enriched at the ID (Smyth, Hong et al. 2010). On the other hand, in the heart with ischemic cardiomyopathy, the decrease of Cx43 signal at the ID correlated with loss of EB1 enrichment (Smyth, Hong et al. 2010). Here, we find enrichment of immunoreactive EB1 with lateralized gap junctions. The presence of EB1 signal at the lateral membrane suggests that forward trafficking of Cx43 is not disrupted but rather preserved and redirected to a different location. This notion is further supported by the finding that Kif5b, an isoform of the motor protein Kinesin-1, also redistributed to lateral membranes in PH hearts. While we do not have direct evidence that Cx43-containing vesicles are driven by kinesin-1 motors, the hypothesis is consistent with recent *in vitro* studies showing that Cx32 in vesicles isolated from hepatocytes are driven along microtubules by

Kinesin-1 (Fort, Murray et al. 2011). Whether Cx43 lateralization depends on Kif5b remains a matter of future studies.

In summary, we have found that, in a large animal model of RV pressure overload, loss of gap junctions at the ID was accompanied by reorganization of junctional complexes in a direction parallel to fiber orientation. We postulate that the latter involves (a) redirectionality of microtubule-mediated forward trafficking and (b) assembly of mechanical junctions that stabilize newly formed gap junction plaques. We speculate that this remodeling may be critical for preservation of electrical synchrony in the afflicted tissue, despite changes in the localization and electrical properties of $Na_V1.5$. As such, lateralization may be not always an arrhythmogenic substrate but, at least this instance, an adaptive mechanism that prevents uncoupling and arrhythmias in the heart.

	$I_{Na,peak}$ (pA)	$V_{1/2,activation}$ (mV)	$V_{1/2,inactivation}$ (mV)	Recovery time constants (ms)
CTL LV	−43.83 ± 7.67 (8)*	−55.47 ± 1.13 (8)†	−85.82 ± 3.76 (8)	9.69 ± 1.29 (8)
CTL RV	−30.17 ± 6.77 (4)	−53.05 ± 0.91 (4)‡	−79.67 ± 1.87 (3)	6.58 ± 0.81 (3)
PH RV	−18.64 ± 3.9 (7)	−44.09 ± 2.41 (7)	−76.47 ± 3.3 (7)	9.07 ± 3.23 (6)

The numbers in parentheses indicate the number of experiments.

CTL = control; I_{Na} = sodium current; LV = left ventricle; PH = pulmonary hypertension; RV = right ventricle.

*P <.05 for CTL LV vs PH RV.

†P <.001 for CTL LV vs CTL RV.

‡P <.05 for CTL RV vs PH RV.

Table 3.1 Parameters of I_{Na} recorded from sheep ventricular myocytes (Chkourko, Guerrero-Serna et al. 2012).

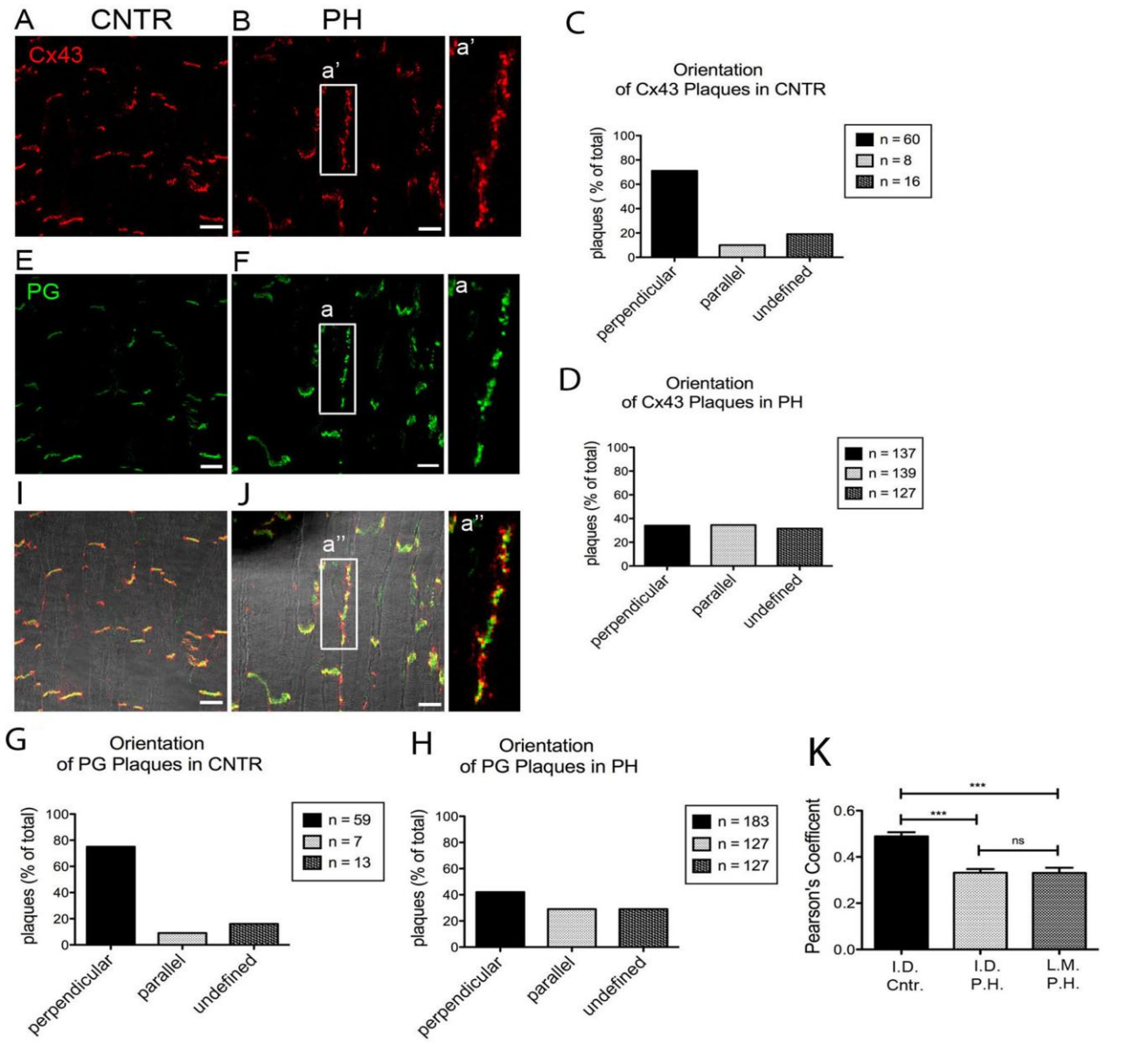

Figure 3.1 Localization of Cx43 and Plakoglobin. Confocal microscopy images obtained from right ventricular tissue of control sheep (CNTR) (**A, E, I**) or sheep afflicted with pulmonary hypertension (PH; **B, F, J)**. Immunoreactive Connexin43 (Cx43; red), and Plakoglobin (PG; green) are presented separately (**A, B**), and (**E, F**) or in merged images (**I, J**). **a, a', a''** enlarged images of Cx43 and PG along the long axis. Bar, 20 µm. **C, D, G,H** Quantification plots representing percentage of Cx43 (**C,D**) or PG (**G,H**) plaques found in a given orientation with respect to the fiber direction in tissue CNTR (**C, G**) or PH (**D, H**). **K,** Colocalization (Pearson's Coefficient) of PG and Cx43 in plaques oriented perpendicular (intercalated disc; I.D.) or parallel (lateral membrane; L.M.) to the fiber orientation. Statistical analysis: One-way ANOVA, Tukey's Multiple Comparison Test. Mean ± SEM. p values: >0.05 (ns); 0.001 to 0.0001 (***). Numbers of regions of interest analyzed: 48, 60, and 60 for I.D. Cntr., I.D. P.H., and L.M. P.H., respectively (Chkourko, Guerrero-Serna et al. 2012).

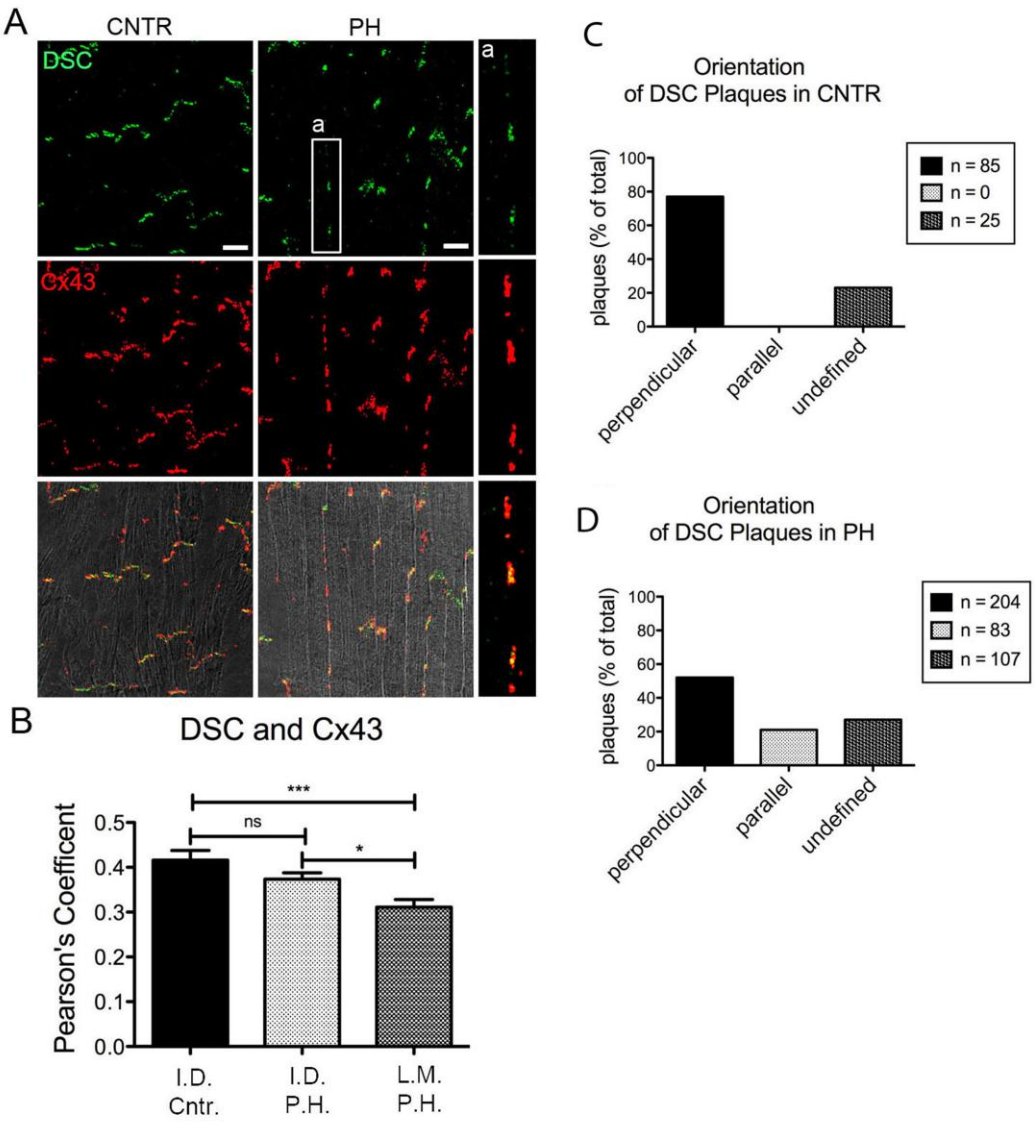

Figure 3.2 Localization of Desmocollin. **A,** Confocal microscopy image obtained from right ventricular tissue of control sheep (CNTR) or sheep afflicted with pulmonary hypertension (PH). Desmocollin (DSC; green), Cx43 (red). Bar, 20 µm. **B,** Colocalization (Pearson's Coefficient) of DSC and Cx43 signals in plaques oriented perpendicular (intercalated disc; I.D.) or parallel (lateral membrane; L.M.) to the fiber orientation. Statistical analysis: One-way ANOVA, Tukey's Multiple Comparison Test. Mean ± SEM. p values: >0.05 (ns); 0.01 to 0.05 (*); 0.001 to 0.0001 (***). Numbers of regions of interest analyzed: 40, 60, and 60 for I.D. Cntr., I.D. P.H., and L.M. P.H., respectively. **C, D,** Quantification plots representing percentage of DSC plaques found in a given orientation with respect to the fiber direction in tissue CNTR (**C**) or PH (**D**) (Chkourko, Guerrero-Serna et al. 2012).

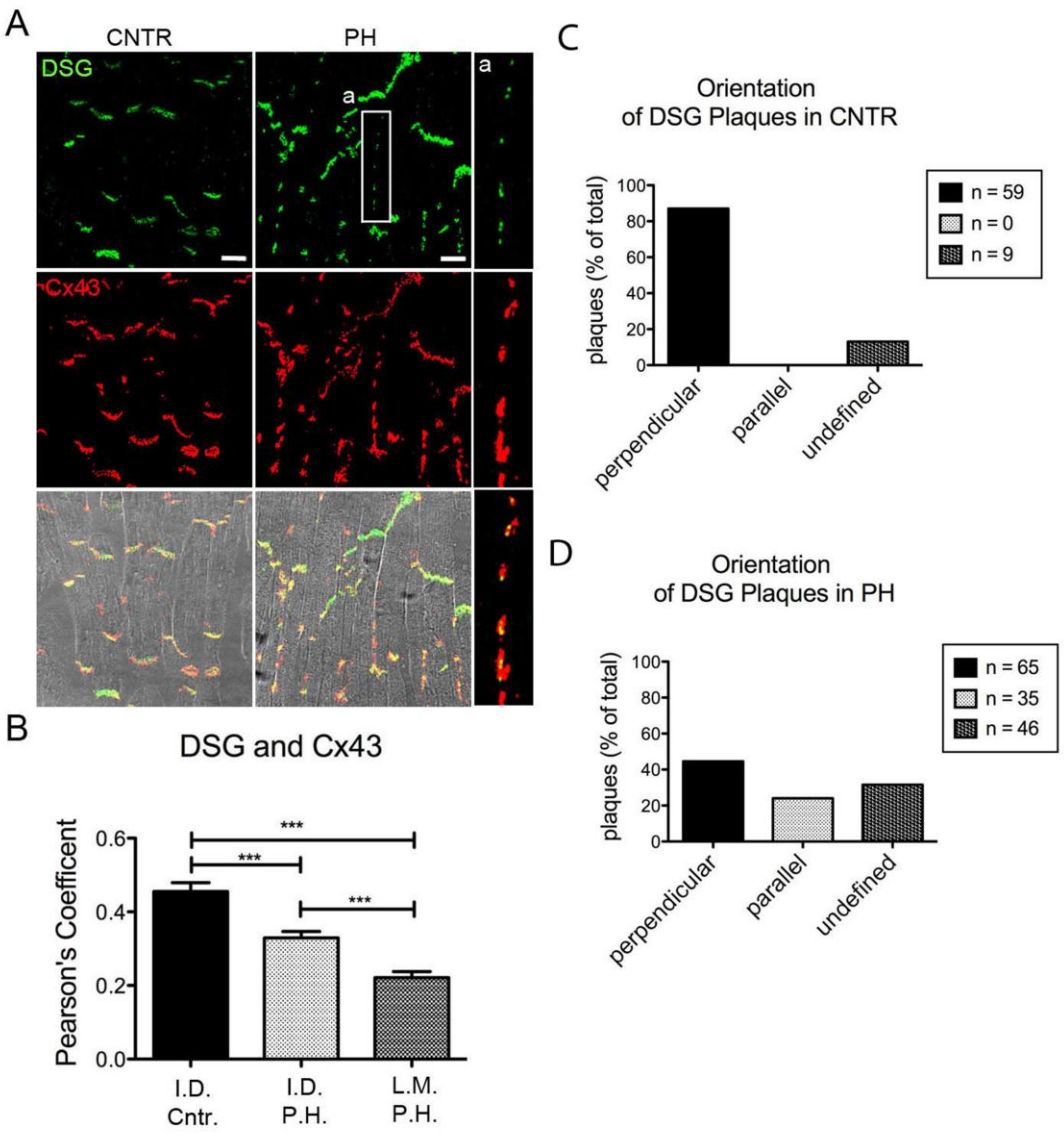

Figure 3.3 Localization of Desmoglein. **A,** Confocal microscopy image obtained from right ventricular tissue of control sheep (CNTR) or sheep afflicted with pulmonary hypertension (PH). Desmoglein, DSG; green. Connexin43, Cx43, red. Nuclei, TO-PRO-3, blue. **a,** enlarged images of Cx43 with DSG along the long axis. Bar, 20 µm. **B,** Colocalization (Pearson's Coefficient) of DSG and Cx43 in plaques oriented perpendicular (intercalated disc; I.D.) or parallel (lateral membrane; L.M) to the fiber orientation. Statistical analysis: ANOVA, Tukey's Multiple Comparison Test. Mean ± SEM. p value < 0.001 (***). Numbers of regions of interest analyzed: 32, 54, and 54 for I.D. Cntr., I.D. P.H., and L.M. P.H., respectively **C, D,** Quantification plots representing percentage of DSG plaques found in a given orientation with respect to the fiber direction in tissue CNTR (**C**) or PH (**D**) (Chkourko, Guerrero-Serna et al. 2012).

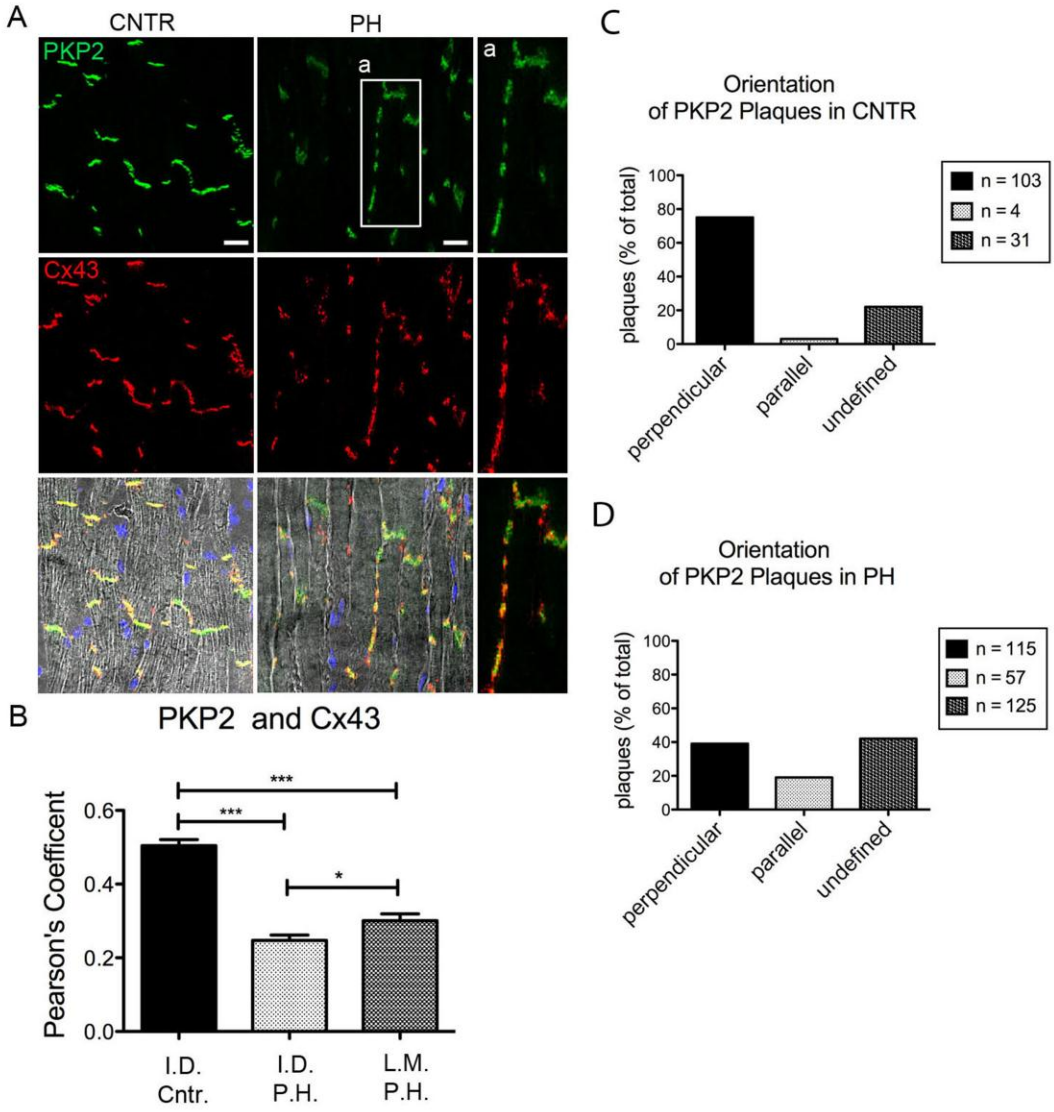

Figure 3.4 Localization of PKP2. **A,** Confocal microscopy image obtained from right ventricular tissue of control sheep (CNTR) or sheep afflicted with pulmonary hypertension (PH). Plakophilin-2, PKP2; green. Connexin43, Cx43, red. Nuclei, TO-PRO-3, blue. **a,** enlarged images of Cx43 with DSG along the long axis. Bar, 20 µm. **B,** Colocalization (Pearson's Coefficient) of PKP2 and Cx43 in plaques oriented perpendicular (intercalated disc; I.D.) or parallel (lateral membrane; L.M) to the fiber orientation. Statistical analysis: ANOVA, Tukey's Multiple Comparison Test. Mean ± SEM. p values: p>0.05 (ns); p 0.01 to 0.05 (*); p value 0.001 to 0.01 (**); p value 0.001 to 0.0001 (***). Numbers of regions of interest analyzed (N): 44, 115, and 67 for I.D. Cntr., I.D. P.H., and L.M. P.H., respectively. **C, D,** Quantification plots representing percentage of PKP2 plaques found in a given orientation with respect to the fiber direction in tissue CNTR (**C**) or PH (**D**) Chkourko, Guerrero-Serna et al. 2012).

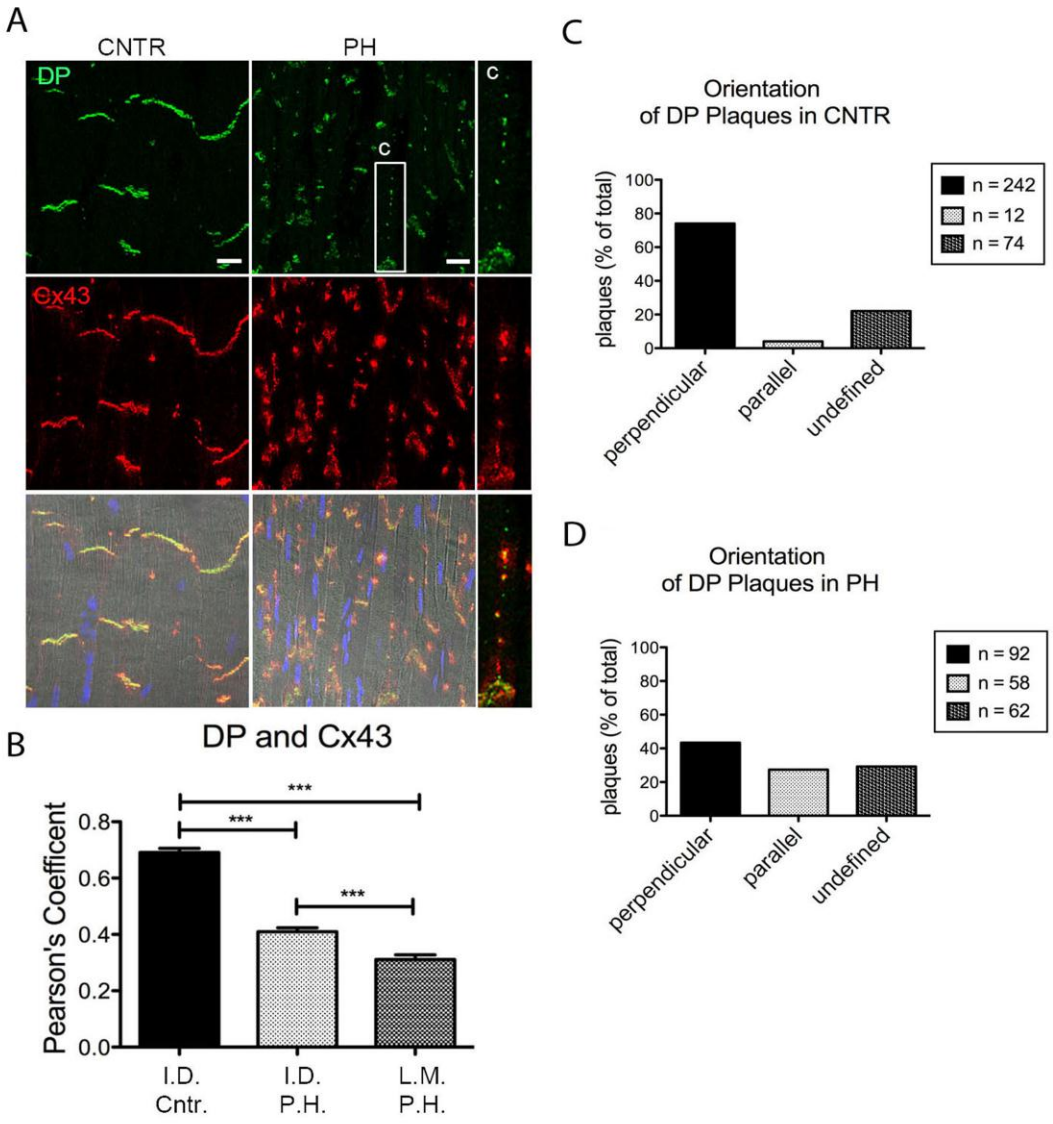

Figure 3.5 Localization of DP. **A,** Confocal microscopy image obtained from right ventricular tissue of control sheep (CNTR) or sheep afflicted with pulmonary hypertension (PH). Desmoplakin, DP; green. Connexin43, Cx43, red. Nuclei, TO-PRO-3, blue. **c,** enlarged images of Cx43 with DP along the long axis. Bar, 20 µm. **B,** Colocalization (Pearson's Coefficient) of DP and Cx43 in plaques oriented perpendicular (intercalated disc; I.D.) or parallel (lateral membrane; L.M) to the fiber orientation. Statistical analysis: ANOVA, Tukey's Multiple Comparison Test. Mean ± SEM. p values: p>0.05 (ns); p 0.01 to 0.05 (*); p value 0.001 to 0.01 (**); p value 0.001 to 0.0001 (***). N=48, 69, and 67 for I.D. Cntr., I.D. P.H., and L.M. P.H., respectively. **C, D,** Quantification plots representing percentage of DP plaques found in a given orientation with respect to the fiber direction in tissue CNTR (**C**) or PH (**D**) (Chkourko, Guerrero-Serna et al. 2012).

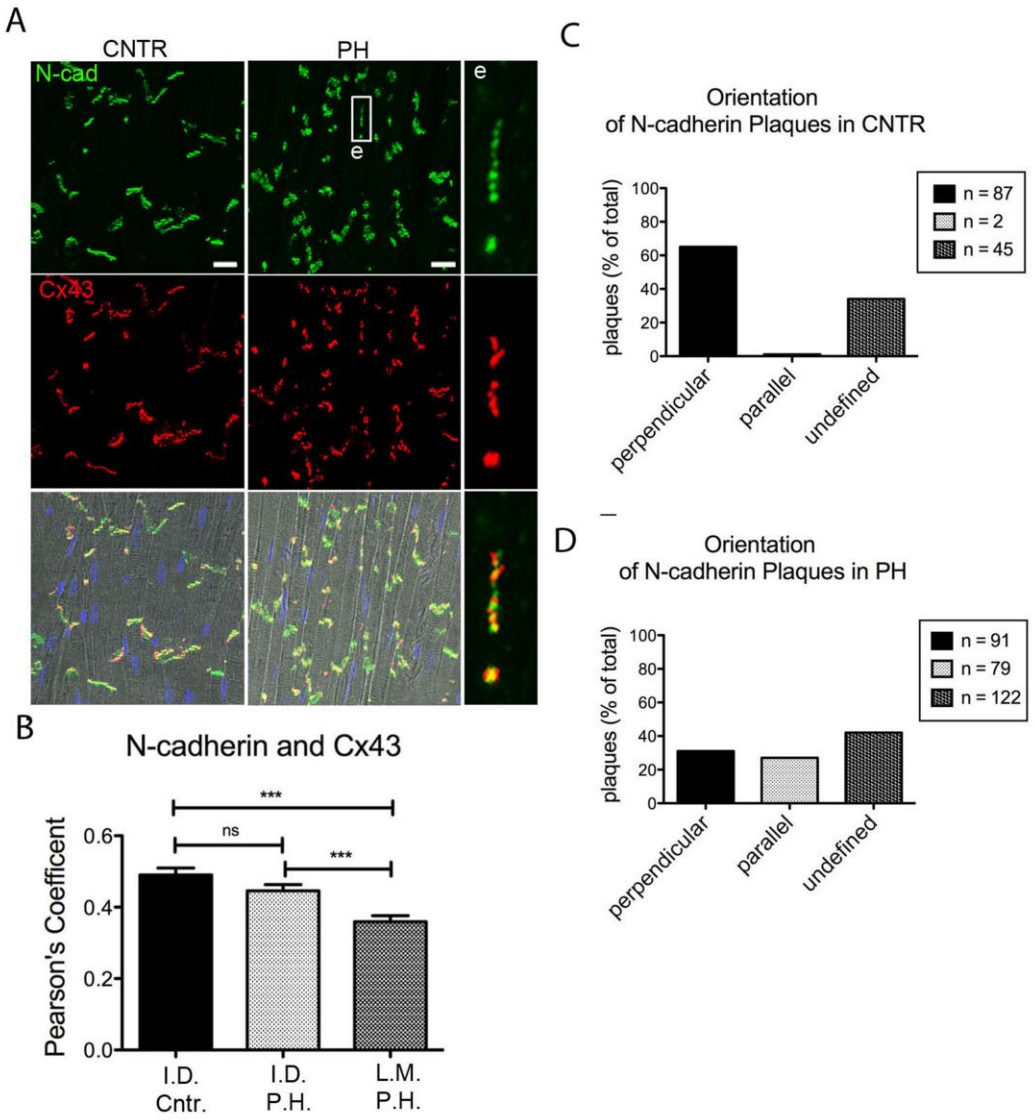

Figure 3.6 Localization of N-cadherin. **A,** Confocal microscopy image obtained from right ventricular tissue of control sheep (CNTR) or sheep afflicted with pulmonary hypertension (PH). N-cadherin, N-cad; green. Connexin43, Cx43, red. Nuclei, TO-PRO-3, blue. **e,** enlarged images of Cx43 with N-cadherin along the long axis. Bar, 20 µm. **B,** Colocalization (Pearson's Coefficient) of N-cadherin and Cx43 in plaques oriented perpendicular (intercalated disc; I.D.) or parallel (lateral membrane; L.M) to the fiber orientation. Statistical analysis: ANOVA, Tukey's Multiple Comparison Test. Mean ± SEM. p values: p>0.05 (ns); p 0.01 to 0.05 (*); p value 0.001 to 0.01 (**); p value 0.001 to 0.0001 (***). N=39, 57, and 51 for I.D. Cntr., I.D. P.H., and L.M. P.H., respectively.**C, D,** Quantification plots representing percentage of DP plaques found in a given orientation with respect to the fiber direction in tissue CNTR (**C**) or PH (**D**) (Chkourko, Guerrero-Serna et al. 2012).

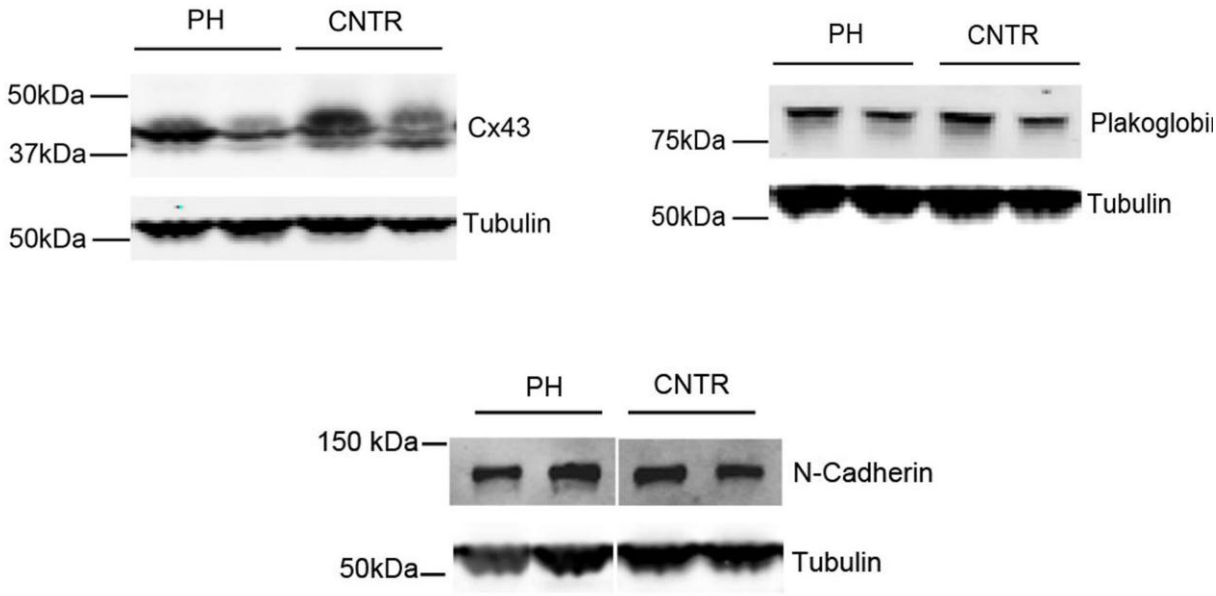

Figure 3.7 Western Blot analysis of CNTR and PH hearts. Duplicate examples of western blots for Cx43, N-cadherin, and plakoglobin showing no differences in protein abundance when compared signals between PH hearts and control (CNTR) (Chkourko, Guerrero-Serna et al. 2012).

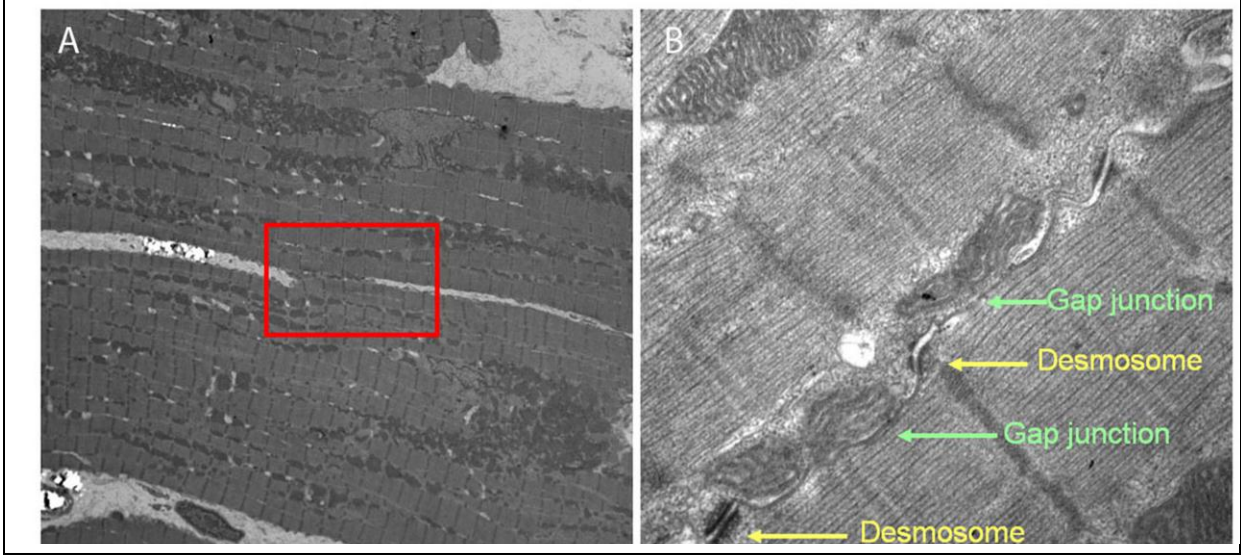

Figure 3.8 Electron Microscopy. Electron microscopy image obtained from the right ventricle of a sheep afflicted with pulmonary hypertension. Low magnification image, 2,600x. **A,** shows the preservation of structures and the orientation of the cells. Area within the red square is shown in **B**, at higher magnification, 34,000x. Notice the presence of lateralized desmosomes and gap junctions oriented parallel to the direction of the fibers. (Chkourko, Guerrero-Serna et al. 2012).

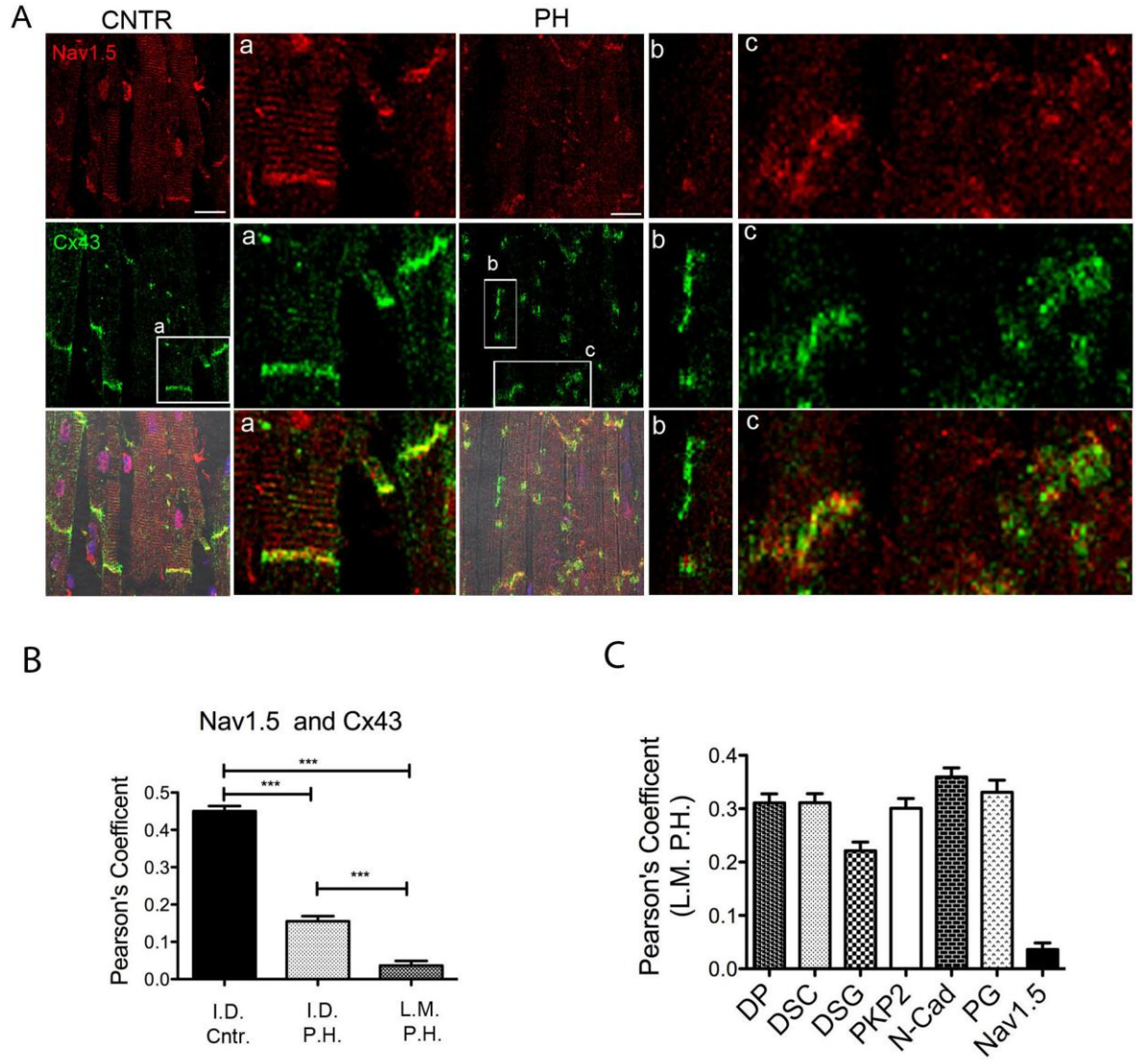

Figure 3.9 $Na_V1.5$ localization in PH hearts. **A,** Confocal microscopy images obtained from CNTR or PH sheep. $Na_V1.5$ (red), Cx43 (green). **a,** enlarged area of intercalated disc from CNTR animal. Notice the colocalization of $Na_V1.5$ and Cx43 highlighted by the yellow color in the merged image. **b,** enlarged area of Cx43 with Nav1.5 along the long axis in the PH tissue. Notice the absence of immunoreactive $Na_V1.5$ where immunoreactive Cx43 is present. **c,** enlarged images of Cx43 and $Na_V1.5$ of two intercalated discs. Notice the presence of immunoreactive $Na_V1.5$ (red) in the "left" intercalated disc and its loss in the "right" one. Bar, 20 μm. **B,** Quantification of Colocalization (Pearson's Coefficient) of Nav1.5 and Cx43 signals at the areas of intercalated disc (ID) in CNTR and PH animals, and at the lateral membrane (LM) of PH animals. Statistical analysis: One-way ANOVA, Tukey's Multiple Comparison Test. Mean ± SEM. P value: 0.001 to 0.0001 (***). Numbers of regions of interest analyzed (N): N=61, 108, and 50 for ID Cntr., ID PH, and LM PH, respectively. C, comparison of Pearson coefficient values for the co-localization of Cx43 with various molecules (noted in abscisae) at the lateral membrane (LM) in PH hearts. ANOVA-Tukey's multiple comparison test showed the value obtained for Cx43- $Na_V1.5$ co-localization was highly different from that obtained for all other junctional molecules ($p<0.0001$) (Chkourko, Guerrero-Serna et al. 2012).

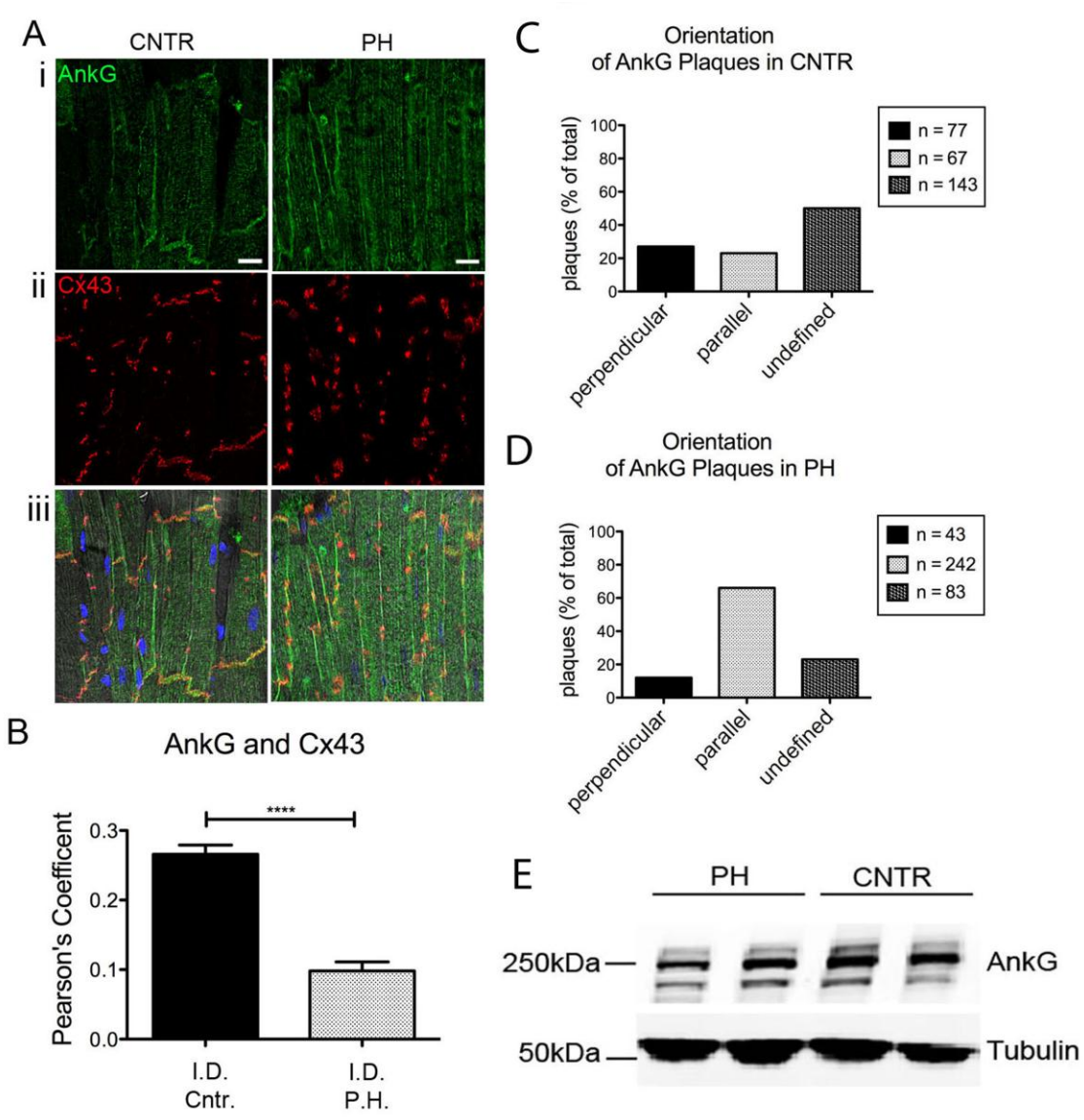

Figure 3.10 Ankyrin-G and Cx43. **A,** Confocal microscopy images obtained from right ventricular tissue of control sheep (CNTR) or sheep afflicted with pulmonary hypertension (PH). Immunoreactive Ankyrin-G (AnkG; green) and Cx43 (red) are presented separately (i, ii) or in a merged image (iii). Nuclei (TO-PRO-3) in blue. **B**, Pearson's coefficient showing the difference in co-localization of AnkG and Cx43 in control, when compared to the PH hearts. Statistical analysis: Unpaired t test. Mean ± SEM. $p<0.0001$ (****) Scale bar: 20 µm **C, D,** Quantification plots representing percentage of AnkG plaques found in a given orientation with respect to the fiber direction in tissue CNTR (**C**) or PH (**D**). **E**, Western Blot analysis of CNTR and PH hearts. Duplicate examples show no changes in protein abundance when compared signal from PH hearts to CNTR (Chkourko, Guerrero-Serna et al. 2012).

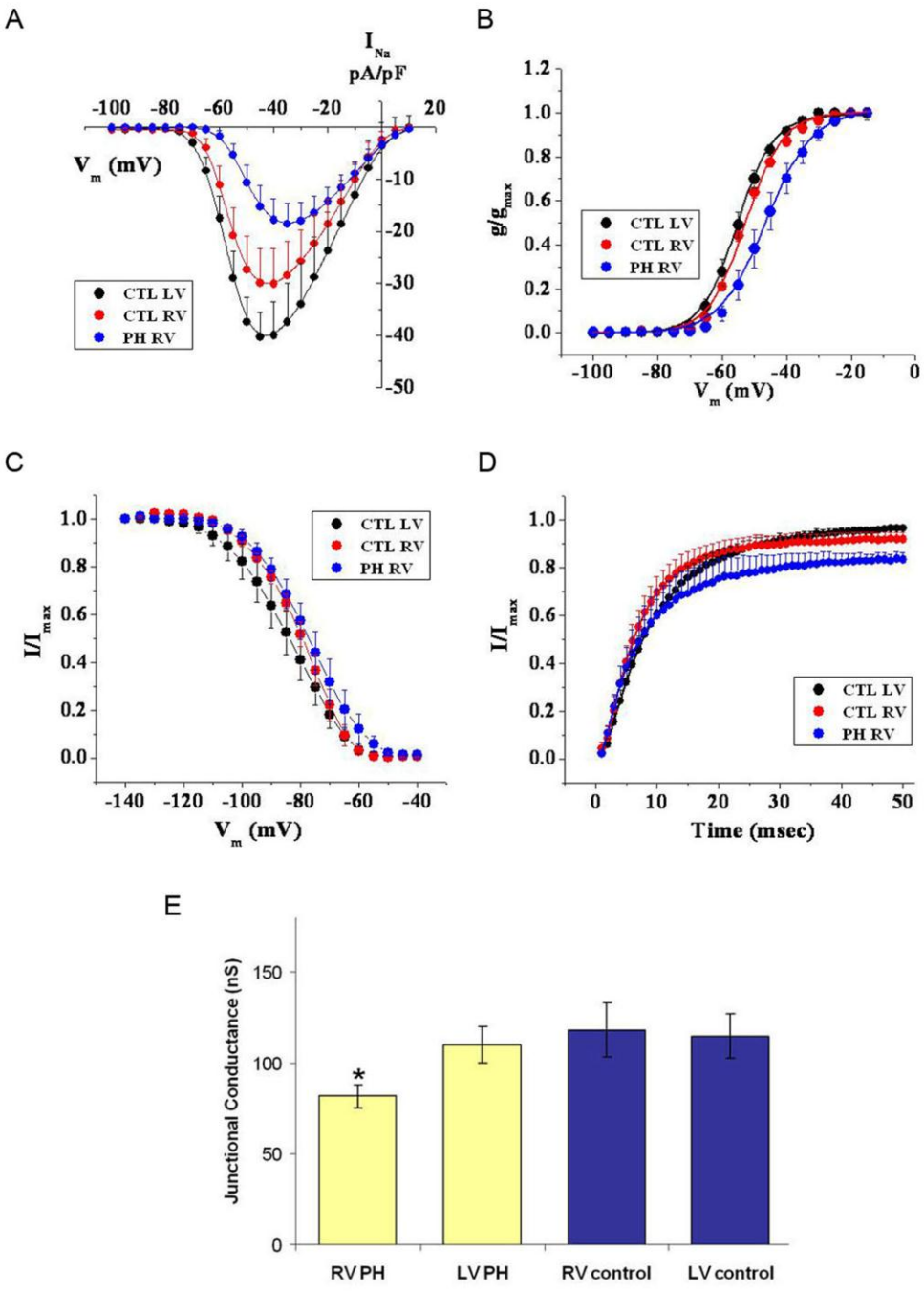

Figure 3.11 Electrophysiological changes. Electrophysiological analysis of ventricular myocytes dissociated from PH-afflicted sheep hearts. **A-D**, Peak average sodium current density (**A**), steady-state activation (**B**), steady-state inactivation (**C**) and recovery from inactivation kinetics (**D**) in ventricular myocytes dissociated from the right (PH RV, blue) or the left ventricle (CTL LV, black) of PH-afflicted sheep hearts, as well as from the right ventricle of a control animal (CTL RV, red). **E**, Junctional conductance measured from cell pairs obtained from either the LV or the RV of control (blue) or PH-afflicted animals (yellow) (Chkourko, Guerrero-Serna et al. 2012).

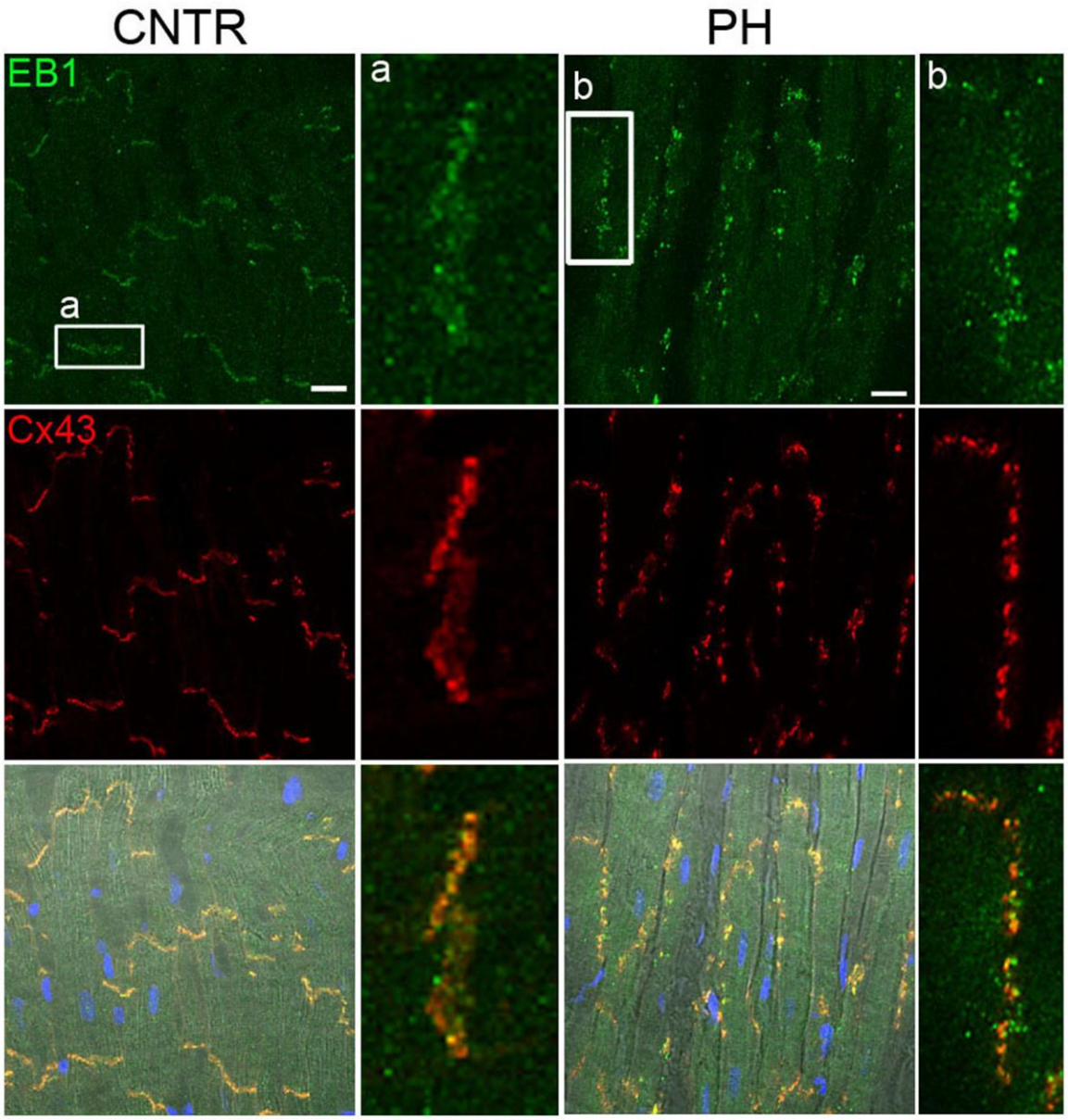

Figure 3.12 Localization of EB1. Confocal microscopy images obtained from right ventricular tissue of CNTR or PH sheep. EB1 (green), Cx43 (red), nuclei (TO-PRO-3, blue). **a**, **b** enlarged areas of intercalated disc in CNTR (**a**) and PH (**b**) tissue. Notice that the area is rotated 90˚ clockwise in (**a**). Scale bar: 20 μm (Chkourko, Guerrero-Serna et al. 2012).

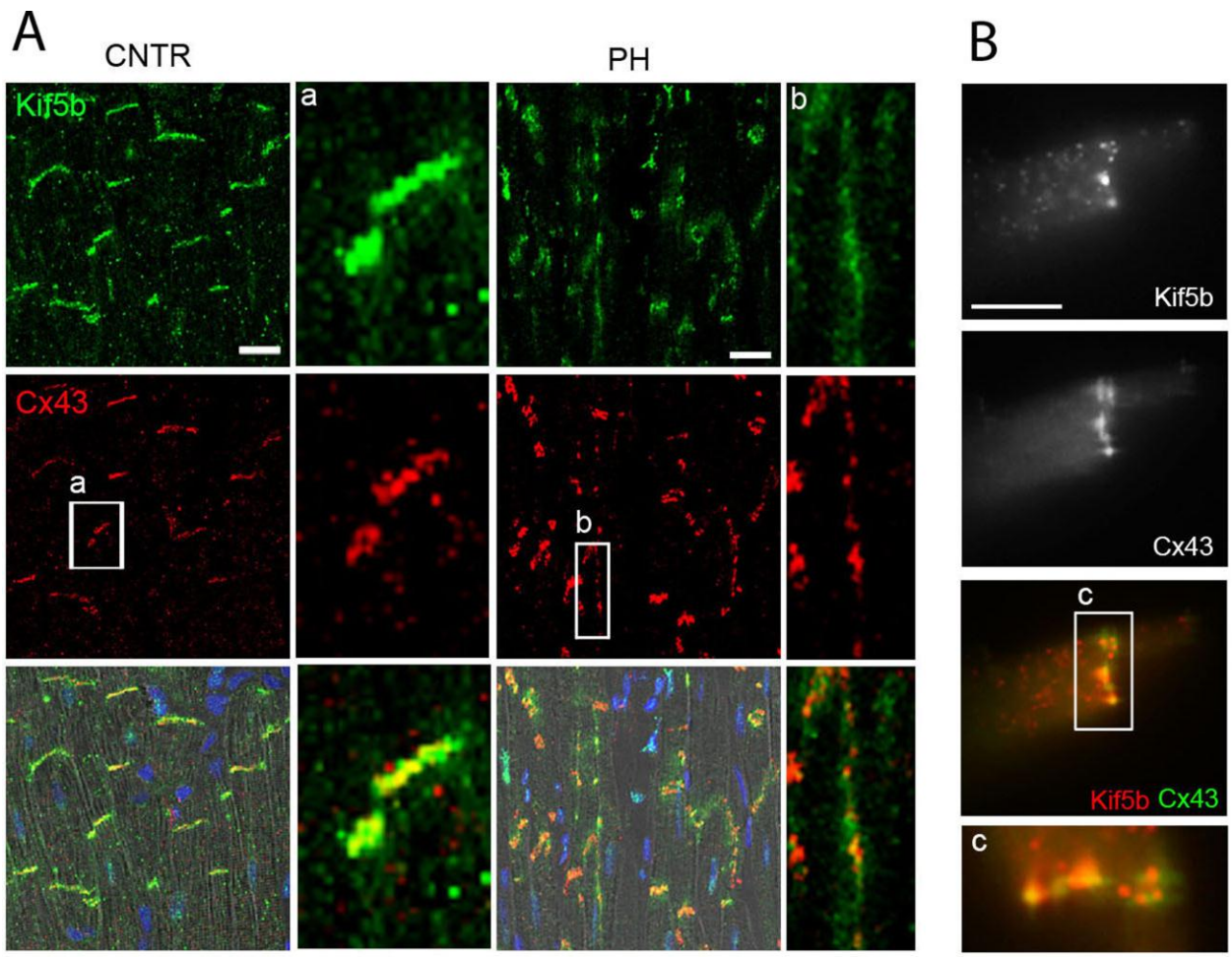

Figure 3.13 Redirection of Kinesin-1 to the lateral membrane. **A,** Confocal microscopy image obtained from right ventricular tissue of CNTR or PH sheep. Kif5b (green), Cx43 (red), nuclei (TO-PRO-3, blue). **a**, enlarged image of Cx43 with Kif5b at the intercalated disc in CNTR. **b**, enlarged image of Cx43 with Kif5b along the long axis. Scale bar: 20 µm. **B,** Localization of Kif5b. TIRF microscopy images obtained from freshly isolated mouse ventricular cardiomyocyte. Notice co-localization of immunoreactive Kif5b and Cx43 (merged panel at the bottom, from box labeled "c"). Scale bar: 5 µm (Chkourko, Guerrero-Serna et al. 2012).

Chapter IV

The Mechanism by Which Connexin43 Regulates Subcellular Localization of $Na_V1.5$

For the preparation of this chapter I performed immunofluorescence, confocal imaging and analysis of the data. I also conducted transfection and western blot experiments. Dr. Xianming Lin performed electrophysiology. Dr. Mingliang Zhang generated the DNA vectors and stable cell lines.

Introduction

The recent report describing the role of gap junctions on the function of ion channels further reinforces the idea of close networking among the proteins residing of the intercalated disc (Jansen, Noorman et al. 2012). Janson et al offered the first evidence implicating connexin43 as a regulator of the function of the VGSC. The study reports that connexin43-deficient mice develop arrhythmias and have decreased immunoreactive $Na_V1.5$ signal at the intercalated disc (Jansen, Noorman et al. 2012). Moreover, the study by Janson et al identifies decreased sodium current as an arrhythmogenic substrate in the connexin43-deficient hearts. The mechanism by which connexin43 regulates $Na_V1.5$ distribution at the cell surface however is not self-evident. Only recently connexin43 was implicated as an accessory to the protein trafficking (Francis, Xu et al. 2011).

Besides its primary role in the cell-cell communication, connexin43 was discovered to participate in cell motility. However, this secondary role of connexin43 is not straightforward since both the overexpression and deficiency (dominant negative) mice models of connexin43 result in hindered cell migration and developmental abnormalities (Ewart, Cohen et al. 1997;

Sullivan, Huang et al. 1998). Moreover, the role of connexin43 on the motility varies among the cell types, i.e. connexin43–deficiency inhibits neuronal cell migration but accelerates migration of keratinocytes (Fushiki, Perez Velazquez et al. 2003; Kretz, Euwens et al. 2003; Mori, Power et al. 2006; Wiencken-Barger, Djukic et al. 2007; Cina, Maass et al. 2009). In the recent study, Francis et al described a mechanism by which connexin43 modulates cell motility through the regulation of microtubule dynamics (Francis, Xu et al. 2011). The study utilizes mouse embryonic fibroblasts (MEFs) and NIH3T3 cells to demonstrate that connexin43 regulates microtubule stability. Loss of connexin43 changes the motility behavior of a cell by altering its polarity, identified by disorientation of microtubule-organizing center (MTOC) and γ-tubulin. Furthermore, the expression level of stabilized detyrosinated microtubules was significantly decreased. Detyrosination is a post-translational modification, and it results from Tyrosine amino acid removal from the carboxy terminus of α-tubulin by a carboxypepetidase. Once Tyrosine is cleaved, Glutamic acid is exposed yielding "Glu-tubulin" (Webster, Gundersen et al. 1987; Hammond, Cai et al. 2008). Stabilization of microtubules by detyrosination was previously reported to play a role in establishing the leading edge of a migrating cell and thus is important for polarization (Gundersen and Bulinski 1988). Francis et al investigated the role of the previously identified tubulin binding domain of connexin43 containing 234-243 residues of the carboxy terminus (Giepmans, Verlaan et al. 2001). The deletion of the tubulin-binding domain (Cx43dT-GFP) resulted in the reduced motility and decreased expression of detyrosinated tubulin (Francis, Xu et al. 2011). Furthermore, Cx43Y17S mutation is found in patients with oculodentodigital dysplasia (ODDD) and it does not hinder delivery of connexin43 to the cell surface but results in non-functional gap junctions (Jordan, Solan et al. 1999; Shibayama, Paznekas et al. 2005). Francis et al utilized this mutation to reveal that the regulation of microtubule stability does not depend on the cell-cell communication because no change in the level of Glu-tubulin was seen in the cells expressing Cx43Y17S when compared to control. Two color TIRF microscopy demonstrated that connexin43 plaques act as tethering molecules for microtubule-capturing at the surface and the deletion of the tubulin binding domain strongly hinders this function (Francis, Xu et al. 2011).

We hypothesized that in cardiac myocytes connexin43 regulates delivery of $Na_V1.5$ to the cellular membrane by modulating microtubule stability. Study by Casini et al demonstrated the

importance of microtubule-cytoskeleton on sodium current (I_{Na}) (Casini, Tan et al. 2010). Although adult cardiomyocytes are not migratory cells, they are highly polarized. We believed that connexin43 plays role in polarization and targeted trafficking of the proteins destined to reside at the intercalated disc. Detyrosination is described as the most abundant post-translational modification of tubulin in healthy ventricular cardiomyocytes (Belmadani, Pous et al. 2004). An expression level of any particular post-translational modification may be important in a scope of delivery of ion channel proteins to the cell membrane. Although we do not know what motor protein delivers $Na_V1.5$, it has been reported that, for instance, Kinesin-1 motor, has a preferential affinity to detyrosinated tubulin when compared to its affinity to tyrosinated (as reviewed in (Liao and Gundersen 1998; Reed, Cai et al. 2006; Hammond, Cai et al. 2008). To explore the regulatory role of connexin43 on the VGSC through microtubule stability in cardiac myocytes we employed immunofluorescence technique combined with the functional assay. We investigated how changes in the expression level of connexin43 affect the expression of Glu-tubulin and, in turn, how alterations of the Glu-tubulin level correlate with distribution of VGSC proteins, and function of the sodium current (I_{Na}). Furthermore, desmosomes are essential for distribution of connexin43 to the cell membrane (Kaplan, Gard et al. 2004; Oxford, Musa et al. 2007). Thus, we investigated whether the deficiency of desmosomal proteins negatively affects the function of the VGSC by mislocalizing connexin43 from the membrane.

Results

Loss of Connexin43 Results in Decrease of Detyrosinated Microtubules in the Cardiac Myocytes

The role of connexin43 on the expression level of stable microtubules in the mouse embryonic fibroblasts and NIH3T3 cells has been explicitly addressed by Francis et al (Francis, Xu et al. 2011). Whether this function of connexin43 is conserved throughout the different cell types and cardiac myocytes, in particular, has not been shown. Thus, we first examined the level of Glu-tubulin in a cell line of cardiac origin. Here we used the mouse atrial myocyte cell line, HL-1, that expresses endogenous connexin43 and $Na_V1.5$ (Claycomb, Lanson et al. 1998). Using lentiviral siRNA technology we generated stable connexin43 deficient HL-1 cell line (Figure 4.1A). As a control, we used HL-1 line that expressed a non-silencing vector (Figure 4.1 A). As expected, connexin43-deficient cells had a significantly lower expression of Glu-tubulin as

determined by western blot (Figure 4.1B and C) and intensity of immunofluorescent signal (Figure 4.1D and E). It is important to note that HL-1 cells originated from the atria and thus they express endogenous connexin40. Whether tubulin- stabilizing function of connexin43 is redundant among various types of connexins was not investigated in this study, but if it is, we are most likely underestimating the effect of connexin43 on Glu-tubulin.

We further assessed the tubulin-stabilizing function of connexin43 in the terminally differentiated cardiomyocytes. For this purpose we used connexin43-deficient mice (α-MHC-Cre:Cx43flox/flox) (Gutstein, Liu et al. 2003). We assessed the level of Glu-tubulin in cardiomyocytes by immunocytochemistry (Figure 4.2A). Importantly, the immonoreactive Glu-tubulin in the connexin43-deficient cardiomyocytes was significantly lower than in the control cells (Figure 4.2B). These results show that in cardiac myocytes – both, undergoing mitosis and terminally differentiated – loss of Cx43 decreases the abundance of Glu-tubulin, likely impairing microtubule stability.

The expression level of Glu-tubulin in connexin43-deficient hearts was also assessed by western blot (Figure 4.2C). Surprisingly, no significant changes in Glu-tubulin between the samples of connexin43 knockout hearts were determined when compared to control. We speculate that these results occurred due to contamination of Glu-tubulin from non-cardiomyocytes. The transcription of Cre is regulated by α-MHC promoter meaning that all non-myocyte cells in the heart preserve its connexin43 and consequently detyrosinated tubulin. In fact, immunofluorescence of freshly isolated heart cells revealed a high abundance of non-cardiomyocyte cells. These cells expressed very high level of Glu-tubulin (Figure 4.2D). Therefore, we speculated that high expression of Glu-tubulin in non-myocyte cells masks the loss of Glu-tubulin in connexin43-deficient cardiac myocytes when assessed by western blot.

Connexin43 affects stabilization of tubulin through detyrosination, but not through polyglutamylation

We asked whether connexin43 modulates other post-translational modifications associated with microtubule stability. Thus, we decided to test connexin43-deficient myocytes

for another type of post-translational modifications - polyglutamylation. No changes in the expression level of polyglutamated tubulin, were detected in HL-1 cells by western blot (Figure 4.3A, B). We also did not find any changes in the immunoreactive polyglutamylated tubulin in the cells from connexin43-deficient mice when compared to control (Figure 4.3C, D). Lack of correlation between the expression level of connexin43 and the level of polyglutamated tubulin suggests a specificity of microtubule stabilization by detyrosination.

Connexin43 mediates microtubule stabilization through its tubulin binding domain

To confirm that loss of Glu-tubulin in connexin43-deficient cells is in fact connexin43-related we performed recovery experiment. Connexin43 was reintroduced into Cx43-deficient HL-1 cells by transient transfection. Since reintroduced connexin43 was labeled with GFP we used vector of GFP alone as a control. Immunoreactive Glu-tubulin signal was measured to determine the expression level. Glu-tubulin expression was significantly higher in the Cx43KO cells expressing Cx43-GFP than in Cx43KO cells expressing GFP (Figure 4.4 A and B).

C-terminus of connexin43 was described to contain a tubulin-binding domain (Giepmans, Verlaan et al. 2001). Francis et al described that the deletion of this domain (Cx43dT-GFP) reduces cellular motility and decreases Glu-tubulin expression (Francis, Xu et al. 2011). On the other hand, Cx43Y17S mutation affects the junctional conductance of gap junctions but does not prevent localization of connexin43 molecules at the cell surface and formation of gap junction plaques (Jordan, Solan et al. 1999; Shibayama, Paznekas et al. 2005). We generated the constructs described by Francis et al and utilized them to confirm the results in the cells of the cardiac origin. Cx43KO cells expressing Cx43dT-GFP have significantly lower expression of Glu-tubulin then Cx43-GFP-expressing cells (Figure 4.4A and B). Tubulin binding domain is necessary for connexin43-mediated stabilization of tubulin. On the other hand, Cx4KO cells expressing Y17S have a similar Glu-tubulin expression as Cx43-GFP expressing cells. Therefore, tubulin-stabilizing function of connexin43 does not depend on channel function of gap junctions. These results are consistent with the findings reported by Francis et al (Francis, Xu et al. 2011).

Connexin43 regulates sodium current via tubulin-stabilization.

Western blot analysis performed on Cx43-deficient HL-1 cells showed that there was no significant difference in the expression of the $Na_V1.5$ protein (Figure 4.5A). The average peak sodium current density is significantly lower in connexin43-deficient HL-1 cells than in control cells (Figure 4.5B). When connexin43 was reintroduced into Cx43KO cells the amplitude of the current significantly increased (Figure 4.5C, GFP (black) and Cx43-GFP (red) traces).

To directly link the function of tubulin-binding domain of connexin43 and VGSC function we measured I_{Na} in connexin43-deficient cells expressing Cx43dT-GFP (Figure 4.5C, green trace). The amplitude of the current in Cx43KO cells transiently expressing Cx43dT-GFP cells was significantly lower than in cells expressing Cx43-GFP (red) (Figure 4.5C).

Connexin43 acts as a tethering molecule for the microtubule growth toward membrane

Francis et al used a two color TIRF technique to demonstrate that besides its role in tubulin stability, tubulin-binding domain is also important for targeting of microtubule to membrane-localized connexin43 (Francis, Xu et al. 2011). This targeting function of connexin43 is very reminiscent of the tethering function of N-cadherin that was earlier described by Shaw et al (Shaw, Fay et al. 2007). In his study, Shaw et al suggested that at the intercalated disc N-cadherin tethers growing end of microtubules (Shaw, Fay et al. 2007). He illustrated it by looking at EB1, microtubule-associated end-plus protein. He demonstrated that in the normal conditions immunoreactive EB1 signal is abundant at the intercalated disc whereas in the failing heart oxidative stress prevents tethering of EB1 resulting in the loss of immunoreactive EB1 signal from the intercalated disc (Shaw, Fay et al. 2007). Therefore, we hypothesized that connexin43 acts as a tethering molecule for a microtubule growing plus end. We performed dual immunolabeling of EB1 and N-cadherin in control and connexin43-deficient tissue to test for microtubule-associated end-plus protein EB1 (Figure 4.6). By measuring Pearson's colocalization coefficient between N-cadherin and EB1 protein, we determined that colocalization in control tissue is significantly higher than in Cx43KO tissue. Since there were

no noticeable changes in the distribution of N-cadherin in connexin43-deficient hearts when compared to control we assumed that EB1 was lost from the intercalated disc.

Loss of Plakophilin-2 Results in Loss of Glu-tubulin

Loss of plakophilin-2 has previously been shown to result in loss of connexin43 expression at the cell membrane and accumulation inside (Oxford, Musa et al. 2007). Thus we hypothesized that PKP2-defficiency will alter distribution of connexin43 and that in turn will lead to a decrease of Glu-tubulin. Employing the previously described method, we generated plakophilin-2-deficient stable HL-1 cell line (Figure 4.7A). As expected, total level of Glu-tubulin was decreased in PKP2-KO HL-1 cells as described by western blot (Figure 4.7B and C) and immunocytochemistry (Figure 4.7D and E). Overexpression of connexin43 in PKP2-KO HL-1 cells did not recover the level of Glu-tubulin. When we compared fluorescence intensity of Glu-tubulin from 19 PKP2KO cells expressing GFP and 26 PKP2KO cells expressing Cx43-GFP constract no significant (p value = 0.953) differences were found. Similar results were found when sodium current (I_{Na}) was measured in PKP2-KO cells expressing GFP or Cx43-GFP.

To confirm these findings in fully differentiated cardiomyocytes we employed plakophilin-2 heterozygote mouse model (Cerrone, Noorman et al. 2012). Measurements of immunoreactive connexin43 in PKP2-deficient cardiomyocytes revealed significant loss of the number of connexin43 gap junction plaques in PKP2+/- cells when compared to wild type (Figure 4.8 A and B). Glu-tubulin was also significant decreased in PKP2-deficient cells (Figure 4.8A and C). Consistent with these findings, patch-clamp experiments on PKP2-deficient HL-1 cells demonstrated loss of I_{Na} (Figure 4.9). Cerone et al reported similar results in PKP2 heterozygote cells (Cerrone, Noorman et al. 2012).

Discussion

The study reported in this chapter describes a mechanism by which connexin43 regulates function and distribution of the VGSC on the cell membrane. These findings further complement

the idea that proteins of the intercalated disc do not function independently as separate entities, but rather interact closely as parts of macromolecular complex.

Connexin43 regulates tubulin cytoskeleton and this function is preserved throughout various cell types. Adult cardiac myocytes are fully differentiated cells that do not divide or undergo migration. Alternatively, these are highly polarized cells with a very precise and consistent subcellular distribution of proteins. Thus we postulated that in cardiac myocytes microtubule stability plays a role in maintaining cellular polarity. Our study with the mutant Cx43 constructs shows that the ability of Cx43 to interact with the microtubules is related to its ability to modulate the sodium current. Study by Casini et al has indicated that the trafficking of $Na_V1.5$ is microtubule-mediated (Casini, Tan et al. 2010). In this study, Casini et al, utilizes non-specific tubulin-stabilizing drug taxol the use of which has been implicated in the development of cardiac arrhythmias. Taxol-induced tubulin polymerization resulted in significant decrease of sodium current amplitude. Whether there is a preferential movement of $Na_V1.5$- delivering machinery along one type of stable microtubules versus the other is yet to be determined. Aside from detyrosination, the only other type of post-translational modifications of tubulin that we examined was polyglutamylation. Although we did not find any changes in the level of polyglutamylated tubulin we cannot exclude the possibility that connexin43 regulates tubulin cytoskeleton through other types of post-translation modifications, i.e. acetylation. When not modified, microtubules are highly unstable structures and undergo constant growth and catastrophe. Thus, connexin43 may just increase global tubulin stability, regardless of the type of post-translational modification, and thus increase the probability rate of anterograde delivery of $Na_V1.5$ to the membrane.

Connexin43-mediated tubulin stabilization may differ from pharmacological agents – mediated tubulin stabilization. Casini et al showed that treatement of HEK293 cells with a tubulin-stabilizing agent, taxol, resulted in 50% decrease in the amplitude of sodium current (I_{Na}) (Casini, Tan et al. 2010). At first glance, this finding contradicts the results we describe in this chapter. On the other hand, in the earlier work by Shaw et al, taxol was also used to study the effect it may have on the abundance of connexin43 gap junction plaques (Shaw, Fay et al. 2007). Treatment with taxol led to the decrease of the number of gap junction plaques at the cell-cell

border (Shaw, Fay et al. 2007). Taxol-induced loss of surface connexin43 may explain why taxol results in the loss of the sodium current. Taxol exhibits its effect by binding to the β-tubulin subunit of microtubule. This taxol-β-tubulin interaction prevents normal dynamic GTP-dependent exchange of α/β-tubulin heterodimer at the growing plus-end of microtubules. Microtubules become stable, rigid and resistant to Ca^{2+} and cold temperature–induced depolymerization (Xiao, Verdier-Pinard et al. 2006). I speculate that taxol-treatment stabilized every microtubule in the cell, some of which were connecting cytoplasmic organnels and some microtubules were approaching but not yet reaching a membrane. This "global stabilization" would eventually deplete all the available pool of tubulin heterodimers resulting in hindering anterograde trafficking. The functional differences between taxol-stabilized microtubules and physiologically stable ones are important to keep in mind when taking cytoskeleton-modulating approach for therapeutic needs.

Besides its role in modulating tubulin stability, connexin43 also acts as a tethering molecule for a microtubule growing end. Earlier, Smyth et al described an abundance of EB1 protein at the intercalated disc in the normal heart and loss of this abundance in the failing heart (Smyth, Hong et al. 2010). The study offered a hypothesis postulating that in the normal heart N-cadherin tethers microtubule growth to the intercalated disc whereas in the failing heart, oxidative stress disrupts the tethering process resulting in the loss of EB1 (Smyth, Hong et al. 2010). On the other hand, at the intercalated disc of the failing heart, N-cadherin signal is preserved whereas connexin43 is lost (Smyth, Hong et al. 2010). Study by Jansen et al described how loss of connexin43 coincides with dislocation of $Na_V1.5$ from the intercalated disc and loss of I_{Na} (Jansen, Noorman et al. 2012). Together with our finding showing that loss of connexin43 results in loss of immunoreactive EB1 at the intercalated disc, we postulated that connexin43 is a primary molecule for targeted microtubule growth to the intercalated disc. It has been well documented that presence of competent N-cadherin and PKP2 at the cell membrane are absolute requirements for the formation of connexin43 gap junctions (Meyer, Laird et al. 1992; Oxford, Musa et al. 2007). Therefore, we suggested that N-cadherin and PKP2, are indirectly involved in tubulin tethering. As a result, loss of either N-cadherin, PKP2, or connexin43 will abrogate tubulin-tethering function and hinder forward trafficking.

PKP2 regulation of I_{Na} is connexin43-mediated. PKP2 is a desmosomal protein participating in maintaining cellular membranes in a close proximity to each other for the generation of gap junctions. Disruption of the function of PKP2 results in the subcellular redistribution of connexin43 and loss of junctional conductance (Oxford, Musa et al. 2007). For a while, loss of PKP2-mediated arrhythmias were attributed to the loss of electrical coupling. Alternatively, loss of PKP2 was also found to result in alteration of I_{Na} (Sato, Musa et al. 2009). Recent *in vivo* studies by Cerone et al suggest that arrhythmias linked to PKP2-deficiency are likely to be provoked by the decreased sodium current than by loss of electrical coupling (Cerrone, Noorman et al. 2012). We do not know if the loss of $Na_V1.5$ in the PH model is related to other effects triggered by the PH, independent from the molecular changes in Cx43 or in desmosomes. That is why we moved onto genetically modified mice, where we can study one protein at a time.

In summary, connexin43 regulates the distribution of $Na_V1.5$ at the cell membrane by regulating microtubule network. There are two possible ways for this regulation to occur. First, connexin43 affects tubulin stability and thus may have a positive effect on the delivery of $Na_V1.5$ to the membrane if there is a preferential delivery of $Na_V1.5$ along stable microtubules. Second, connexin43 tethers microtubule growth toward intercalated disc and thus increases chances for $Na_V1.5$ to be delivered to intercalated disc as opposed to elsewhere. Connexin-43-mediated tubulin stabilization and tethering to the intercalated disc involve tubulin-binding domain of connexin43.

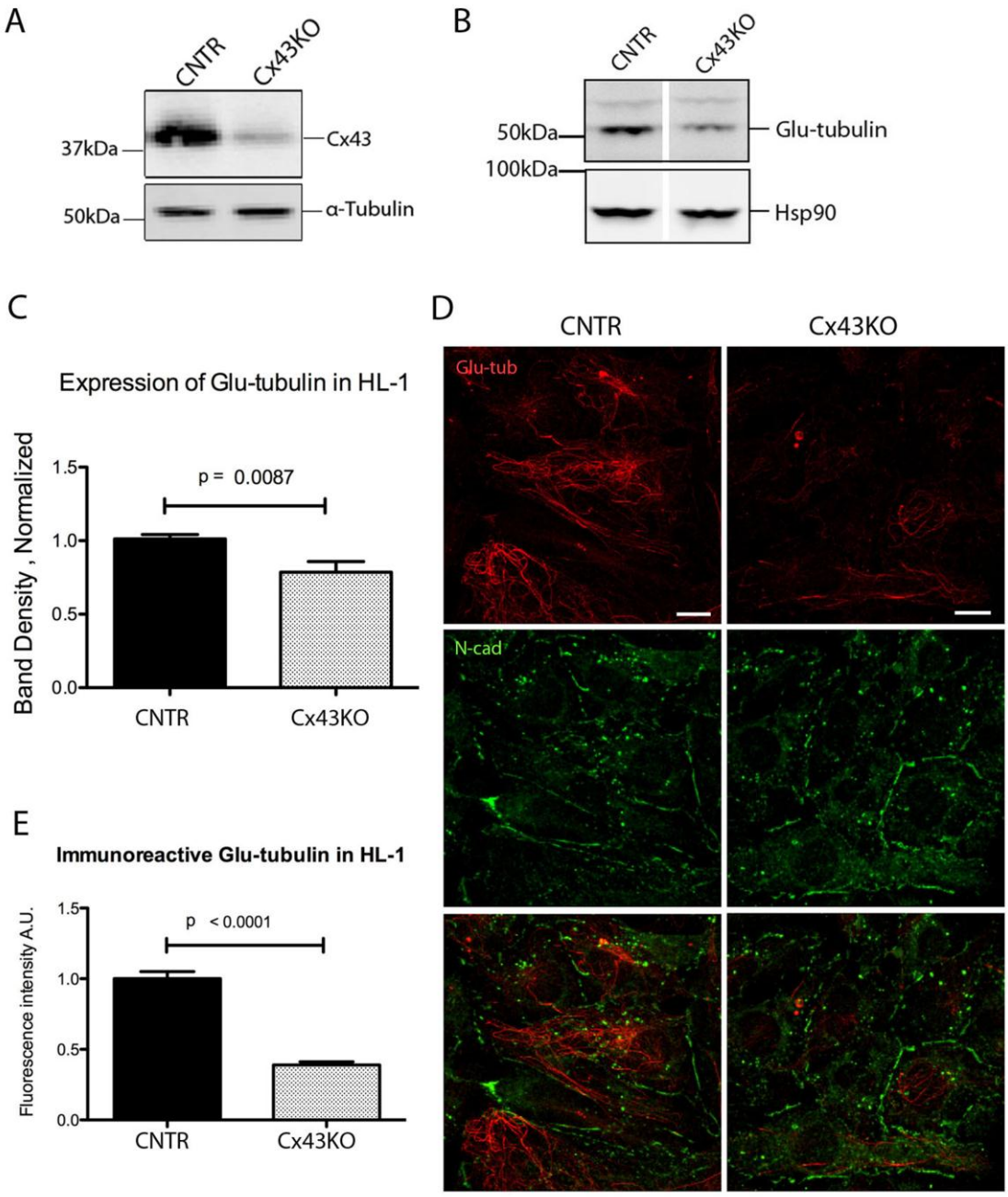

Figure 4.1 Loss of connexin43 decreases total Glu-tubulin in HL-1 cells. **A, B** Western blots of Cx43(**A**) and Glu-tubulin(**B**) expression in control (CNTR) and connexin43-deficient HL-1 cells (Cx43KO). A-Tubulin and Hsp90 are loading controls. **C,** Densitometry analysis of Glu-tubulin. Each band was normalized to its loading control. n= number of lysates. CNTR (n=14) and Cx43KO (n=15).**D,** Immunocytochemistry of immunoreactive Glu-tubulin and N-cadherin. Scale bar =10 μm. **E,** Quantitative assessment of fluorescence intensity of Glu-tubulin in individual CNTR (n =191) and Cx43KO (n= 154) cells. Regions of interest (or n) were oriented by immunoreactive N-cadherin.

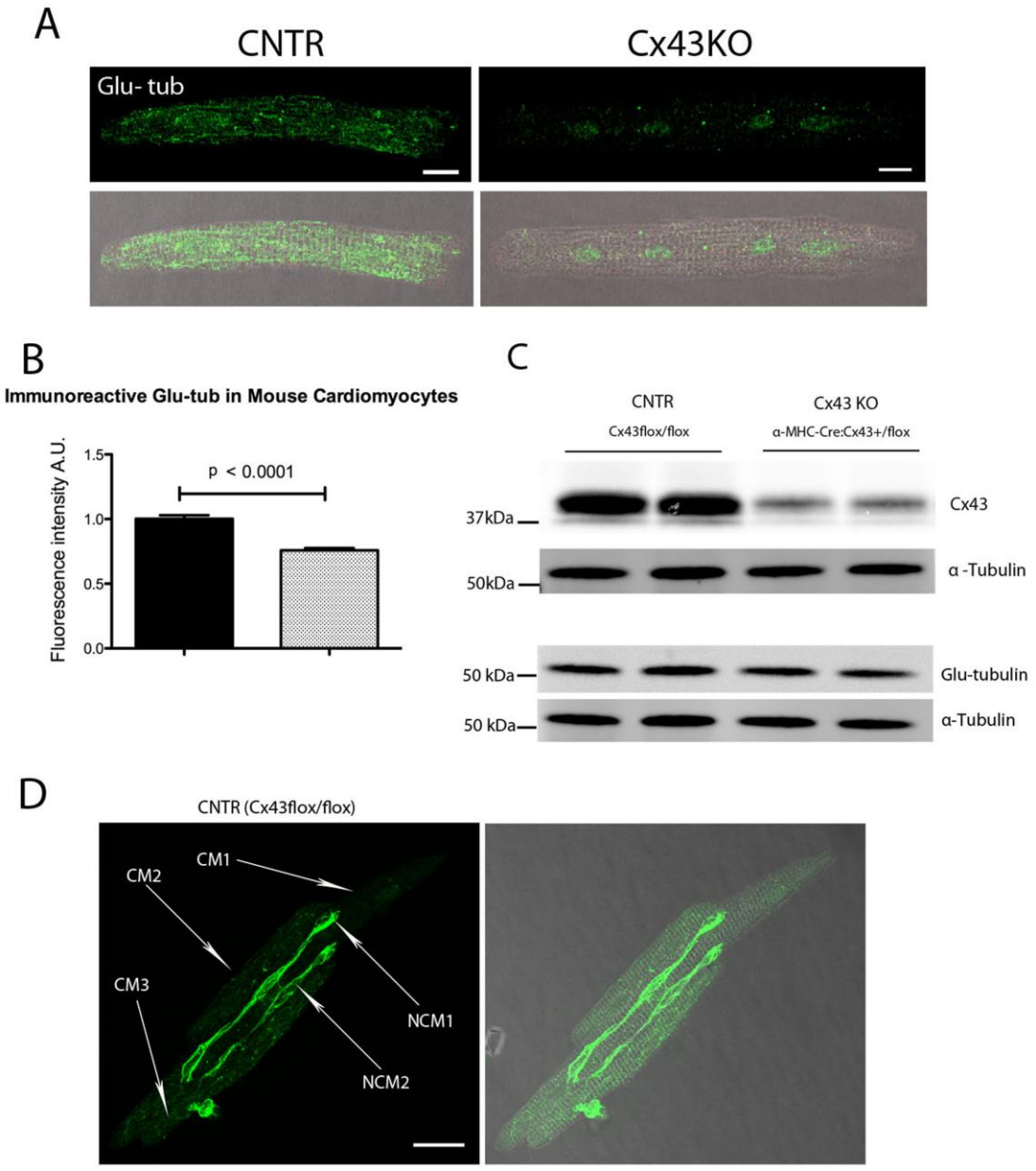

Figure 4.2 Glu-tubulin is decreased in connexin43 deficient cardiac myocytes. **A,** Immunoreactive Glu-tubulin in mouse cardiomyocytes from CNTR (Cx43flox/flox) or Cx43KO (α-MHC-Cre:Cx43flox/flox) animal. Scale, 20 μm. **B,** Quantitative assessment of Glu-tubulin in CNTR (N=3, n=77) vs Cx43KO cardiomyocytes (N=4, n=136), N= number of animals, n=number of cells. **C,** Western blots of Cx43 and Glu-tubulin in CNTR (Cx43flox/flox) and Cx43 null (Cx43KO, α-MHC-Cre:Cx43+/flox) hearts. α-Tubulin is loading control. **D,** Immunoreactive Glu-tubulin in a mixture of non-fully dissociated cardiomyocytes (CM) and non-cardiomyocytes (NCM) from CNTR mouse. Note the difference in the intensity of the signal between CM and NCM. Scale, 20 μm.

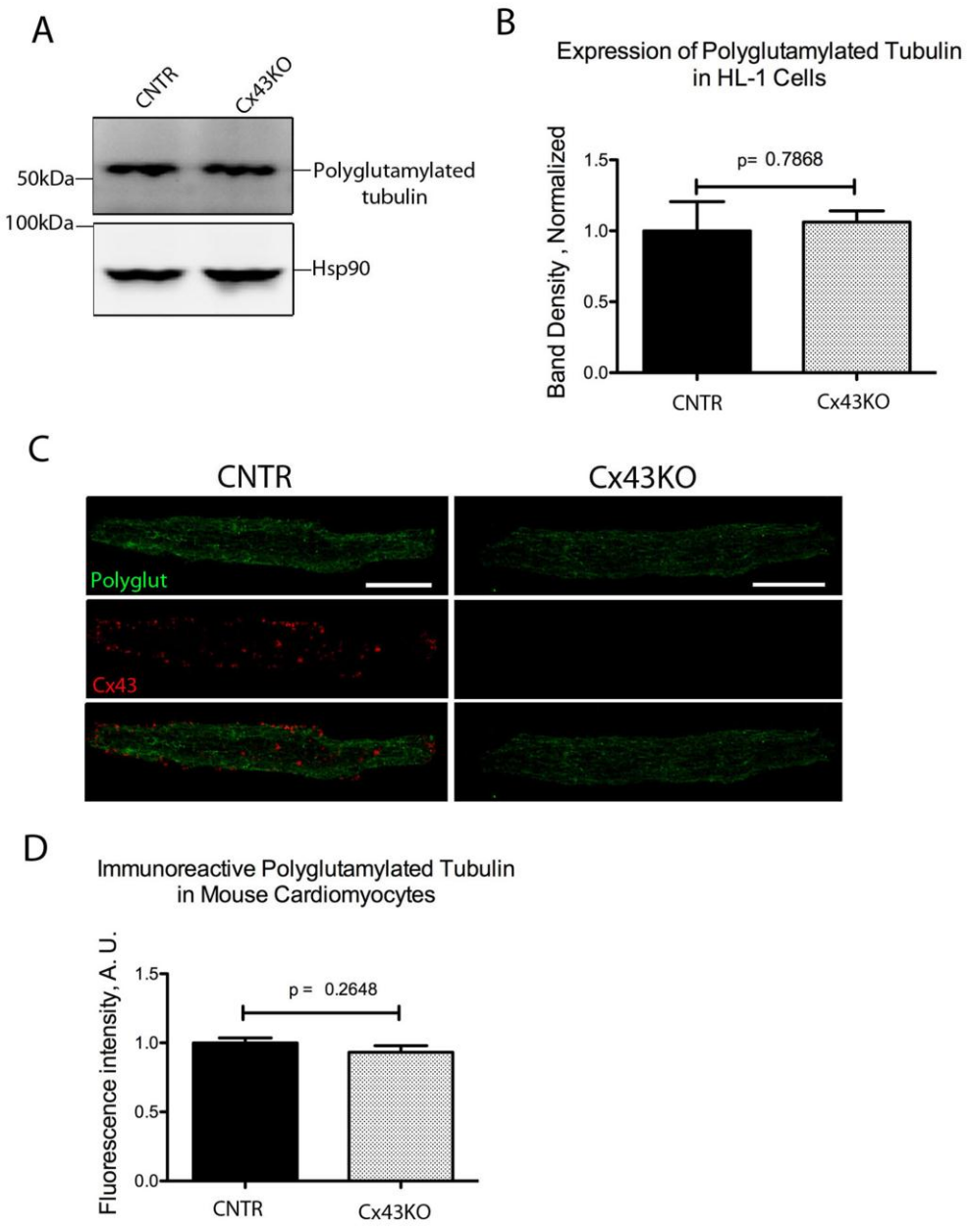

Figure 4.3 No difference in polyglutamylated tubulin in connexin43 deficient cardiac myocytes. **A**, Western blot of polyglutamylated tubulin expression in control (CNTR) and connexin43-deficient HL-1 cells (Cx43KO). Hsp90 is a loading control. **B,** Densitometry analysis. Each band was normalized to its loading control. n= number of lysates. CNTR (n=4) and Cx43KO (n=4).**C,** Immunoreactive polyglutamylated (polyglot) in mouse cardiomyocytes from CNTR (Cx43flox/flox) or Cx43KO (α-MHC-Cre:Cx43flox/flox) animal. Scale, 20 μm. **D,** Quantitative assessment of Glu-tubulin in CNTR (n=21) vs Cx43KO cardiomyocytes (n=23), n= number of cells.

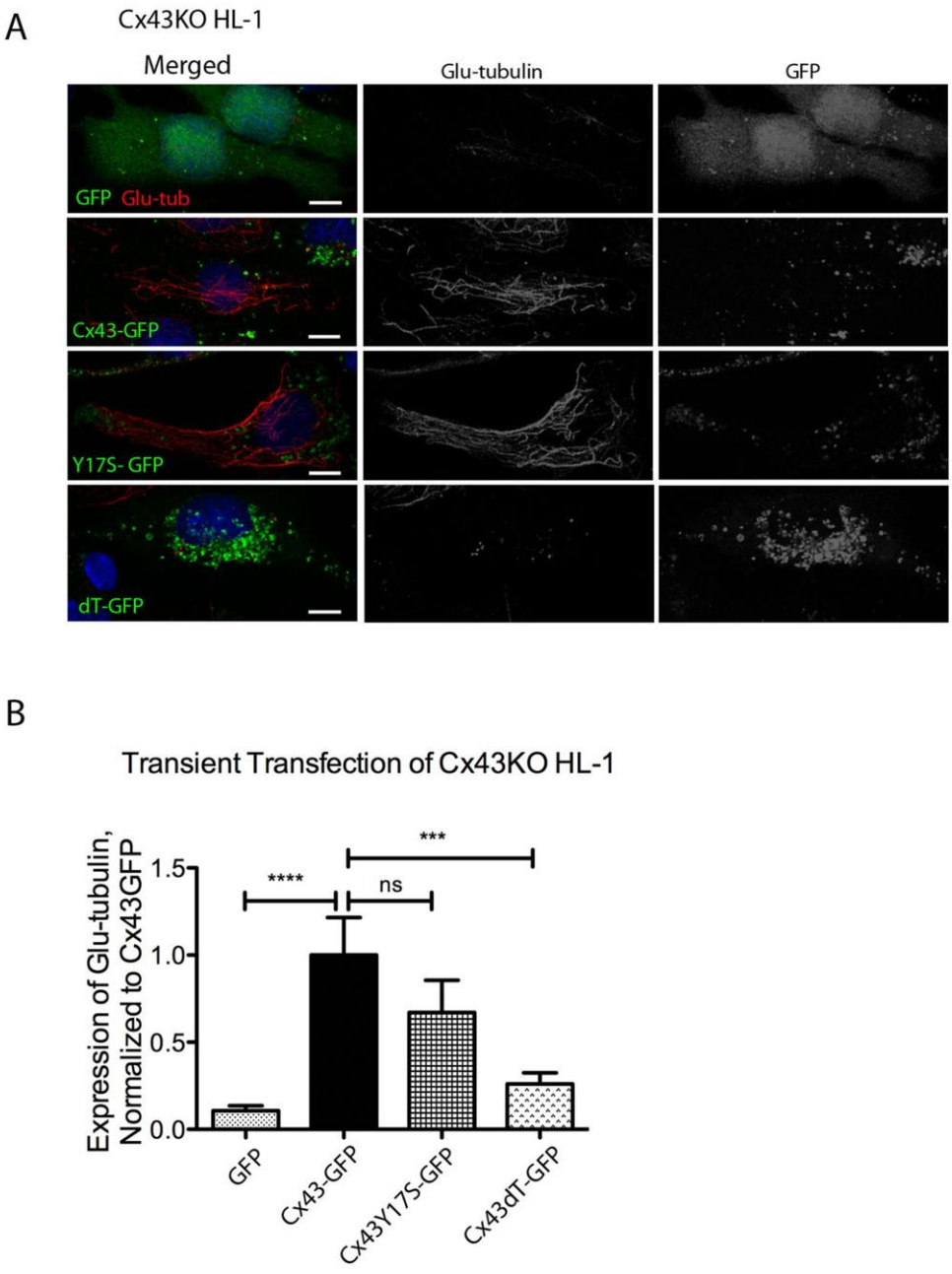

Figure 4.4 Tubulin-binding domain is important for tubulin-stabilizing function of connexin43. **A.** Cx43KO HL-1 cells transiently transfected with plasmids GFP, Cx43-GFP, Cx43dT-GFP and Cx43Y17S-GFP and immunolabeled with Glu-tubulin (red). Scale bar: 10μm. **B,** Quantitative assessment of Glu-tubulin staining in Cx43KO cells expressing GFP (n=22), Cx43-GFP (n=20), Cx43Y17S-GFP (n=17), and Cx43dT-GFP (n=29). For statistical comparison Bonferroni's Multiple Comparison Test was performed.

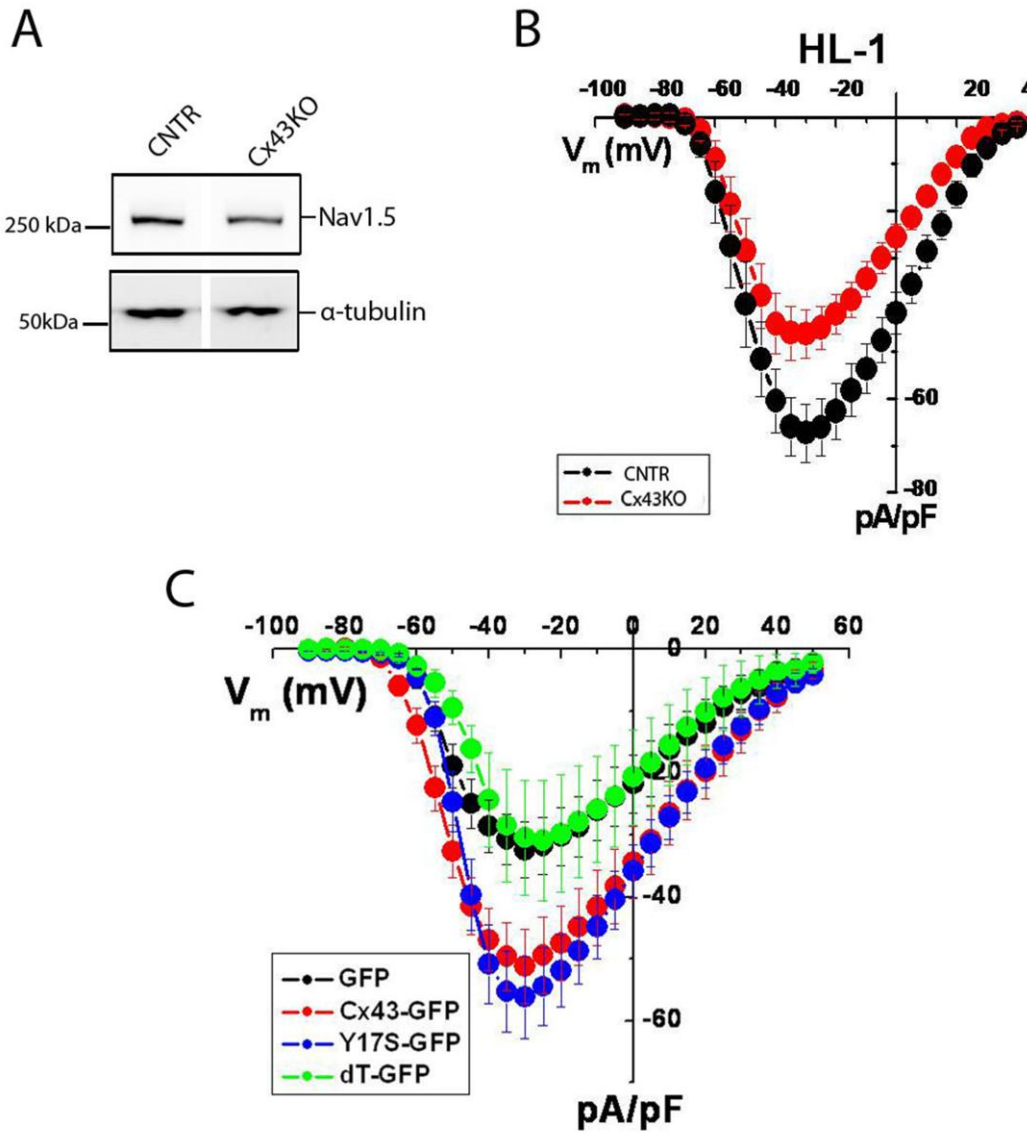

Figure 4.5 A, Western blot of $Na_V1.5$ from CNTR (n=10) and Cx43KO (n=9) HL-1 lysates. α-tubulin is a loading control. **B,** Average peak sodium current density as a function of voltage command in CNTR or Cx43KO HL-1 cells. Peak current amplitude at -30mV: CNTR: -67.30±6.16 pA/pF; n=13. Cx43KO:-46.18±5.18pA/pF; n=11. P<0.016. **C,** Average peak sodium current density as a function of voltage command in Cx43KO HL-1 cells transiently expressing GFP (black, n=11), Cx43-GFP (red, n=13), Cx43Y17S- GFP (blue, n=11) and Cx43dT-GFP (green, n=11). Peak current amplitude at -30 mV: Cx43-GFP: -51.15±5.566pA/pF. Cx43dT-GFP: - 30.45 pA/pF; P=0.0467. Statistical analysis is performed using unpaired student t-test.

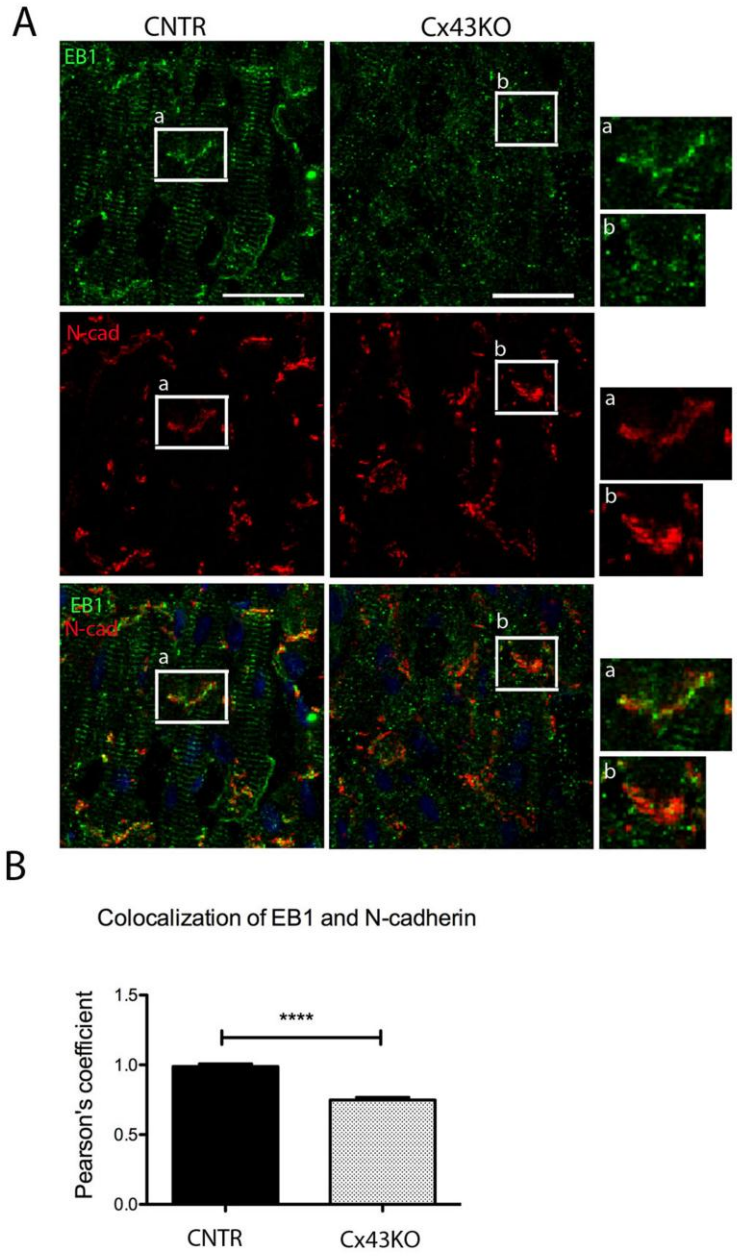

Figure 4.6 Loss of EB1 from the intercalated disc in Cx43KO animals. **A,** Immunolabeling of CNTR (cre negative) and Cx43KO cardiac tissue for EB1 (green) and N-cadherin (red). Scale bar = 20 μm. **B,** Quantitative assessment of co-localization of EB1 and N-cadherin by Pearson's coefficient in CNTR (n=169) and Cx43KO (n=184). n= region of interest.

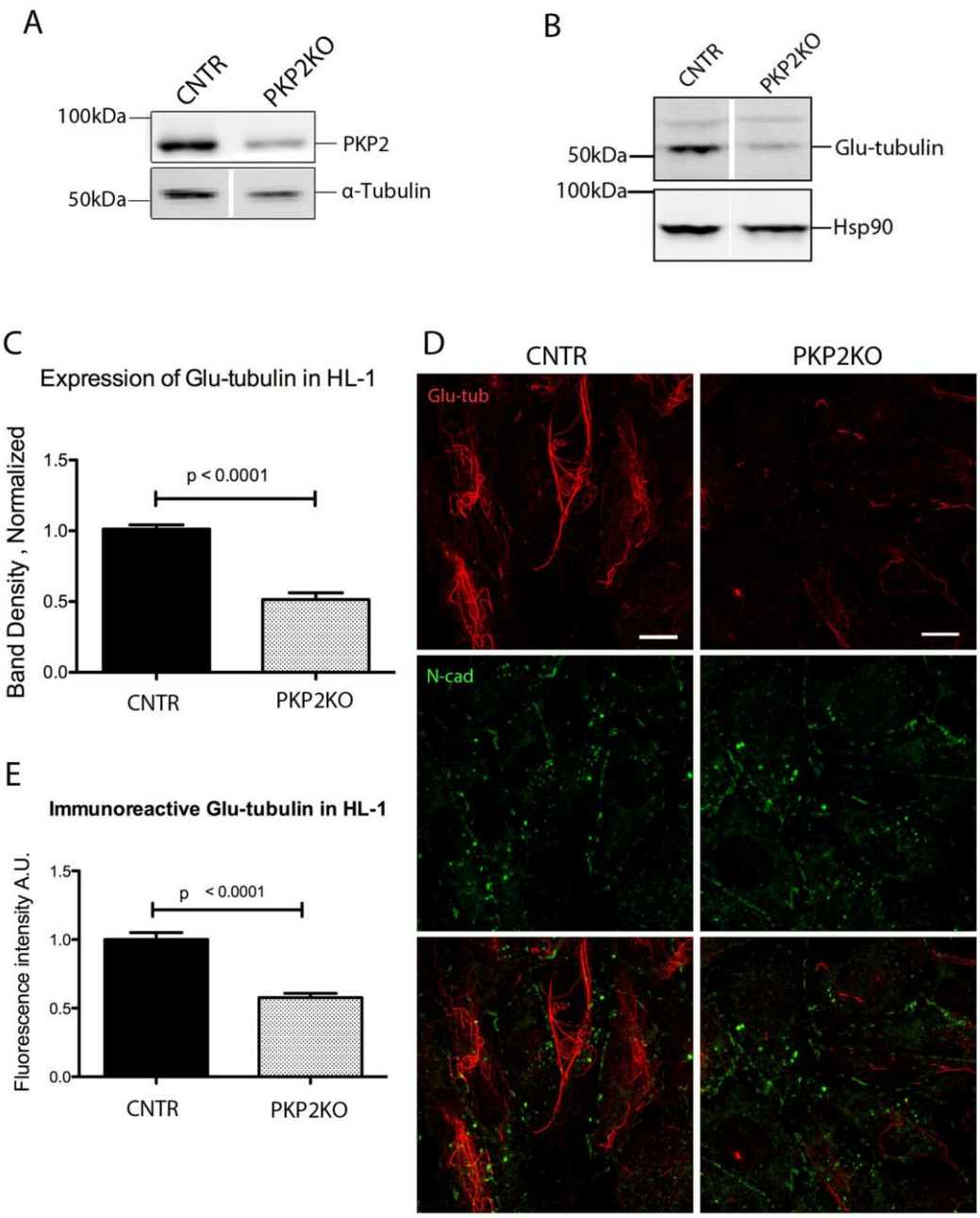

Figure 4.7 Loss of Glu-tubulin expression in PKP2 deficient HL-1 cells. **A,** western blot HL-1 cells stably transfected with non-silencing vector (CNTR) and connexin43-silencing vector (Cx43KO). **B,** immunoblotting of Glu-tubulin in CNTR (N=4, n=14) and PKP2KO (N=4, n=15) HL-1 cells. **C,** densitometry analysis of Glu-tubulin bands from CNTR and PKP2 KO cells. **D,** Immunocytochemistry of immunoreactive Glu-tubulin and N-cadherin. Scale bar =10 μm. **D,** Measurements of fluorescence intensity of Glu-tubulin in individual CNTR (n =191) and PKP2KO (n= 201) cells.

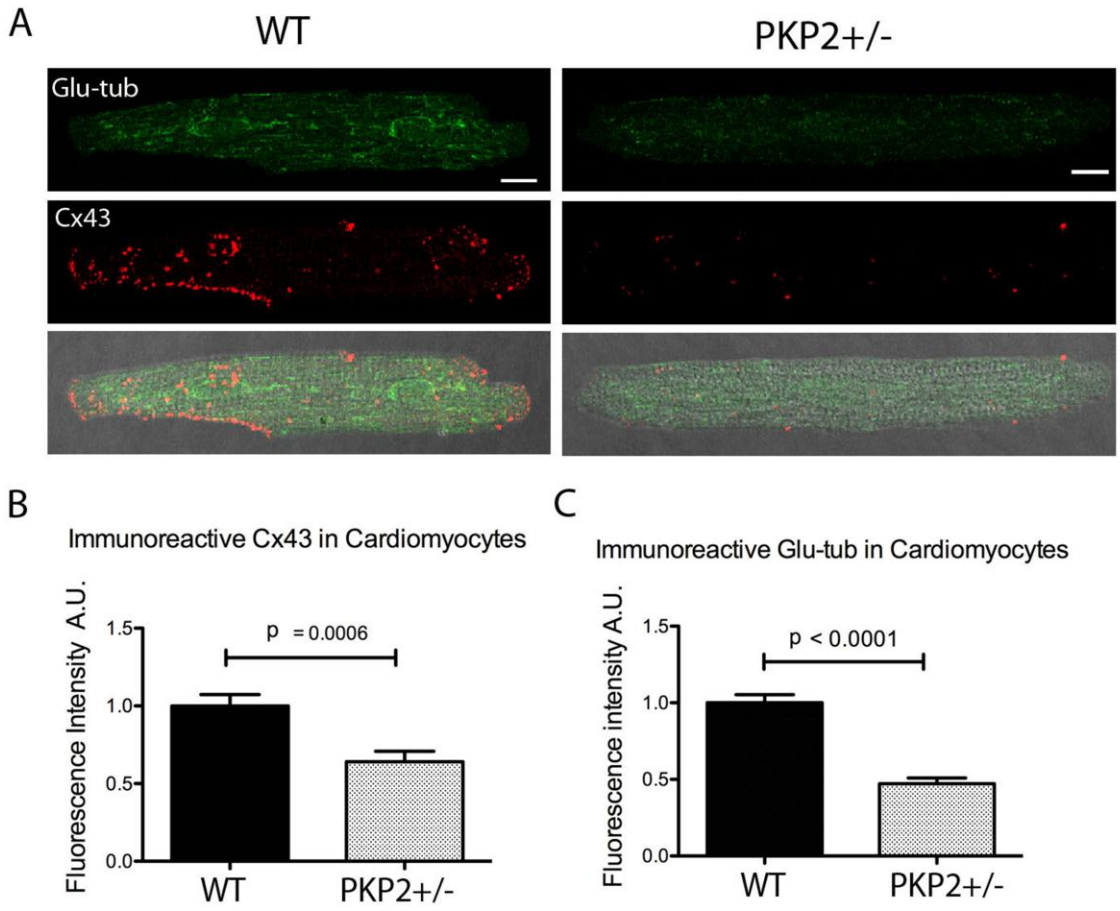

Figure 4.8 Loss of Glu-tubulin in PKP2 dedicient cardiac myocytes. **A,** Immunolabeling of Glu-tubulin (green) and connexin43 (red) in wild type (WT) control or PKP2-heterozygote (PKP2+/-) cells. **B,** quantitative assessment of immonoreactive connexin43 signal in WT (N=2, n=40) and PKP2KO (N=3, n=51). **C,** quantitative assessment of Glu-tubulin signal (N=2, n=40) and PKP2KO (N=3, n=51).

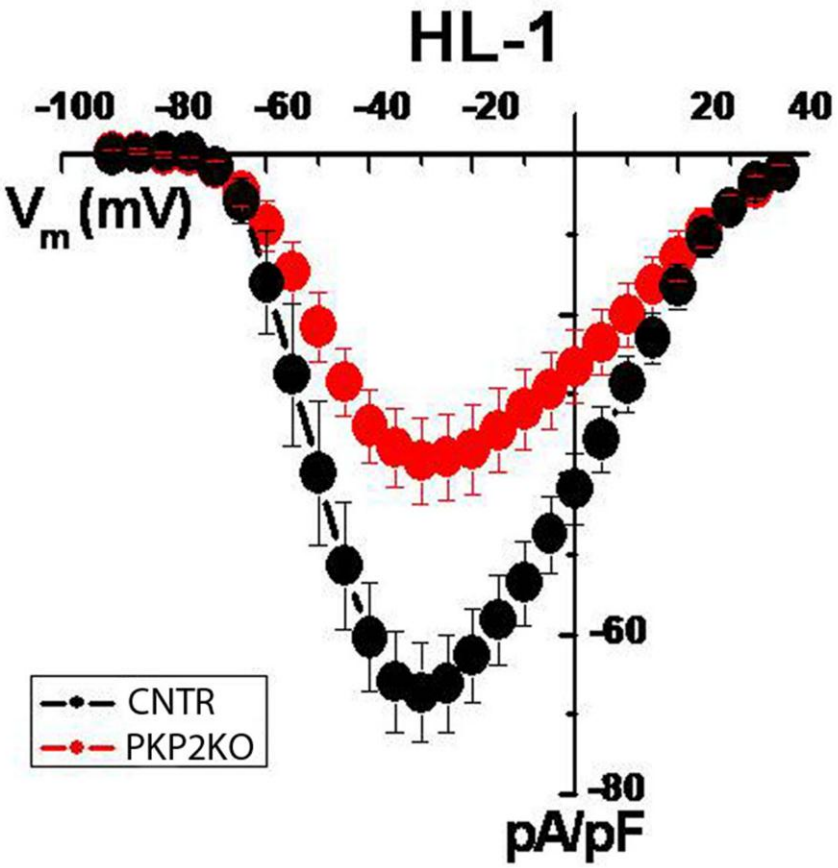

Figure 4.9 Average peak sodium current density as a function of voltage command in CNTR or PKP2-KO HL-1 cells. Peak current amplitude at -30 mV: CNTR: -67.30±6.16pA/pF; n=13. Cx43KO: - 38.30±5.35 pA/pF; n=10. $p<0.0025$.

Chapter V

Summary, Final Discussion and Unanswered Questions

The central idea of this thesis was to convey a thought that proteins residing at the intercalated disc function together as macromolecular complexes. The closer look we took into the functional interactions between desmosomal proteins, gap junctions and VGSC the more convinced we have become that none of these proteins are functionally segregated.

One approach to study how one protein influences the other is by looking at it from the angle of a disease. In an attempt to understand the mechanism of gap junctions remodeling in the diseased heart we implemented the pulmonary hypertension model of a sheep. Going into the study we had a set of questions to address. First, do mechanical junction proteins accompany connexin43 appearance at the lateral membrane? We knew that mechanical junctions are critical for the formation of gap junction plaques, but there had been no evidence placing desmosomes to the lateral membrane. Based on the data from the confocal and electron microscopy studies we drew the conclusion that desmosomal proteins undergo remodeling and most likely precede the formation of lateralized connexin43 gap junction plaques. The next question – what is the fate of $Na_V1.5$ in the scope of connexin43 remodeling? Jansen et al study offered the first evidence that the function of the VGSC was dependent on connexin43 expression (Jansen, Noorman et al. 2012). At this point, we could not be certain of what contributed to the loss of $Na_V1.5$ at the intercalated disc. Remodeling of what is considered to be the most stable protein of the intercalated disc, N-cadherin, prevented us from having a point of comparison. Thus, we were unable to find out whether the abundance of connexin43 and desmosomal molecules was changed at the intercalated disc. On the other hand, western blot studies did not reveal any changes in the total expression level of these proteins. Thus, we could only speculate that

perhaps the number of Cx43 and desmosomal proteins was lower at the intercalated disc because a significant amount of gap junctions and desmosomes was found at the lateral membrane. It is plausible to think that either potential change in the abundance of gap junctions and desmosomes at the intercalated disc or decrease of immunoreactive ankyrin-G may have contributed to the loss of $Na_V1.5$ at the intercalated disc.

The studies in Chkourko et al indicated that VGSC did not follow connexin43 to the lateral membrane. I speculate that this result may be associated with remodeling of the *perinexus*. Rhett et al described this structure as an area that surrounds gap junction plaques and where ZO-1 interacts with connexons (Rhett, Jourdan et al. 2011). The same group later discovered that in the vicinity of connexin43 gap junctions, $Na_V1.5$ is localized solely at the perinexus and not at the gap junction plaque itself (Rhett, Ongstad et al. 2012). From the study by Hesketh et al we know that during remodeling ZO-1 does not lateralize together with connexin43, meaning that no perinexus may form at the lateral membrane (Hesketh, Shah et al. 2010). Whether perinexus is an absolute requirement for $Na_V1.5$ localization remains to be determined, but if it is, then lack of perinexus at the lateral membrane may explain why $Na_V1.5$ does not lateralize.

The last question that we tried to address in the study described in Chapter III was "how"? How does connexin43 ends up at the lateral membrane? Do connexin43 gap junctions plaques rearrange themselves and in diffusive manner redistribute themselves to the lateral membrane? Or, are they strategically targeted to the lateral membrane? Due to the groundwork laid by Smyth et al and Fort et al we focused on the proteins involved in trafficking (Smyth, Hong et al. 2010; Fort, Murray et al. 2011). We found that, microtubule plus-end tracking protein, EB1, and motor protein of anterograde trafficking, Kinesin-1, undergo remodeling and accumulate at the lateral membrane. We interpreted these findings by postulating that remodeling is a result of changes in the targeted trafficking of connexin43.

The aforementioned findings support the idea that mechanical junctions are required for gap junctions to form. We then expanded on the concept that desmosomal proteins and connexin43 are also critical for the function of VGSC. Role of connexin43 on the redistribution and function of VGSC was demonstrated in connexin43-deficient cardiomyocytes in the study of

Jansen et al (Jansen, Noorman et al. 2012). We wanted to know more about the intimate mechanism of connexin43-mediated regulation of VGSC. To address the question we turned to the recent study by Francis et al that identified connexin43 as a protein that stabilizes tubulin and tethers targeted microtubule growth (Francis, Xu et al. 2011). This novel function was explored in the scope of regulation of $Na_V1.5$. We found that just like in embryonic fibroblasts and NIH3T3 cells, connexin43 mediates the abundance of Glu-tubulin subpopulation via its tubulin-biding domain in cardiac myocytes. We also found that connexin43 expression relates to the localization of the tethering protein EB1. Importantly, we found that the function of VGSC is tied closely to the integrity of tubulin-binding domain of connexin43. This makes a direct connection between cytoskeleton-regulating function of connexin43 and I_{Na}. Although Casini et al established the importance of microtubule network on the function of the VGSC, no evidence on preferential delivery of $Na_V1.5$ along stable versus unstable microtubules has been reported (Casini, Tan et al. 2010). The key unanswered question about trafficking of $Na_V1.5$ remains to be a question about molecular machinery. It has been reported that motor proteins preferentially bind to the stable microtubules (Dunn, Morrison et al. 2008; Cai, McEwen et al. 2009). Thus, knowing what motor protein is involved in the delivery of $Na_V1.5$ may give us a clue to a preferential modification of tubulin for $Na_V1.5$ trafficking.

In this study we looked at the role of detyrosination on the function of I_{Na}. Detyrosination results from a cleavage of Tyrosine from a C-terminus of α-tubulin by an unidentified carboxypeptidase (Westermann and Weber 2003; Verhey and Gaertig 2007; Hammond, Cai et al. 2008). Pharmacological agents have been used to modify tubulin. Carboxypeptidase A (CPA) was described as an agent inducing tubulin detyrosination (Konishi and Setou 2009). Konishi et al demonstrated that detyrosination provides a "directional cue" for Kinesin-1 to move to neuronal axon. On one hand, carboxypeptidase A (CPA) is not a specific carboxypeptidase and may potentially affect a number of cellular functions making an interpretation of results potentially difficult. On the other hand, it might be useful to test the effect of treatment with CPA on connexin43 distribution and I_{Na}. Similarly, trachostatin A (TSA) may be used to induce acetylation (Konishi and Setou 2009). Although we provide compelling evidence supporting the notion that tubulin-tethering and stabilizing function of connexin43 regulates function of VGSC, the information on motor proteins involved in $Na_V1.5$ delivery is still missing.

In summary, we found that in the diseased heart desmosomes are formed at the lateral membrane. These lateralized desmosomes probably participate in the targeted delivery of connexin43 and gap junction formation. Although desmosomes and connexin43 are essential for the function and distribution of the VGSC, we found that $Na_V1.5$ does not follow desmosomes and connexin43 to the lateral membrane, an effect that might be related to the loss of a Cx43-ZO1 interaction upon remodeling. Our data also lead us to propose the hypothesis that through its tubulin binding domain, connexin43 regulates the distribution and function of VGSC by stabilizing and tethering tubulin. In the future, it may be important to assess the role of perinexus in the tubulin tethering. Immunofluorescence study of EB1 signal might reveal whether tubulin-tethering function is impaired. Furthermore, connexin43 is regulated by phoshporylation. Studies in the heart failure model of a dog showed change in the phosphorylation state resulting in almost two fold increase in dephosphorylated Cx43 at the late stage of disease (Akar, Nass et al. 2007). Importantly, remodeled connexin43 has been reported to be predominantly dephoshporylated. Thus, one may use genetically-engineered mice with compromised sites of phosphorylation to address the role of this post-translational modification on the tethering function (Huang, Xie et al. 2011; Remo, Qu et al. 2011).

One more question comes to mind and serves as a platform for the future directions of this study. Although the predominant subpopulation of $Na_V1.5$ is localized at the intercalated disc and interacts with SAP97, a lesser fraction exists at the T-tubule membranes and interacts with syntrophyn-dystrophin complex (Petitprez, Zmoos et al. 2011). Under the normal conditions connexin43 is not present at the T-tubule membrane and thus it is not clear what proteins at the lateral membrane substitute for the role of connexin43? We know that lateralized $Na_V1.5$ interacts with syntrophin–dystrophin complex via its PDZ-binding domain (Gavillet, Rougier et al. 2006). Studies on dystrophin- deficient (mdx^{5cv}) revealed the decrease in the expression of $Na_V1.5$ and decrease in I_{Na} (Gavillet, Rougier et al. 2006). Given that syntrophin-dystrophin complex interacts with actin cytoskeleton the first question one should address is whether delivery of T-tubule $Na_V1.5$ is dependent on microtubulin cytoskeleton. The study by Lin et al had shown that the amplitude and gating properties of I_{Na} localized at the lateral membrane differ from those distributed at the intercalated disc (Lin, Liu et al. 2011). This information may come

handy when one decides to test the role of tubulin-modulating agents, such as nocadozole or taxol, on the function of $Na_V1.5$. Alternatively, cell-attached micropatch studies may be performed in combination with these treatments. Once the importance of tubulin in the function of the lateral VGSC is established one should examine plus-end-tracking proteins (+TIPs) and their binding partners (i.e. EB1, p150(Glued)) that may localize to the T-tubules. Expecting that the abundance of these proteins at the T-tubules may be lower than what is seen at the intercalated discs, the higher magnification and resolution microscopy (i.e. TIRF) should be employed. Once the +TIPs producing T-tubule pattern is established the next step may be to use the dystrophin- deficient (mdx^{5cv}) mouse to detect any changes in the immunoreactive EB1 pattern. If dystrophin-deficiency will result in the loss of +TIPs signal, one may want to examine the role of binding partners of dystrophin-syntrophin complex on the +TIPs distribution with the hope to pinpoint a microtubule-tethering protein.

Bibliography

Akar, F. G., R. D. Nass, et al. (2007). "Dynamic changes in conduction velocity and gap junction properties during development of pacing-induced heart failure." American journal of physiology. Heart and circulatory physiology **293**(2): H1223-1230.

Akar, F. G., R. D. Nass, et al. (2007). "Dynamic changes in conduction velocity and gap junction properties during development of pacing-induced heart failure." Am J Physiol Heart Circ Physiol **293**(2): H1223-1230.

Akar, F. G., D. D. Spragg, et al. (2004). "Mechanisms underlying conduction slowing and arrhythmogenesis in nonischemic dilated cardiomyopathy." Circulation research **95**(7): 717-725.

Akhmanova, A. and C. C. Hoogenraad (2005). "Microtubule plus-end-tracking proteins: mechanisms and functions." Current opinion in cell biology **17**(1): 47-54.

Al-Amoudi, A. and A. S. Frangakis (2008). "Structural studies on desmosomes." Biochemical Society transactions **36**(Pt 2): 181-187.

Allouis, M., F. Le Bouffant, et al. (2006). "14-3-3 is a regulator of the cardiac voltage-gated sodium channel Nav1.5." Circulation research **98**(12): 1538-1546.

Argyropoulos, G., A. M. Stutz, et al. (2009). "KIF5B gene sequence variation and response of cardiac stroke volume to regular exercise." Physiol Genomics **36**(2): 79-88.

Barker, R. J., R. L. Price, et al. (2002). "Increased association of ZO-1 with connexin43 during remodeling of cardiac gap junctions." Circ Res **90**(3): 317-324.

Bass-Zubek, A. E., L. M. Godsel, et al. (2009). "Plakophilins: multifunctional scaffolds for adhesion and signaling." Current opinion in cell biology **21**(5): 708-716.

Beams, H. W., T. C. Evans, et al. (1949). "Electron microscope studies on the structure of cardiac muscle." The Anatomical record **105**(1): 59-81, incl 53 pl.

Beardslee, M. A., J. G. Laing, et al. (1998). "Rapid turnover of connexin43 in the adult rat heart." Circulation research **83**(6): 629-635.

Beardslee, M. A., D. L. Lerner, et al. (2000). "Dephosphorylation and intracellular redistribution of ventricular connexin43 during electrical uncoupling induced by ischemia." Circulation research **87**(8): 656-662.

Belmadani, S., C. Pous, et al. (2004). "Post-translational modifications of tubulin and microtubule stability in adult rat ventricular myocytes and immortalized HL-1 cardiomyocytes." Molecular and cellular biochemistry **258**(1-2): 35-48.

Bennett, V. and J. Healy (2009). "Membrane domains based on ankyrin and spectrin associated with cell-cell interactions." Cold Spring Harbor perspectives in biology **1**(6): a003012.

Beyder, A., J. L. Rae, et al. (2010). "Mechanosensitivity of Nav1.5, a voltage-sensitive sodium channel." The Journal of physiology **588**(Pt 24): 4969-4985.

Boassa, D., J. L. Solan, et al. (2010). "Trafficking and recycling of the connexin43 gap junction protein during mitosis." Traffic **11**(11): 1471-1486.

Borlak, J. and T. Thum (2003). "Hallmarks of ion channel gene expression in end-stage heart failure." FASEB journal : official publication of the Federation of American Societies for Experimental Biology **17**(12): 1592-1608.

Borrmann, C. M., C. Grund, et al. (2006). "The area composita of adhering junctions connecting heart muscle cells of vertebrates. II. Colocalizations of desmosomal and fascia adhaerens molecules in the intercalated disk." Eur J Cell Biol **85**(6): 469-485.
Brackenbury, W. J. and L. L. Isom (2011). "Na Channel beta Subunits: Overachievers of the Ion Channel Family." Frontiers in pharmacology **2**: 53.
Bruce, A. F., S. Rothery, et al. (2008). "Gap junction remodelling in human heart failure is associated with increased interaction of connexin43 with ZO-1." Cardiovascular research **77**(4): 757-765.
Cabo, C., J. Yao, et al. (2006). "Heterogeneous gap junction remodeling in reentrant circuits in the epicardial border zone of the healing canine infarct." Cardiovasc Res **72**(2): 241-249.
Cai, D., D. P. McEwen, et al. (2009). "Single molecule imaging reveals differences in microtubule track selection between Kinesin motors." PLoS biology **7**(10): e1000216.
Cannon, S. C. (1996). "Sodium channel defects in myotonia and periodic paralysis." Annual review of neuroscience **19**: 141-164.
Casini, S., H. L. Tan, et al. (2007). "Characterization of a novel SCN5A mutation associated with Brugada syndrome reveals involvement of DIIIS4-S5 linker in slow inactivation." Cardiovascular research **76**(3): 418-429.
Casini, S., H. L. Tan, et al. (2010). "Tubulin polymerization modifies cardiac sodium channel expression and gating." Cardiovascular research **85**(4): 691-700.
Catterall, W. A. (1992). "Cellular and molecular biology of voltage-gated sodium channels." Physiological reviews **72**(4 Suppl): S15-48.
Cerrone, M., M. Noorman, et al. (2012). "Sodium Current Deficit and Arrhythmogenesis in a Murine Model of Plakophilin-2 Haploinsufficiency." Cardiovascular research.
Chen, X., S. Bonne, et al. (2002). "Protein binding and functional characterization of plakophilin 2. Evidence for its diverse roles in desmosomes and beta -catenin signaling." The Journal of biological chemistry **277**(12): 10512-10522.
Chkourko, H. S., G. Guerrero-Serna, et al. (2012). "Remodeling of mechanical junctions and of microtubule-associated proteins accompany cardiac connexin43 lateralization." Heart rhythm : the official journal of the Heart Rhythm Society **9**(7): 1133-1140 e1136.
Cina, C., K. Maass, et al. (2009). "Involvement of the cytoplasmic C-terminal domain of connexin43 in neuronal migration." The Journal of neuroscience : the official journal of the Society for Neuroscience **29**(7): 2009-2021.
Claycomb, W. C., N. A. Lanson, Jr., et al. (1998). "HL-1 cells: a cardiac muscle cell line that contracts and retains phenotypic characteristics of the adult cardiomyocyte." Proceedings of the National Academy of Sciences of the United States of America **95**(6): 2979-2984.
Cohen, S. A. (1996). "Immunocytochemical localization of rH1 sodium channel in adult rat heart atria and ventricle. Presence in terminal intercalated disks." Circulation **94**(12): 3083-3086.
Colussi, C., J. Rosati, et al. (2011). "Nepsilon-lysine acetylation determines dissociation from GAP junctions and lateralization of connexin 43 in normal and dystrophic heart." Proceedings of the National Academy of Sciences of the United States of America **108**(7): 2795-2800.
Cooper, C. D. and P. D. Lampe (2002). "Casein kinase 1 regulates connexin-43 gap junction assembly." The Journal of biological chemistry **277**(47): 44962-44968.
Cowin, P., H. P. Kapprell, et al. (1986). "Plakoglobin: a protein common to different kinds of intercellular adhering junctions." Cell **46**(7): 1063-1073.

Davis, J. Q. and V. Bennett (1984). "Brain ankyrin. A membrane-associated protein with binding sites for spectrin, tubulin, and the cytoplasmic domain of the erythrocyte anion channel." The Journal of biological chemistry **259**(21): 13550-13559.
De Mello, W. C. (1999). "Cell coupling and impulse propagation in the failing heart." Journal of cardiovascular electrophysiology **10**(10): 1409-1420.
Della Rocca, G., F. Pugliese, et al. (1997). "Hemodynamics during inhaled nitric oxide in lung transplant candidates." Transplant Proc **29**(8): 3367-3370.
Della Rocca, G., F. Pugliese, et al. (1997). "Hemodynamics during inhaled nitric oxide in lung transplant candidates." Transplantation proceedings **29**(8): 3367-3370.
Delmar, M. (2012). "Connexin43 regulates sodium current; ankyrin-G modulates gap junctions: the intercalated disc exchanger." Cardiovascular research **93**(2): 220-222.
Delmar, M. and F. X. Liang (2011). "Connexin43, and the regulation of intercalated disc function." Heart Rhythm.
Delmar, M. and F. X. Liang (2012). "Connexin43 and the regulation of intercalated disc function." Heart rhythm : the official journal of the Heart Rhythm Society **9**(5): 835-838.
Delmar, M. and W. J. McKenna (2010). "The cardiac desmosome and arrhythmogenic cardiomyopathies: from gene to disease." Circulation research **107**(6): 700-714.
Dhar Malhotra, J., C. Chen, et al. (2001). "Characterization of sodium channel alpha- and beta-subunits in rat and mouse cardiac myocytes." Circulation **103**(9): 1303-1310.
Dominguez, J. N., A. de la Rosa, et al. (2008). "Tissue distribution and subcellular localization of the cardiac sodium channel during mouse heart development." Cardiovasc Res **78**(1): 45-52.
Dunn, S., E. E. Morrison, et al. (2008). "Differential trafficking of Kif5c on tyrosinated and detyrosinated microtubules in live cells." Journal of cell science **121**(Pt 7): 1085-1095.
Dupont, E., T. Matsushita, et al. (2001). "Altered connexin expression in human congestive heart failure." Journal of molecular and cellular cardiology **33**(2): 359-371.
Emdad, L., M. Uzzaman, et al. (2001). "Gap junction remodeling in hypertrophied left ventricles of aortic-banded rats: prevention by angiotensin II type 1 receptor blockade." J Mol Cell Cardiol **33**(2): 219-231.
Escayg, A., B. T. MacDonald, et al. (2000). "Mutations of SCN1A, encoding a neuronal sodium channel, in two families with GEFS+2." Nature genetics **24**(4): 343-345.
Ewart, J. L., M. F. Cohen, et al. (1997). "Heart and neural tube defects in transgenic mice overexpressing the Cx43 gap junction gene." Development **124**(7): 1281-1292.
Fernandes, R., H. Girao, et al. (2004). "High glucose down-regulates intercellular communication in retinal endothelial cells by enhancing degradation of connexin 43 by a proteasome-dependent mechanism." The Journal of biological chemistry **279**(26): 27219-27224.
Fialova, M., K. Dlugosova, et al. (2008). "Adaptation of the heart to hypertension is associated with maladaptive gap junction connexin-43 remodeling." Physiol Res **57**(1): 7-11.
Forbes, M. S. and N. Sperelakis (1985). "Intercalated discs of mammalian heart: a review of structure and function." Tissue & cell **17**(5): 605-648.
Fort, A. G., J. W. Murray, et al. (2011). "In vitro motility of liver connexin vesicles along microtubules utilizes kinesin motors." J Biol Chem **286**(26): 22875-22885.
Fort, A. G., J. W. Murray, et al. (2011). "In vitro motility of liver connexin vesicles along microtubules utilizes kinesin motors." The Journal of biological chemistry **286**(26): 22875-22885.

Francis, R., X. Xu, et al. (2011). "Connexin43 modulates cell polarity and directional cell migration by regulating microtubule dynamics." PloS one **6**(10): e26379.
Franke, W. W., C. M. Borrmann, et al. (2006). "The area composita of adhering junctions connecting heart muscle cells of vertebrates. I. Molecular definition in intercalated disks of cardiomyocytes by immunoelectron microscopy of desmosomal proteins." Eur J Cell Biol **85**(2): 69-82.
Frohnwieser, B., L. Q. Chen, et al. (1997). "Modulation of the human cardiac sodium channel alpha-subunit by cAMP-dependent protein kinase and the responsible sequence domain." The Journal of physiology **498 (Pt 2)**: 309-318.
Fushiki, S., J. L. Perez Velazquez, et al. (2003). "Changes in neuronal migration in neocortex of connexin43 null mutant mice." Journal of neuropathology and experimental neurology **62**(3): 304-314.
Gaietta, G., T. J. Deerinck, et al. (2002). "Multicolor and electron microscopic imaging of connexin trafficking." Science **296**(5567): 503-507.
Garcia-Gras, E., R. Lombardi, et al. (2006). "Suppression of canonical Wnt/beta-catenin signaling by nuclear plakoglobin recapitulates phenotype of arrhythmogenic right ventricular cardiomyopathy." The Journal of clinical investigation **116**(7): 2012-2021.
Gavillet, B., J. S. Rougier, et al. (2006). "Cardiac sodium channel Nav1.5 is regulated by a multiprotein complex composed of syntrophins and dystrophin." Circulation research **99**(4): 407-414.
Gee, S. H., R. Madhavan, et al. (1998). "Interaction of muscle and brain sodium channels with multiple members of the syntrophin family of dystrophin-associated proteins." The Journal of neuroscience : the official journal of the Society for Neuroscience **18**(1): 128-137.
Gerull, B., A. Heuser, et al. (2004). "Mutations in the desmosomal protein plakophilin-2 are common in arrhythmogenic right ventricular cardiomyopathy." Nature genetics **36**(11): 1162-1164.
Getsios, S., A. C. Huen, et al. (2004). "Working out the strength and flexibility of desmosomes." Nature reviews. Molecular cell biology **5**(4): 271-281.
Giepmans, B. N. and W. H. Moolenaar (1998). "The gap junction protein connexin43 interacts with the second PDZ domain of the zona occludens-1 protein." Current biology : CB **8**(16): 931-934.
Giepmans, B. N., I. Verlaan, et al. (2001). "Gap junction protein connexin-43 interacts directly with microtubules." Current biology : CB **11**(17): 1364-1368.
Giepmans, B. N., I. Verlaan, et al. (2001). "Connexin-43 interactions with ZO-1 and alpha- and beta-tubulin." Cell communication & adhesion **8**(4-6): 219-223.
Goossens, S., B. Janssens, et al. (2007). "A unique and specific interaction between alphaT-catenin and plakophilin-2 in the area composita, the mixed-type junctional structure of cardiac intercalated discs." Journal of cell science **120**(Pt 12): 2126-2136.
Green, K. J. and C. L. Simpson (2007). "Desmosomes: new perspectives on a classic." The Journal of investigative dermatology **127**(11): 2499-2515.
Grossmann, K. S., C. Grund, et al. (2004). "Requirement of plakophilin 2 for heart morphogenesis and cardiac junction formation." The Journal of cell biology **167**(1): 149-160.

Gundersen, G. G. and J. C. Bulinski (1988). "Selective stabilization of microtubules oriented toward the direction of cell migration." Proceedings of the National Academy of Sciences of the United States of America **85**(16): 5946-5950.
Gutstein, D. E., F. Y. Liu, et al. (2003). "The organization of adherens junctions and desmosomes at the cardiac intercalated disc is independent of gap junctions." Journal of cell science **116**(Pt 5): 875-885.
Gutstein, D. E., G. E. Morley, et al. (2001). "Conduction slowing and sudden arrhythmic death in mice with cardiac-restricted inactivation of connexin43." Circulation research **88**(3): 333-339.
Hallaq, H., Z. Yang, et al. (2006). "Quantitation of protein kinase A-mediated trafficking of cardiac sodium channels in living cells." Cardiovascular research **72**(2): 250-261.
Hammond, J. W., D. Cai, et al. (2008). "Tubulin modifications and their cellular functions." Current opinion in cell biology **20**(1): 71-76.
Harris, A. L. (2007). "Connexin channel permeability to cytoplasmic molecules." Progress in biophysics and molecular biology **94**(1-2): 120-143.
Herve, J. C., N. Bourmeyster, et al. (2007). "Gap junctional complexes: from partners to functions." Progress in biophysics and molecular biology **94**(1-2): 29-65.
Hesketh, G. G., M. H. Shah, et al. (2010). "Ultrastructure and regulation of lateralized connexin43 in the failing heart." Circulation research **106**(6): 1153-1163.
Huang, G. Y., L. J. Xie, et al. (2011). "Evaluating the role of connexin43 in congenital heart disease: Screening for mutations in patients with outflow tract anomalies and the analysis of knock-in mouse models." Journal of cardiovascular disease research **2**(4): 206-212.
Huber, O. (2003). "Structure and function of desmosomal proteins and their role in development and disease." Cellular and molecular life sciences : CMLS **60**(9): 1872-1890.
Hunter, A. W., R. J. Barker, et al. (2005). "Zonula occludens-1 alters connexin43 gap junction size and organization by influencing channel accretion." Molecular biology of the cell **16**(12): 5686-5698.
Jansen, J. A., M. Noorman, et al. (2012). "Reduced heterogeneous expression of Cx43 results in decreased Nav1.5 expression and reduced sodium current that accounts for arrhythmia vulnerability in conditional Cx43 knockout mice." Heart rhythm : the official journal of the Heart Rhythm Society **9**(4): 600-607.
Jespersen, T., B. Gavillet, et al. (2006). "Cardiac sodium channel Na(v)1.5 interacts with and is regulated by the protein tyrosine phosphatase PTPH1." Biochemical and biophysical research communications **348**(4): 1455-1462.
Jordan, K., R. Chodock, et al. (2001). "The origin of annular junctions: a mechanism of gap junction internalization." Journal of cell science **114**(Pt 4): 763-773.
Jordan, K., J. L. Solan, et al. (1999). "Trafficking, assembly, and function of a connexin43-green fluorescent protein chimera in live mammalian cells." Molecular biology of the cell **10**(6): 2033-2050.
Kaplan, S. R., J. J. Gard, et al. (2004). "Remodeling of myocyte gap junctions in arrhythmogenic right ventricular cardiomyopathy due to a deletion in plakoglobin (Naxos disease)." Heart rhythm : the official journal of the Heart Rhythm Society **1**(1): 3-11.
Kaprielian, R. R., S. Stevenson, et al. (2000). "Distinct patterns of dystrophin organization in myocyte sarcolemma and transverse tubules of normal and diseased human myocardium." Circulation **101**(22): 2586-2594.

Kar, R., N. Batra, et al. (2012). "Biological role of connexin intercellular channels and hemichannels." Archives of biochemistry and biophysics.
Konishi, Y. and M. Setou (2009). "Tubulin tyrosination navigates the kinesin-1 motor domain to axons." Nature neuroscience **12**(5): 559-567.
Kostin, S., S. Dammer, et al. (2004). "Connexin 43 expression and distribution in compensated and decompensated cardiac hypertrophy in patients with aortic stenosis." Cardiovasc Res **62**(2): 426-436.
Kostin, S., M. Rieger, et al. (2003). "Gap junction remodeling and altered connexin43 expression in the failing human heart." Molecular and cellular biochemistry **242**(1-2): 135-144.
Kostin, S., M. Rieger, et al. (2003). "Gap junction remodeling and altered connexin43 expression in the failing human heart." Mol Cell Biochem **242**(1-2): 135-144.
Kretz, M., C. Euwens, et al. (2003). "Altered connexin expression and wound healing in the epidermis of connexin-deficient mice." Journal of cell science **116**(Pt 16): 3443-3452.
Kreuzberg, M. M., G. Sohl, et al. (2005). "Functional properties of mouse connexin30.2 expressed in the conduction system of the heart." Circulation research **96**(11): 1169-1177.
Kucera, J. P., S. Rohr, et al. (2002). "Localization of sodium channels in intercalated disks modulates cardiac conduction." Circulation research **91**(12): 1176-1182.
Kucera, J. P., S. Rohr, et al. (2002). "Localization of sodium channels in intercalated disks modulates cardiac conduction." Circ Res **91**(12): 1176-1182.
Laing, J. G. and E. C. Beyer (1995). "The gap junction protein connexin43 is degraded via the ubiquitin proteasome pathway." The Journal of biological chemistry **270**(44): 26399-26403.
Laing, J. G., P. N. Tadros, et al. (1997). "Degradation of connexin43 gap junctions involves both the proteasome and the lysosome." Experimental cell research **236**(2): 482-492.
Laird, D. W. (2006). "Life cycle of connexins in health and disease." The Biochemical journal **394**(Pt 3): 527-543.
Lampe, P. D., C. D. Cooper, et al. (2006). "Analysis of Connexin43 phosphorylated at S325, S328 and S330 in normoxic and ischemic heart." Journal of cell science **119**(Pt 16): 3435-3442.
Lauf, U., B. N. Giepmans, et al. (2002). "Dynamic trafficking and delivery of connexons to the plasma membrane and accretion to gap junctions in living cells." Proc Natl Acad Sci U S A **99**(16): 10446-10451.
Lauf, U., B. N. Giepmans, et al. (2002). "Dynamic trafficking and delivery of connexons to the plasma membrane and accretion to gap junctions in living cells." Proceedings of the National Academy of Sciences of the United States of America **99**(16): 10446-10451.
Leithe, E. and E. Rivedal (2004). "Epidermal growth factor regulates ubiquitination, internalization and proteasome-dependent degradation of connexin43." Journal of cell science **117**(Pt 7): 1211-1220.
Leithe, E. and E. Rivedal (2004). "Ubiquitination and down-regulation of gap junction protein connexin-43 in response to 12-O-tetradecanoylphorbol 13-acetate treatment." The Journal of biological chemistry **279**(48): 50089-50096.
Lerner, D. L., K. A. Yamada, et al. (2000). "Accelerated onset and increased incidence of ventricular arrhythmias induced by ischemia in Cx43-deficient mice." Circulation **101**(5): 547-552.
Lettieri, C. J., S. D. Nathan, et al. (2006). "Prevalence and outcomes of pulmonary arterial hypertension in advanced idiopathic pulmonary fibrosis." Chest **129**(3): 746-752.

Leykauf, K., M. Salek, et al. (2006). "Ubiquitin protein ligase Nedd4 binds to connexin43 by a phosphorylation-modulated process." Journal of cell science **119**(Pt 17): 3634-3642.
Li, J., S. Goossens, et al. (2012). "Loss of alphaT-catenin alters the hybrid adhering junctions in the heart and leads to dilated cardiomyopathy and ventricular arrhythmia following acute ischemia." Journal of cell science **125**(Pt 4): 1058-1067.
Li, J., V. V. Patel, et al. (2005). "Cardiac-specific loss of N-cadherin leads to alteration in connexins with conduction slowing and arrhythmogenesis." Circulation research **97**(5): 474-481.
Liao, G. and G. G. Gundersen (1998). "Kinesin is a candidate for cross-bridging microtubules and intermediate filaments. Selective binding of kinesin to detyrosinated tubulin and vimentin." The Journal of biological chemistry **273**(16): 9797-9803.
Lin, X., N. Liu, et al. (2011). "Subcellular heterogeneity of sodium current properties in adult cardiac ventricular myocytes." Heart rhythm : the official journal of the Heart Rhythm Society **8**(12): 1923-1930.
Lombardi, R., J. Dong, et al. (2009). "Genetic fate mapping identifies second heart field progenitor cells as a source of adipocytes in arrhythmogenic right ventricular cardiomyopathy." Circulation research **104**(9): 1076-1084.
Lopez-Santiago, L. F., L. S. Meadows, et al. (2007). "Sodium channel Scn1b null mice exhibit prolonged QT and RR intervals." Journal of molecular and cellular cardiology **43**(5): 636-647.
Lossin, C., D. W. Wang, et al. (2002). "Molecular basis of an inherited epilepsy." Neuron **34**(6): 877-884.
Lowe, J. S., O. Palygin, et al. (2008). "Voltage-gated Nav channel targeting in the heart requires an ankyrin-G dependent cellular pathway." The Journal of cell biology **180**(1): 173-186.
Lu, T., H. C. Lee, et al. (1999). "Modulation of rat cardiac sodium channel by the stimulatory G protein alpha subunit." The Journal of physiology **518 (Pt 2)**: 371-384.
Maass, K., J. Shibayama, et al. (2007). "C-terminal truncation of connexin43 changes number, size, and localization of cardiac gap junction plaques." Circ Res **101**(12): 1283-1291.
Maier, S. K., R. E. Westenbroek, et al. (2004). "Distinct subcellular localization of different sodium channel alpha and beta subunits in single ventricular myocytes from mouse heart." Circulation **109**(11): 1421-1427.
Maier, S. K., R. E. Westenbroek, et al. (2002). "An unexpected role for brain-type sodium channels in coupling of cell surface depolarization to contraction in the heart." Proceedings of the National Academy of Sciences of the United States of America **99**(6): 4073-4078.
Maltsev, V. A. and A. I. Undrovinas (1997). "Cytoskeleton modulates coupling between availability and activation of cardiac sodium channel." The American journal of physiology **273**(4 Pt 2): H1832-1840.
Matsushita, S., H. Kurihara, et al. (2006). "Alterations of phosphorylation state of connexin 43 during hypoxia and reoxygenation are associated with cardiac function." The journal of histochemistry and cytochemistry : official journal of the Histochemistry Society **54**(3): 343-353.
McKoy, G., N. Protonotarios, et al. (2000). "Identification of a deletion in plakoglobin in arrhythmogenic right ventricular cardiomyopathy with palmoplantar keratoderma and woolly hair (Naxos disease)." Lancet **355**(9221): 2119-2124.

Meadows, L. S. and L. L. Isom (2005). Sodium channels as macromolecular complexes: implications for inherited arrhythmia syndromes. 67 Review.

Meyer, R. A., D. W. Laird, et al. (1992). "Inhibition of gap junction and adherens junction assembly by connexin and A-CAM antibodies." The Journal of cell biology **119**(1): 179-189.

Mohler, P. J., I. Rivolta, et al. (2004). "Nav1.5 E1053K mutation causing Brugada syndrome blocks binding to ankyrin-G and expression of Nav1.5 on the surface of cardiomyocytes." Proceedings of the National Academy of Sciences of the United States of America **101**(50): 17533-17538.

Montpetit, M. L., P. J. Stocker, et al. (2009). "Regulated and aberrant glycosylation modulate cardiac electrical signaling." Proceedings of the National Academy of Sciences of the United States of America **106**(38): 16517-16522.

Moreno, A. P., J. C. Saez, et al. (1994). "Human connexin43 gap junction channels. Regulation of unitary conductances by phosphorylation." Circulation research **74**(6): 1050-1057.

Mori, R., K. T. Power, et al. (2006). "Acute downregulation of connexin43 at wound sites leads to a reduced inflammatory response, enhanced keratinocyte proliferation and wound fibroblast migration." Journal of cell science **119**(Pt 24): 5193-5203.

Morley, G. E., D. Vaidya, et al. (1999). "Characterization of conduction in the ventricles of normal and heterozygous Cx43 knockout mice using optical mapping." Journal of cardiovascular electrophysiology **10**(10): 1361-1375.

Musil, L. S. and D. A. Goodenough (1991). "Biochemical analysis of connexin43 intracellular transport, phosphorylation, and assembly into gap junctional plaques." The Journal of cell biology **115**(5): 1357-1374.

Musil, L. S. and D. A. Goodenough (1993). "Multisubunit assembly of an integral plasma membrane channel protein, gap junction connexin43, occurs after exit from the ER." Cell **74**(6): 1065-1077.

North, A. J., W. G. Bardsley, et al. (1999). "Molecular map of the desmosomal plaque." Journal of cell science **112 (Pt 23)**: 4325-4336.

Ou, Y., P. Strege, et al. (2003). "Syntrophin gamma 2 regulates SCN5A gating by a PDZ domain-mediated interaction." The Journal of biological chemistry **278**(3): 1915-1923.

Oxford, E. M., H. Musa, et al. (2007). "Connexin43 remodeling caused by inhibition of plakophilin-2 expression in cardiac cells." Circulation research **101**(7): 703-711.

Papadatos, G. A., P. M. Wallerstein, et al. (2002). "Slowed conduction and ventricular tachycardia after targeted disruption of the cardiac sodium channel gene Scn5a." Proceedings of the National Academy of Sciences of the United States of America **99**(9): 6210-6215.

Patino, G. A., L. R. Claes, et al. (2009). "A functional null mutation of SCN1B in a patient with Dravet syndrome." The Journal of neuroscience : the official journal of the Society for Neuroscience **29**(34): 10764-10778.

Peters, M. F., M. E. Adams, et al. (1997). "Differential association of syntrophin pairs with the dystrophin complex." The Journal of cell biology **138**(1): 81-93.

Peters, N. S., J. Coromilas, et al. (1997). "Disturbed connexin43 gap junction distribution correlates with the location of reentrant circuits in the epicardial border zone of healing canine infarcts that cause ventricular tachycardia." Circulation **95**(4): 988-996.

Peters, N. S., C. R. Green, et al. (1993). "Reduced content of connexin43 gap junctions in ventricular myocardium from hypertrophied and ischemic human hearts." Circulation **88**(3): 864-875.
Peters, N. S., C. R. Green, et al. (1995). "Cardiac arrhythmogenesis and the gap junction." Journal of molecular and cellular cardiology **27**(1): 37-44.
Petitprez, S., A. F. Zmoos, et al. (2011). "SAP97 and dystrophin macromolecular complexes determine two pools of cardiac sodium channels Nav1.5 in cardiomyocytes." Circulation research **108**(3): 294-304.
Pfenniger, A., J. P. Derouette, et al. (2010). "Gap junction protein Cx37 interacts with endothelial nitric oxide synthase in endothelial cells." Arteriosclerosis, thrombosis, and vascular biology **30**(4): 827-834.
Piehl, M., C. Lehmann, et al. (2007). "Internalization of large double-membrane intercellular vesicles by a clathrin-dependent endocytic process." Molecular biology of the cell **18**(2): 337-347.
Pilichou, K., A. Nava, et al. (2006). "Mutations in desmoglein-2 gene are associated with arrhythmogenic right ventricular cardiomyopathy." Circulation **113**(9): 1171-1179.
Pohlmann JR, A. B., Camboni D, Koch KL, Mervak BM, Cook KE "A low mortality model of chronic pulmonary hypertension in sheep. Surgical Research, in press." Surgical Research.
Priori, S. G., C. Napolitano, et al. (2002). "Natural history of Brugada syndrome: insights for risk stratification and management." Circulation **105**(11): 1342-1347.
Procida, K., L. Jorgensen, et al. (2009). "Phosphorylation of connexin43 on serine 306 regulates electrical coupling." Heart rhythm : the official journal of the Heart Rhythm Society **6**(11): 1632-1638.
Qin, H., Q. Shao, et al. (2003). "Lysosomal and proteasomal degradation play distinct roles in the life cycle of Cx43 in gap junctional intercellular communication-deficient and -competent breast tumor cells." The Journal of biological chemistry **278**(32): 30005-30014.
Qu, J., F. M. Volpicelli, et al. (2009). "Gap junction remodeling and spironolactone-dependent reverse remodeling in the hypertrophied heart." Circ Res **104**(3): 365-371.
Rampazzo, A., A. Nava, et al. (2002). "Mutation in human desmoplakin domain binding to plakoglobin causes a dominant form of arrhythmogenic right ventricular cardiomyopathy." American journal of human genetics **71**(5): 1200-1206.
Reed, N. A., D. Cai, et al. (2006). "Microtubule acetylation promotes kinesin-1 binding and transport." Current biology : CB **16**(21): 2166-2172.
Remo, B. F., J. Qu, et al. (2011). "Phosphatase-resistant gap junctions inhibit pathological remodeling and prevent arrhythmias." Circulation research **108**(12): 1459-1466.
Rhett, J. M., J. Jourdan, et al. (2011). "Connexin 43 connexon to gap junction transition is regulated by zonula occludens-1." Molecular biology of the cell **22**(9): 1516-1528.
Rhett, J. M., E. L. Ongstad, et al. (2012). "Cx43 Associates with Na(v)1.5 in the Cardiomyocyte Perinexus." The Journal of membrane biology **245**(7): 411-422.
Rizzo, S., K. Pilichou, et al. (2012). "The changing spectrum of arrhythmogenic (right ventricular) cardiomyopathy." Cell and tissue research **348**(2): 319-323.
Rodriguez-Sinovas, A., K. Boengler, et al. (2006). "Translocation of connexin 43 to the inner mitochondrial membrane of cardiomyocytes through the heat shock protein 90-dependent

TOM pathway and its importance for cardioprotection." Circulation research **99**(1): 93-101.
Rohr, S. (2007). "Molecular crosstalk between mechanical and electrical junctions at the intercalated disc." Circ Res **101**(7): 637-639.
Rook, M. B., M. M. Evers, et al. (2012). "Biology of cardiac sodium channel Nav1.5 expression." Cardiovascular research **93**(1): 12-23.
Rowinsky, E. K. and R. C. Donehower (1995). "Paclitaxel (taxol)." The New England journal of medicine **332**(15): 1004-1014.
Rowinsky, E. K., W. P. McGuire, et al. (1991). "Cardiac disturbances during the administration of taxol." Journal of clinical oncology : official journal of the American Society of Clinical Oncology **9**(9): 1704-1712.
Saez, J. C., K. A. Schalper, et al. (2010). "Cell membrane permeabilization via connexin hemichannels in living and dying cells." Experimental cell research **316**(15): 2377-2389.
Sasano, C., H. Honjo, et al. (2007). "Internalization and dephosphorylation of connexin43 in hypertrophied right ventricles of rats with pulmonary hypertension." Circulation journal : official journal of the Japanese Circulation Society **71**(3): 382-389.
Sato, H., C. M. Hall, et al. (2008). "Large animal model of chronic pulmonary hypertension." ASAIO J **54**(4): 396-400.
Sato, H., C. M. Hall, et al. (2008). "Large animal model of chronic pulmonary hypertension." ASAIO journal **54**(4): 396-400.
Sato, P. Y., W. Coombs, et al. (2011). "Interactions between ankyrin-G, Plakophilin-2, and Connexin43 at the cardiac intercalated disc." Circ Res **109**(2): 193-201.
Sato, P. Y., W. Coombs, et al. (2011). "Interactions between ankyrin-G, Plakophilin-2, and Connexin43 at the cardiac intercalated disc." Circulation research **109**(2): 193-201.
Sato, P. Y., H. Musa, et al. (2009). "Loss of plakophilin-2 expression leads to decreased sodium current and slower conduction velocity in cultured cardiac myocytes." Circulation research **105**(6): 523-526.
Sato, P. Y., H. Musa, et al. (2009). "Loss of plakophilin-2 expression leads to decreased sodium current and slower conduction velocity in cultured cardiac myocytes." Circ Res **105**(6): 523-526.
Schreibmayer, W. (1999). "Isoform diversity and modulation of sodium channels by protein kinases." Cellular physiology and biochemistry : international journal of experimental cellular physiology, biochemistry, and pharmacology **9**(4-5): 187-200.
Schreibmayer, W., B. Frohnwieser, et al. (1994). "Beta-adrenergic modulation of currents produced by rat cardiac Na+ channels expressed in Xenopus laevis oocytes." Receptors & channels **2**(4): 339-350.
Schulz, R. and G. Heusch (2004). "Connexin 43 and ischemic preconditioning." Cardiovascular research **62**(2): 335-344.
Scriven, D. R., P. Dan, et al. (2000). "Distribution of proteins implicated in excitation-contraction coupling in rat ventricular myocytes." Biophysical journal **79**(5): 2682-2691.
Severs, N. J., A. F. Bruce, et al. (2008). "Remodelling of gap junctions and connexin expression in diseased myocardium." Cardiovascular research **80**(1): 9-19.
Severs, N. J., S. R. Coppen, et al. (2004). "Gap junction alterations in human cardiac disease." Cardiovascular research **62**(2): 368-377.
Severs, N. J., E. Dupont, et al. (2004). "Remodelling of gap junctions and connexin expression in heart disease." Biochimica et biophysica acta **1662**(1-2): 138-148.

Shaw, R. M., A. J. Fay, et al. (2007). "Microtubule plus-end-tracking proteins target gap junctions directly from the cell interior to adherens junctions." Cell **128**(3): 547-560.
Shibayama, J., W. Paznekas, et al. (2005). "Functional characterization of connexin43 mutations found in patients with oculodentodigital dysplasia." Circulation research **96**(10): e83-91.
Smyth, J. W., T. T. Hong, et al. (2010). "Limited forward trafficking of connexin 43 reduces cell-cell coupling in stressed human and mouse myocardium." J Clin Invest **120**(1): 266-279.
Smyth, J. W., T. T. Hong, et al. (2010). "Limited forward trafficking of connexin 43 reduces cell-cell coupling in stressed human and mouse myocardium." The Journal of clinical investigation **120**(1): 266-279.
Smyth, J. W. and R. M. Shaw (2012). "The gap junction life cycle." Heart rhythm : the official journal of the Heart Rhythm Society **9**(1): 151-153.
Smyth, J. W., J. M. Vogan, et al. (2012). "Actin cytoskeleton rest stops regulate anterograde traffic of connexin 43 vesicles to the plasma membrane." Circulation research **110**(7): 978-989.
Sohl, G. and K. Willecke (2004). "Gap junctions and the connexin protein family." Cardiovascular research **62**(2): 228-232.
Spragg, D. D., F. G. Akar, et al. (2005). "Abnormal conduction and repolarization in late-activated myocardium of dyssynchronously contracting hearts." Cardiovasc Res **67**(1): 77-86.
Stevenson, S. A., M. J. Cullen, et al. (2005). "High-resolution en-face visualization of the cardiomyocyte plasma membrane reveals distinctive distributions of spectrin and dystrophin." European journal of cell biology **84**(12): 961-971.
Sullivan, R., G. Y. Huang, et al. (1998). "Heart malformations in transgenic mice exhibiting dominant negative inhibition of gap junctional communication in neural crest cells." Developmental biology **204**(1): 224-234.
Syrris, P., D. Ward, et al. (2006). "Arrhythmogenic right ventricular dysplasia/cardiomyopathy associated with mutations in the desmosomal gene desmocollin-2." American journal of human genetics **79**(5): 978-984.
Tan, H. L., S. Kupershmidt, et al. (2002). "A calcium sensor in the sodium channel modulates cardiac excitability." Nature **415**(6870): 442-447.
Tan, X. Y. and J. G. He (2009). "The remodeling of connexin in the hypertrophied right ventricular in pulmonary arterial hypertension and the effect of a dual ET receptor antagonist (bosentan)." Pathol Res Pract **205**(7): 473-482.
Tepass, U., K. Truong, et al. (2000). "Cadherins in embryonic and neural morphogenesis." Nature reviews. Molecular cell biology **1**(2): 91-100.
Thabut, G., G. Dauriat, et al. (2005). "Pulmonary hemodynamics in advanced COPD candidates for lung volume reduction surgery or lung transplantation." Chest **127**(5): 1531-1536.
Thabut, G., H. Mal, et al. (2003). "Survival benefit of lung transplantation for patients with idiopathic pulmonary fibrosis." The Journal of thoracic and cardiovascular surgery **126**(2): 469-475.
Thabut, G., H. Mal, et al. (2003). "Survival benefit of lung transplantation for patients with idiopathic pulmonary fibrosis." J Thorac Cardiovasc Surg **126**(2): 469-475.
Thomas, T., K. Jordan, et al. (2005). "Mechanisms of Cx43 and Cx26 transport to the plasma membrane and gap junction regeneration." Journal of cell science **118**(Pt 19): 4451-4462.

Thomas, T., K. Jordan, et al. (2005). "Mechanisms of Cx43 and Cx26 transport to the plasma membrane and gap junction regeneration." J Cell Sci **118**(Pt 19): 4451-4462.
Toyofuku, T., Y. Akamatsu, et al. (2001). "c-Src regulates the interaction between connexin-43 and ZO-1 in cardiac myocytes." The Journal of biological chemistry **276**(3): 1780-1788.
Toyofuku, T., M. Yabuki, et al. (1998). "Direct association of the gap junction protein connexin-43 with ZO-1 in cardiac myocytes." The Journal of biological chemistry **273**(21): 12725-12731.
Undrovinas, A. I., G. S. Shander, et al. (1995). "Cytoskeleton modulates gating of voltage-dependent sodium channel in heart." The American journal of physiology **269**(1 Pt 2): H203-214.
Uzzaman, M., H. Honjo, et al. (2000). "Remodeling of gap junctional coupling in hypertrophied right ventricles of rats with monocrotaline-induced pulmonary hypertension." Circ Res **86**(8): 871-878.
Valdivia, C. R., W. W. Chu, et al. (2005). "Increased late sodium current in myocytes from a canine heart failure model and from failing human heart." Journal of molecular and cellular cardiology **38**(3): 475-483.
Valiunas, V., Y. Y. Polosina, et al. (2005). "Connexin-specific cell-to-cell transfer of short interfering RNA by gap junctions." The Journal of physiology **568**(Pt 2): 459-468.
van Bemmelen, M. X., J. S. Rougier, et al. (2004). "Cardiac voltage-gated sodium channel Nav1.5 is regulated by Nedd4-2 mediated ubiquitination." Circulation research **95**(3): 284-291.
Venuta, F., E. A. Rendina, et al. (2000). "Pulmonary hemodynamics contribute to indicate priority for lung transplantation in patients with cystic fibrosis." The Journal of thoracic and cardiovascular surgery **119**(4 Pt 1): 682-689.
Venuta, F., E. A. Rendina, et al. (2000). "Pulmonary hemodynamics contribute to indicate priority for lung transplantation in patients with cystic fibrosis." J Thorac Cardiovasc Surg **119**(4 Pt 1): 682-689.
Verhey, K. J. and J. Gaertig (2007). "The tubulin code." Cell cycle **6**(17): 2152-2160.
Vizza, C. D., J. P. Lynch, et al. (1998). "Right and left ventricular dysfunction in patients with severe pulmonary disease." Chest **113**(3): 576-583.
Watson, C. L. and M. R. Gold (1997). "Modulation of Na+ current inactivation by stimulation of protein kinase C in cardiac cells." Circulation research **81**(3): 380-386.
Webster, D. R., G. G. Gundersen, et al. (1987). "Differential turnover of tyrosinated and detyrosinated microtubules." Proceedings of the National Academy of Sciences of the United States of America **84**(24): 9040-9044.
Weitzenblum, E., M. Ehrhart, et al. (1983). "Pulmonary hemodynamics in idiopathic pulmonary fibrosis and other interstitial pulmonary diseases." Respiration **44**(2): 118-127.
Weitzenblum, E., M. Ehrhart, et al. (1983). "Pulmonary hemodynamics in idiopathic pulmonary fibrosis and other interstitial pulmonary diseases." Respiration; international review of thoracic diseases **44**(2): 118-127.
Westermann, S. and K. Weber (2003). "Post-translational modifications regulate microtubule function." Nature reviews. Molecular cell biology **4**(12): 938-947.
Wiencken-Barger, A. E., B. Djukic, et al. (2007). "A role for Connexin43 during neurodevelopment." Glia **55**(7): 675-686.

Wu, L., S. L. Yong, et al. (2008). "Identification of a new co-factor, MOG1, required for the full function of cardiac sodium channel Nav 1.5." The Journal of biological chemistry **283**(11): 6968-6978.
Xiao, H., P. Verdier-Pinard, et al. (2006). "Insights into the mechanism of microtubule stabilization by Taxol." Proceedings of the National Academy of Sciences of the United States of America **103**(27): 10166-10173.
Yu, F. H., V. Yarov-Yarovoy, et al. (2005). "Overview of molecular relationships in the voltage-gated ion channel superfamily." Pharmacological reviews **57**(4): 387-395.
Zadeh, A. D., Y. Cheng, et al. (2009). "Kif5b is an essential forward trafficking motor for the Kv1.5 cardiac potassium channel." J Physiol **587**(Pt 19): 4565-4574.
Zhou, J., H. G. Shin, et al. (2002). "Phosphorylation and putative ER retention signals are required for protein kinase A-mediated potentiation of cardiac sodium current." Circulation research **91**(6): 540-546.
Zhou, J., J. Yi, et al. (2000). "Activation of protein kinase A modulates trafficking of the human cardiac sodium channel in Xenopus oocytes." Circulation research **87**(1): 33-38.